ISTANBUL TECHNICAL UNIVERSITY ★ GRADUATE SCHOOL OF SCIENCE ENGINEERING AND TECHNOLOGY

EFFECT OF PREPARATION METHODS ON MORPHOLOGY AND RHEOLOGICAL PROPERTIES OF PLA/CNC NANOCOMPOSITES

M.Sc. THESIS

Burcu ÖZDEMİR

Department of Materials Science and Engineering

Material Science and Engineering Graduate Programme

JULY 2020

ISTANBUL TECHNICAL UNIVERSITY ★ GRADUATE SCHOOL OF SCIENCE ENGINEERING AND TECHNOLOGY

EFFECT OF PREPARATION METHODS ON MORPHOLOGY AND RHEOLOGICAL PROPERTIES OF PLA/CNC NANOCOMPOSITES

M.Sc. THESIS

Burcu ÖZDEMİR
(521171006)

Department of Materials Science and Engineering

Material Science and Engineering Graduate Programme

Thesis Advisor: Assoc. Prof. M. Reza NOFAR

JULY 2020

İSTANBUL TEKNİK ÜNİVERSİTESİ ★ FEN BİLİMLERİ ENSTİTÜSÜ

ÜRETİM YÖNTEMLERİNİN PLA/CNC NANOKOMPOZİTLERİNİN MORFOLOJİK VE REOLOJİK ÖZELLİKLERİNE ETKİSİ

YÜKSEK LİSANS TEZİ

Burcu ÖZDEMİR
(521171006)

Malzeme Bilimi ve Mühendisliği Ana Bilim Dalı

Malzeme Bilimi ve Mühendisliği Programı

Tez Danışmanı: Doç. Dr. M. Reza NOFAR

TEMMUZ 2020

Burcu Özdemir, a M.Sc. student of ITU Graduate School of Science Engineering and Technology student ID 521171006, successfully defended the thesis/dissertation entitled "EFFECT OF PREPARATION METHODS ON MORPHOLOGY AND RHEOLOGICAL PROPERTIES OF PLA/CNC NANOCOMPOSITES", which she prepared after fulfilling the requirements specified in the associated legislations, before the jury whose signatures are below.

Thesis Advisor:	**Assoc. Prof. M. Reza Nofar** Istanbul Technical University	....
Jury Members:	**Prof. F. Seniha Güner** Istanbul Technical University	....
	Prof. Göknur Bayram Middle East Technical University	....

Date of Submission : 12 June 2020
Date of Defense : 22 July 2020

To my family

FOREWORD

I would like to express my deepest gratitude to my supervisor Assoc. Prof. M. Reza NOFAR for his precious guidance, encouragement, and support. It was a great opportunity to be in his undergraduate courses and now to be in his guidance during my master's study.

I would like to thank Prof. Seniha GÜNER, Prof. Gürbüz GÜNEŞ, Prof. Beraat ÖZÇELİK, and Prof. Metin Hayri ACAR for their supports in running experiments in their laboratories, for providing rheometer, compression molding, water bath sonicator, and DSC respectively. I also express my gratitude to Prof. Kürşat KAZMANLI and to all technical and administrative staff of ITU Faculty of Chemical and Metallurgical Engineering for their kind cooperation during this work. I would also like to thank Academic Yonca Alkan for helping in running FTIR experiments and for her kind support in the analysis.

I express my sincere appreciation to Merve GÜÇLÜ, Doğan ARSLAN, Ece GÜLER, Emre VATANSEVER, and Deniz Sema SARUL for their precious friendship, and support as teammates.

I would like to thank Murat RAZİ for his love and support.

Finally, I would like to dedicate my thesis to my family: my mother Nisa ÖZDEMİR, my father Metin ÖZDEMİR, my brother Burak ÖZDEMİR, my little sister, Bahar ÖZDEMİR, and the cute cat members of our family, Gudil and Mutlu. I am very grateful to have them and to feel their love.

July 2020

Burcu ÖZDEMİR
(Metallurgical and Materials Engineer)

TABLE OF CONTENTS

Page

ABBREVIATIONS

PLA	: Polylactide
ABS	: Acrylonitrile butadiene styrene
BC	: Bacterial cellulose
CE	: Chain extender
CHL	: Chloroform
CNC	: Cellulose nanocrystals
CNCFD	: Freeze-dried CNC
CNCSD	: Spray-dried CNC
CNF	: Cellulose nanofibers
CNT	: Carbon nanotube
DMF	: Dimethylformamide
DMSO	: Dimethyl sulfoxide
DSC	: Differential scanning calorimetry
FCNC	: Freeze-dried CNC
GHG	: Global greenhouse gas
H_2SO_4	: Sulphuric acid
HCl	: Hydrochloric acid
HNT	: Halloysite nanotube
LCB	: Long-chain branched
MS	: Magnetic stirrer
NC	: Nanocomposite
PA6	: Polyamide 6
PBAT	: Polybutylene adipate terephthalate
PDLA	: Poly(D-lactic acid)
PEG	: Polyethylene glycol
PET	: Polyethylene terephthalate
PLLA	: Poly(L-lactic acid)
PLM	: Polarized light microscope
PMMA	: Plexiglas 7N
PP	: Polypropylene

PS	: Polystyrene
SCNC	: Spray-dried CNC
SEM	: Scanning electron microscope
TEMPO	: 2,2,6,6-tetramethylpiperidin-1-yl)oxyl
THF	: Tetrahydrofuran
TNPP	: Tris(nony1- phenyl) phosphite
WS	: Water bath sonicator

SYMBOLS

G'	**:** Storage modulus
G''	**:** Loss modulus
G*	**:** Complex modulus
t	**:** Time
λ	**:** Relaxation time
η	: Steady-shear viscosity
η'	**:** Real part of the complex viscosity
η″	**:** Imaginary part of the complex viscosity
η*	**:** Complex viscosity
tan δ	**:** Loss tangent
δ	**:** Phase angle
ϕ	**:** Volume fraction
ϕ_c	**:** Critical volume fraction of percolation network
σ	: Tensile strength
$\boldsymbol{\gamma}$	: Strain amplitude
ε	**:** Engineering (nominal) strain
ω	**:** frequency of oscillation

LIST OF TABLES

Page

LIST OF FIGURES

EFFECT OF PREPARATION METHODS ON MORPHOLOGY AND RHEOLOGICAL PROPERTIES OF PLA/CNC NANOCOMPOSITES

SUMMARY

Bio-based and biodegradable polymers are produced from biomass which is renewable by cultivation. The biopolymers degrade in natural environments decomposing into non-toxic substances. Moreover, during the cultivation process of raw material, biomass, of biopolymers CO_2 is consumed and the amount of CO_2 emission from the life cycle of biopolymers is much lower compared to that of petroleum-based polymers. Poly(lactic acid) or polylactide, PLA, is both Bio-based and biodegradable polyester-based polymer. It has comparable mechanical and physical properties with commonly used petroleum-based polymers. Thus, it is considered as a candidate to be replaced with widely used petroleum-based polymers. However, PLA has some drawbacks which limits is processability and applications. The shortcomings of PLA are slow crystallization kinetics and poor rheological properties. They result in slow crystallization rate, low thermal properties, low melt strength hence limited processability. Studies have shown that making nanocomposites of PLA by incorporation of nanoparticles into the PLA matrix could enhance its crystallization kinetics and viscoelastic properties. Cellulose nanocrystals (CNC) as being a biodegradable and Bio-based polymer has outstanding mechanical and thermal properties. Studies have shown that making PLA/CNC nanocomposites improve the thermal, crystallization, and rheological properties of PLA by preserving its biodegradable and Bio-based characteristics. However, the hydrophilic character of CNCs challenges its homogeneous dispersion in the hydrophobic PLA matrix which is crucial to improve PLAs properties, especially at low percolation concentrations.

Studies have shown that without the use of any modification, the melt mixing process is not successful to disperse CNCs since the shear force applied during the process is not enough to break the strong hydrogen bonds between CNCs. Although it is not industrially feasible as melt mixing, it is possible to deagglomerate CNCs and to obtain good dispersion by solution casting method. The solution casting method involves the dispersion of CNC and PLA in proper solvents by using a water bath sonicator, tip sonicator, or magnetic stirrer followed by casting the mixture and followed by evaporation of the solvent. Studies have shown that the application of solution casting greatly differs in the instrument, the sequence of application, duration, PLA type, CNC type, and solvent type.

This study aims to investigate the effect of preparation method, solvent, and CNC type on CNC dispersion thus the rheological and thermal properties of PLA/CNC nanocomposites. Low molecular weight and highly crystallizable PLA and two types of CNC were used to make nanocomposites. CNCs differ in their drying processes: spray-dried CNC (SCNC) in powder form and freeze-dried CNC (FCNC) in flake form. The rheological analysis was used as a characterization method to analyze the CNC dispersion. As the first step of the study, four different solvents were used to prepare nanocomposites of PLA/SCNC and PLA/FCNC at a fixed amount of CNC (3

wt.%). The solvents are tetrahydrofuran (THF), chloroform (CHL), dimethylformamide (DMF), and dimethyl sulfoxide (DMSO). The preparation method is followed as first dispersing CNC in the solvent using a bath sonicator for 2 hours at room temperature. Then PLA was added to the CNC solvent mixture and mixed with a magnetic stirrer for 2.5 hours (4 hours for DMSO). The temperature during magnetic stirring was selected according to the type of solvent. It was 55^{o}C for THF and CHL since PLA is soluble in those solvents. PLA is not soluble in DMF and DMSO in room temperature thus, the temperature was increased above the glass transition temperature of PLA and it was 75^{o}C for DMF and 95^{o}C for DMSO (gradually increased). After the mixing process, the solvent containing PLA and CNC were casted into petri dishes and left to dry for 2 days under the fume hood followed by vacuum drying at 85^{o}C for 2 days. After two days of vacuum drying, the films were ground with a coffee grinder and powders were further dried for 2 days under vacuum at 85^{o}C.

Nanocomposites prepared with DMSO revealed the highest improvement in rheological properties followed by DMF. THF resulted in a slight increase in total compared to neat PLA due to its much lower dielectric constant. However, nonpolar CHL couldn't deagglomerate CNC thus nanocomposites prepared with CHL revealed much lower viscoelastic properties than neat PLA. PLA/SCNC nanocomposites revealed slightly higher improvement in DMF and DMSO however, the difference was insignificant in THF and CHL.

To investigate the effect of the preparation method, DMSO was chosen. Both PLA/SCNC and PLA/FCNC nanocomposites were prepared with varying water sonication times and sequences. In total four different methods were compared: 0WS-4MS, 2WS-4MS, 4WS-4MS, and 2WS-4MS-2WS. As an example, 2WS-4MS means 2 hours of water sonication followed by 4 hours of magnetic stirring. The highest improvement achieved with PLA/SCNC by the 4WS-4MS method. The increased water sonication time increased the dispersion of CNC however, the other methods displayed similar improvements. Moreover, since the CNC was in powder form only four hours of vigorous stirring at elevated temperature resulted in the second best improvement. It could be due to the DMSO's higher ability to disperse CNCs even without a bath sonicator. In the case of PLA/FCNC, 0WS-4MS revealed the highest improvement. Since the FCNC is in flake form the bath sonication at room temperature was not enough to disperse them. The method 2WS-4MS-2WS revealed the second-best result and better than the 2WS-4MS method. In the first method after 4 hours of magnetic stirring the PLA/FCNC and solvent mixture is placed in the bath sonicator when it was still hot. Thus, the high temperature of the solvent could aid the further dispersion of FCNC.

To see the effect of CNC content (1, 2, 3, and 5 wt.%) it was decided to continue with SCNC since the results were more consistent. PLA/SCNC nanocomposites with DMSO by using 2WS-4MS method with varying CNC contents were prepared. To compare the results, nanocomposites with DMF was also prepared. PLA/SCNC nanocomposites with 5 wt.% revealed the highest improvement in rheological properties. In nanocomposites prepared with DMF, except PLA/SCNC1, nanocomposites revealed increased rheological properties. For the NCs prepared with DMSO, this increase was more pronounced. The rheological percolation threshold of NCs prepared with DMF and DMSO was calculated by employing the empirical power-law equation and found to be 1.59 and 0.44 wt.% respectively. The percolation concentration again revealed that DMSO is much more effective to obtain high quality dispersion of CNC.

The apparent yield stress of NCs were calculated by employing Modified Herschel-Bulkley equation. NCs prepared with DMSO revealed much higher apparent yield stress values compared to ones prepared with DMF. Both the modified cole-cole plot analysis and Herschel-Bulkley plots of NCs revealed solid like behaviour started at percolation concentration.

The isothermal DSC analysis of NCs revealed that due to better dispersion of CNC with DMSO, the NCs prepared with DMSO exhibit faster crystallisation kinetics. However, no significant change was observed between FCNC and SCNC. The neat PLA processes with DMSO revealed faster crystallisation compared to one with DMF. This could be due to higher plasticizing effect of DMSO since it is expected that higher amount of DMSO is remained in samples. Similarly, NCs prepared with different CNC content revealed that crystallisation time is close to that of neat PLAs. Those, results shows the effect of remaining solvent on NCs crystallisation.

ÜRETİM YÖNTEMLERİNİN PLA/CNC NANOKOMPOZİTLERİNİN MORFOLOJİK VE REOLOJİK ÖZELLİKLERİNE ETKİSİ

ÖZET

Biyobazlı ve biyobozunur polimerler yenilenebilir biyokaynaklardan üretilmektedirler. Bu biyopolimerler doğal ortamlarda toksik olmayan bileşenlere ayrılabilirler. Ayrıca, hammaeddeleri olan biyokütleler yetiştirilme esnasında CO_2 tükettikleri için biyopolimerlerin ömür boyu CO_2 salınımları petrol bazlı polimerlere göre çok daha azdır. Biyopolimerlerin bir türü olan poli(laktik asit) ya da polilaktit (PLA) polyester bazlı biyobazlı ve biyobozunur termoplastik bir polimerdir. PLA, yaygın olarak kullanılan petrol bazlı polimerlerle rekabet edebilecek mekanik ve fiziksel özelliklere sahiptir. Bu sebeple, PLA endüstride ve emtia uygulamalarında yaygın olarak kullanılan petrol bazlı polimerlerin yerini almaya uygun bir aday olarak değerlendirilmektedir. Ancak, söz konusu karşılaştırılabilir mekanik ve fiziksel özelliklerine rağmen PLA'nın bazı dezavantajları mevcuttur. Bu dezavantajlar PLA'nın işlenebilme ve dolayısıyla uygulanabilmesini kısıtlamaktadır. PLA'nın dezavantajları şu şekilde özetlenebilir: yavaş kristalizasyon kinetiği ve düşük viskoelastik (reolojik) özellikler. Bu özellikler, PLA'nın kristalleşebilmesini kısıtlamakta ve düşük eriyik mukavemetine sebep olmaktadır.

PLA'nın kristalizasyon kinetiğini ve reolojik özelliklerini iyileştirmek adına farklı yöntemler mevcuttur. Bunlardan yaygın olarak çalışılanları: zincir uzatıcı kullanımı, söz konusu özellikler bakımından daha üstün başka bir polimerle harmanlanması ve nano-parçacıklar kullanarak nanokompozit yapılmasıdır. Söz konusu çalışmalar karşılaştırıldığında, nanoparçacıkların kristalizasyon için çekirdeklenme noktası olarak davranmasıyla PLA'nın kristalizasyon kinetiğini iyileştirdiği ve ayrıca homojen bir şekilde dağılmış olan nanoparçacıklar ile PLA moleküllerinin etkileşimi sayesinde reolojik özelliklerini de iyileştirdiği görülmüştür. Bu kapsamda çeşitli türde nanoparçacıklar kullanılmaktadır. Bunların arasında, biyobazlı ve biyobozunur olan selüloz nanokristalleri (CNC) yaygın olarak kullanılan nanoparçacıklarla karşılaştırılabilir mekanik özellikleri, düşük yoğunluğu ve yüksek yüzey/hacim oranı ile öne çıkmaktadır. Çalışmalar, PLA/CNC nanokompozitlerinin PLA'nın biyobazlı ve biyobozunur özelliklerinden ödün vermeden, PLA'nın dezavantajlarını iyileştirdiğini göstermiştir.

Yüksek molekül ağırlığına sahip selüloz biyopolimeri, amorf ve kristal bölgeler içeren selüloz mikrofibrillerinden oluşur. Selüloz nanokristalleri ise selüloz mikrofibrillerindeki amorf bölgelerin asit ile hidrolize edilmesiyle elde edilir. CNC üretimi ticari olarak sülfürik asit hidrolizi ile yapılmaktadır. CNC'nin sülfürik asit ile hidrolizi esnasında yüzeyine negatif olarak yüklü sülfat yarı ester grupları yerşleşir. Bu gruplar, CNC yüzeyinin negatif olarak yüklenmesine sebep olur ve CNC'ye hidrofilik karakter kazandırır. CNC hidroliz işleminden sonra kurutmaya tabi tutulur. Kurutma işleminin amacı sulu CNC çözeltisinden suyun uzaklaştırılarak hidrofobik polimer ile işlenebilir hale getirmektedir. İki tür kurutma işlemi vardır: sprey kurutma

ve dondurulmuş halde kurutma. Sprey kurutulmuş CNC (SCNC) toz formunda elde edilir ve dondurularak kurutulmuş CNC (FCNC) pul formundadır.

PLA/CNC nanokompozitlerinin hazırlanması temel olarak iki yöntemle gerçekleştirilebilir: eriyik karıştırma ve çözelti dökümü yöntemleri. Çalışmalar eriyik karıştırma yönteminin hidrofilik CNC'yi hidrofobik PLA içerisinde homojen olarak dağıtmada başırlı olmadığını göstermiştir. Sebebi, eriyik karıştırma yöntemi sırasında uygulanan kesme gerilmelerini CNC partikülleri arasındaki güçlü hidrojen bağlarını kıracak kadar güçlü olmamasıdır. Eriyik karıştırma yöntemi her ne kadar endüstriyel olarak uygulanmaya ve seri üretime uygun olsa da yapılan çalışmalar CNC'nin PLA içerisinde topak olarak kaldığını göstermiştir. Yalnızca bir çalışmada, aslında ilaç üretim ve seramik sektörlerinde kullanılan bir yöntem olan sprey dondurularak kurutma (spray freze drying) ile kurutulmuş CNC, PLA matris içerisinde eriyik karıştırılma yöntemi ile başarılı bir şekilde dağıtılmıştır.

PLA/CNC üretmek için kullanılan bir diğer yöntem olan çözelti döküm yöntemi ise PLA uygun bir çözücüde çözülmesi ve CNC'nin ise uygun bir çözücüde disperse edilmesine dayanır. Yapılan çalışmalar bu yöntemi kullanarak CNC'nin PLA matris içerisinde homojen olarak disperse edilebildiğini göstermiştir. Çözelti döküm yöntemi parametrelerinin CNC'nin dispersiyonunu etkilediği çeşitli çalışmalarda görülmüştür. Malzeme türü ile alakalı olarak güncel bir çalışma düşük molekül ağırlığına sahip yarı-kristal PLA'nın, çözelti döküm yöntemi ile hazırlanan PLA/CNC nanokompozitler için en uygun matris olduğunu göstermiştir. Düşük molekül ağırlığına sahip yarı kristal PLA içerisinde CNC kristalizasyon için çekirdeklenme noktası olarak davranmakta, matris içerisinde disperse olmuş CNC etrafında oluşmaya başlayan kristaller CNC'yi bulunduğu yere sabitleyerek CNC'nin matris içerisinde tekrar birleşmesini önlemektedir. SCNC ve FCNC'nin etkileri ile alakalı yapılan çalışmalar eriyik karıştırma yöntemi ile sınırlı kalmıştır. Ayrıca, çözelti döküm yönteminde kullanılan karıştırma yöntemleri (su banyosu, uç sonikatörü (tip sonicator)), bu yöntemlerin süresi ve sırası açısından farklıdır.

Bu çalışmanın amacı, çözelti döküm yöntemi parametrelerinin CNC'nin dispersiyonu üzerindeki etkisini ve dolayısıyla PLA/CNC nanokompozitlerinin kristalizasyon ve reolojik özelliklerine etkisini incelemektir. CNC'nin dispersiyonunu ve nanokompozitlerin viskoelastik özelliklerini analiz etmek adına reoloji karakterizasyon için kullanılmıştır.

Bu kapsamda, tüm çalışma boyunca düşük molekül ağırlığına sahip ve kristallenebilirliği yüksek tek bir tür PLA matris olarak kullanılmıştır. Hem PLA-SCNC hem de PLA/FCNC nankompozitler dört farklı türde çözelti kullanarak hazırlanmış bu sayede çözeltinin ve CNC kurutma türünün etkileri araştırılmıştır. Kullanılan çözeltiler sırasıyla şu şekildedir: tetrahidrofuran (THF), kloroform (CHL), dimetil formamid (DMF) ve dimetilsülfoksit (DMSO). Üretim aşamaları şu şekildedir: öncelikle CNC çözelti içerisinde disperse olabilmesi için su banyosu sonikatöründe 2 saat boyunca (oda sıcaklığında) bekletilmiş, daha sonra CNC solvent karışımı manyetik karıştırıcıya yerleştirilmiş, daha sonra PLA eklenmiş ve 2.5 saat (DMSO için 4 saat) boyunca yüksek hızda karıştırılmıştır. Manyetik karıştırma sıcaklığı THF ve CHL için 55^{o}C, DMF için 75^{o}C ve DMSO için (kademeli olarak artırarak) 95^{o}C'dir. Karıştırma sıcaklığı DMF ve DMSO için özellikle camso geçiş sıcaklığının üzerinde seçilmiştir. Karıştırma sonrası, karışımlar petri kaplarına dökülerek 2 gün çeker ocak altında oda sıcaklığında bekletilmiş, 2 gün film halinde vakum altında 85^{o}C'de bekletilmiştir. 2 gün vakum fırında bekleyen filmler kahve öğütücü yardımı ile toz haline getirilerek 2 gün daha vakum altında 85^{o}C'de bekletilmiştir. DMSO'nun kaynama noktası yüksek olduğu için film halinde bekleme süresi DMSO ile üretilen nanokompozitlerde 5 gün olarak uygulanmıştır.

Reolojik analizler sonucunda, viskoelastik özelliklerdeki en çok iyileşme DMSO ile üretilmiş nanokompozitlerde görülmüştür. Ardından, ikinci en iyi iyileşme DMF ile üretilenlerde görülmüştür. Bunun sebebi, DMSO ve DMF'in yüksek dielektirik sabiti ve polar yapıları sayesinde CNC'nin dispersiyonunda daha etikili olmuş olmalarıdır. Öte yandan, polar yapıda olmasına rağmen, THF'li nanokompozitlerde iyileşme çok daha az olmuştur. Bunun sebebi THF'in çok daha düşük dielektrik sabitine sahip olması olabilir. Kloroform ile hazırlanan nanokompozitlerin viskoelastik özellikleri ise katkısız PLA'nın özelliklerinden bile daha düşük çıkmıştır. Sebebi, apolar kloroformun CNC'yi disperse edememesi ve CNC'nin büyük yığınlar halinde yapıda kalmasıdır. CNC türleri karşılaştırıldığında, SCNC'nin FCNC'ye göre daha iyi disperse olduğu, bu farkın DMSO ve DMF'te daha belirgin olduğu ancak, THF ve CHL için aradaki farkın çok az olduğu görülmektedir.

Üretim metodunun etkileri DMSO kullanılarak PLA/SCNC ve PLA/FCNC nanokompozitleri hazırlanarak araştırılmıştır. Bu kapsamda dört farklı üretim metodu karşılaştırılmıştır. Metotlar, su banyosu süresi ve sırası bakımından farklı olmak üzere şu şekildedir: 0WS-4MS, 2WS-4MS, 4WS-4MS ve 2WS-4MS-2WS. Örnek olarak 2WS-4MS şu anlama gelmektedir: 2 saat su banyosu (WS) ardından 4 saat manyetik karıştırıcı. Öncelikle, en yüksek iyileşme 4WS-4MS yöntemi ile üretilen PLA/SCNC nanokompozitinde görülmüştür. PLA/SCNC nanokompozitlerine bakıldığında sonikasyon süresinin artması SCNC'nin dispersiyonunu arttırmıştır. Ancak, ikinci en yüksek iyileşme 0WS-4MS yöntemi ile elde edilmiştir. Bu durumun sebebi, toz formunda olan CNC'nin yüksek sıcaklıkta ve yüksek karıştırma hızında polar yapıda ve yüksek dielektrik sabite sahip DMSO içerisinde kolaylıkla disperse olmuş olmasıdır. PLA/FCNC nanokompozitler karşılaştırıldığında, en çok iyileşme 0WS-4MS metodunda görülmüştür. Su banyosu oda sıcaklığında gerçekleştiğinden, pul formundaki büyük FCNC yığınlarını disperse etmekte başarılı olamamıştır. İkinci en iyi sonuçları veren 2WS-4MS-2WS yönteminin başarılı olmasının sebebi, 4 saatlik manyetik karıştırma işleminden sonra 2 saat daha su banyosuna koyulduğunda karışımın hala çok sıcak olması ve bu sıcaklığın FCNC'nin dispersiyonunu kolaylaştırmasıdır.

Sonuç olarak, en etkili iyileşme DMSO kullanılarak görülmüş ve toz formundaki SCNC kullanılan PLA nanokompozitlerinin viskoelastik özellikleri daha çok iyileşmiş ve daha tutarlı sonuçlar elde edilmiştir. Çalışmanın devamında, CNC oranının etkisini incelemek adına DMF ve DMSO kullanılarak PLA/SCNC nanokompozitleri farklı CNC yüzdeleri (ağırlıkça % 1, 2, 3 ve 5) ile hazırlanmıştır. DMSO için 2WS-4MS yöntemi ve DMF için ise 2WS-2.5MS yöntemleri kullanılmıştır. DMF ile hazırlanan numunelerde PLA-SCNC1 hariç nanokompozitlerde CNC oranı arttıkça reolojik özelliklerin de iyileştiği görülmüştür. PLA-SCNC1'in ise neat PLA'ya göre daha kötü reolojik özellik göstermesi DMF'in düşük oranlarda CNC'yi disperse edemediğinden kaynaklanmış olabilir. DMSO ile hazırlanan nanokompozitlerde ise ağırlıkça %1 SCNC kullanımında bile reolojik özelliklerde çok etkili iyileşmeler görülmüştür. Nanokompozitlerin perkolasyon konsantrasyonu deneysel üstel yasayı (empirical power-law equation) kullanarak hesaplanmıştır. Perkolasyon konsantrasyonu DMF ile hazırlanan numelerde % 1.59 ve DMSO ile hazırlananlarda % 0.44 olarak hesaplanmıştır. Nanokompozitlerin akma gerilmesi (apparent yield stress) Modified Herschel-Bulkley denklemi kullanarak hesaplanmış ve DMSO ile üretilen numunelerde DMF ile üretilenlere göre çok daha yüksek sonuç alınmıştır. Ayrıca, akma gerilmesinin CNC oranı ile beraber arttığı görülmüştür.

Nanokompositlerin eşısıl olmayan DSC analizlerine göre DMSO ile üretilmiş olanlar DMF'e göre daha hızlı kristalizasyon kinetiği göstermiştir. FCNC ve SCNC'nin kristalizasyona etkisi arasında kayda değer bir fark görülmemiştir. Farklı oranlarda SCNC içeren nanokompozitler saf PLA ile karşılaştırıldığında benzer kristalizasyon kinetiği sergilemişler ve bunun sebebi olarak uzaklaştırılamamış çözücünün plastikleştirici etkisi olduğu düşünülmüştür.

1. INTRODUCTION

Bioplastics stand out as a sustainable alternative to conventional plastics since they have several advantages. Source of bioplastics is biomass which is a renewable source and consumes CO_2 during cultivation. Compared to petroleum-based counterparts bioplastics' CO_2 emission is much lower [1]. The amount of global production of bioplastics in 2018 was around 2.11 million tones and it is expected to increase further [2, 3]. Among those bioplastics, poly(lactic acid) or polylactide (PLA) as being both Bio-based and biodegradable becomes prominent as a driver for growth. PLA is an aliphatic polyester-based bioplastic that is both biodegradable, bio-based, and biocompatible. Monomers of PLA could be lactic acid or lactide which can be produced from non-toxic and annually renewable sources such as corn sugar, potato, and sugar cane [4, 5]. In addition to its eco-friendly and biocompatible characteristics, PLA has comparable mechanical and physical properties to those of polystyrene (PS) and polyethylene terephthalate (PET) and it is considered as a candidate to be replaced with fossil-based polymers [6]. PLA based articles are already used in various applications and it is assumed that PLAs production rate will continue to increase [7, 8]. However, PLA suffers from some drawbacks that limit its processability and applications. Those limitations are low T_g (or low transition temperatures) which limits its service temperature and results in narrow processing window [9-12]; slow crystallization kinetics that limits processability notably in productions with fast cycles which results in a low amount of crystallinity (negatively affects mechanical, thermal and barrier properties), and poor melt strength (which greatly influence the processability) [6]; and poor rheological (or viscoelastic) properties that limit processability and application which also results in poor melt strength [13, 14].

Different methods such as copolymerization, blending with other polymers, plasticizing, chemical modification, use of chain extender, and composite-making have been employed to overcome the aforementioned drawbacks of PLA [5, 6, 14, 15]. Among those methods, making nanocomposites of PLA by using nanosized particles as reinforcement proved to be an effective way which enables to tailor the properties of PLA for a wide range of applications [14, 16]. The use of nanosized reinforcements not only improves the mechanical, thermal, and barrier properties but also improves the rheological properties and enhances the crystallization kinetics by acting as nucleating points which in the end, improve the processability and application of PLA [5, 14, 17]. Different kinds of nanosized fillers have been widely incorporated into PLA such as clay-based nanofillers (sepiolites, layered silicates (montmorillonite), and halloysite nanotube (HNT) [18, 19], carbonaceous nanofillers (carbon nanotube (CNT), carbon nanofiber (CNF), and graphene) [20, 21], silicon-based nanoparticles (nano-silica and POSS) [14, 22], metal and metal oxide nanoparticles (silver, titanium dioxide, etc) [23], and cellulose-based nanofillers (cellulose nanocrystals (CNC), cellulose nanofibers (CNF), and bacterial cellulose (BC)) [16, 23, 24]. Cellulose nanocrystals (CNC) stand out among other filler with its higher mechanical properties, low density, and the potential for surface modification meanwhile being renewable, Bio-based, and biodegradable [25-27]. Studies shown that PLA/CNC nanocomposites successfully improved the rheological and thermal properties of PLA [28-30].

PLA nanocomposites (NCs) are mainly produced with two main methods: melt mixing and solution casting. It is important to achieve a good level of dispersion in PLA however, the sulfate half ester groups ($O\text{-}SO^{3-}$) are on the CNC surface make its surface negatively charged thereby, make the dispersion of hydrophilic CNC in hydrophobic polymer quite challenging [25, 27]. Bagheriasl et al. [28] prepared PLA/CNC nanocomposites with both melt mixing and solution casting to compare the effect of the method on CNC dispersion. Since the shear forces applied during the melt mixing process are not enough to break down the hydrogen bonds between CNC particles, the deagglomeration of CNC in PLA couldn’t be achieved with the melt mixing process [16]. The solution casting method was found to be effective to achieve a good level of dispersion. Bagheriasl et al. [31] prepared PLA/CNC nanocomposites by first preparing masterbatches through solution casting then diluted with TSE. The method was found to be effective compared to the direct melt mixing process. Vatansever et al. [17] compared the effect of PLAs molecular weight and crystallinity on rheological properties and crystal structure on PLA/CNC nanocomposites produced by solution casting. The rheological analysis revealed that the dispersion of CNC in crystalline PLA was the best in semi-crystalline low molecular weight PLA.

Since CNCs are produced from the acid hydrolysis of cellulose the final product is an aqueous suspension that is not suitable to incorporate into hydrophobic media especially in polymer nanocomposite production. Thus, CNC aqueous suspension is objected to a drying step to obtain dry CNC. There are two methods namely spray drying and freeze-drying that resulted in CNC in powder and flake form, respectively [26]. Khoshkava and Kamal [32] compared the effect of the CNC drying method in PLA/CNC nanocomposites by using the melt mixing method. Khoshkava and Kamal [33] compared the dispersion of the spray-dried (CNCSD) and spray freeze-dried CNC (CNCSFD) in the PLA matrix using a melt mixing method. They prepared spray freeze-dried CNC (CNCSFD) by using spray freeze-drying method which is commercially used in the pharmaceutical and ceramic industry. They achieved a good level of dispersion due to the highly porous structure of CNCSFD enabled infiltration of polymer into CNC particles.

Studies have shown the success of the solution casting method to obtain a good level of CNC dispersion that resulted in improved rheological and thermal properties. The objective of this study is to further investigate the effect of preparation methods, the effect of solvent, and drying type of CNC. To do that four types of solvents namely tetrahydrofuran (THF), chloroform (CHL), dimethylformamide (DMF), and dimethyl sulfoxide (DMSO) were used to prepare both PLA/SCNC and PLA/FCNC nanocomposites. Thereby, the effect of SCNC and FCNC was also compared. After the selection of the best solvent, four different preparation methods were used to prepare PLA/SCNC and PLA/FCNC nanocomposites. The preparation methods differ in water bath sonication time and sequence. By selecting the most effective method, CNC, and solvent PLA/CNC nanocomposites were prepared with different amounts of CNC contents. The rheological analysis was used to analyze the viscoelastic properties of nanocomposites and to investigate the quality of dispersion of CNC. Nonisothermal crystallization was also investigated with differential scanning calorimetry (DSC).

2. BIOPLASTICS

2.1 Need for Bioplastics and Their Classification

The use of plastics has steadily increased in the last half-century and 359 million tons of plastics were produced in 2018. Today, for the production of plastics almost 6% of the world's fossil source is used as raw material and energy in half. That amount is estimated to increase to 20% in 2050 by considering similar rates of use. Meanwhile, the share of the plastic industry in the global annual carbon budget is also expected to increase from 1% to 15%. On the other hand, in global almost 150 million tons of post-consumer plastic waste is generated every year and only 2% of this amount is recycled. During recycling or from the landfill sites chemical additives in plastics that are hazardous for organisms also leak into soil or groundwater. Moreover, the amount of global plastic waste that ends up in the ocean is estimated to be 5 to 13 million tons [1, 8, 34]. Due to small recycling rates, huge carbon emission, and limited source of petroleum-based plastics, plastics produced from renewable sources become prominent to provide sustainable production [34].

Bioplastics stand out as a sustainable alternative to conventional plastics since they have several advantages. Figure 2.1 summaries the life cycle of bioplastics. Source of raw material of bioplastics is biomass which is a renewable source. Plants used as raw material for bioplastics could be replaced annually. Moreover, during the cultivation process the source of bioplastics consume CO_2 thus, reduces the global greenhouse gas emissions (GHG). Post-consumer waste of bioplastics, if it is biodegradable, would decompose into the water, carbon dioxide, and compost which are natural substances. This residue can again be used for plant growth. Moreover, the degradation time of bioplastics is too short as compared to fossil-based ones [1]. Bioplastics are defined under three different categories based on their source and degradation which is shown in Figure 2.2. Plastics are first divided as Bio-based (renewable source) and fossil-based (unrenewable source) then, as biodegradable and nonbiodegradable. Thus, bioplastics could be classified as:

1. Bio-based and biodegradable (e.g. PLA, PHA, PBS),
2. Bio-based and nonbiodegradable (e.g. PE, PET, PA, PTT),
3. Fossil based and biodegradable (e.g. PBAT, PCL).

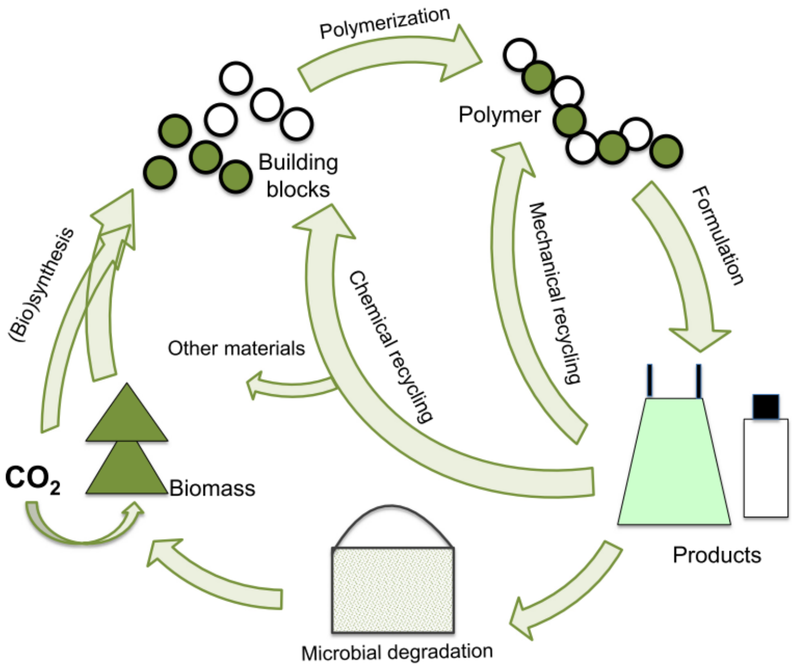

Figure 2.1: The life cycle of bioplastics [1].

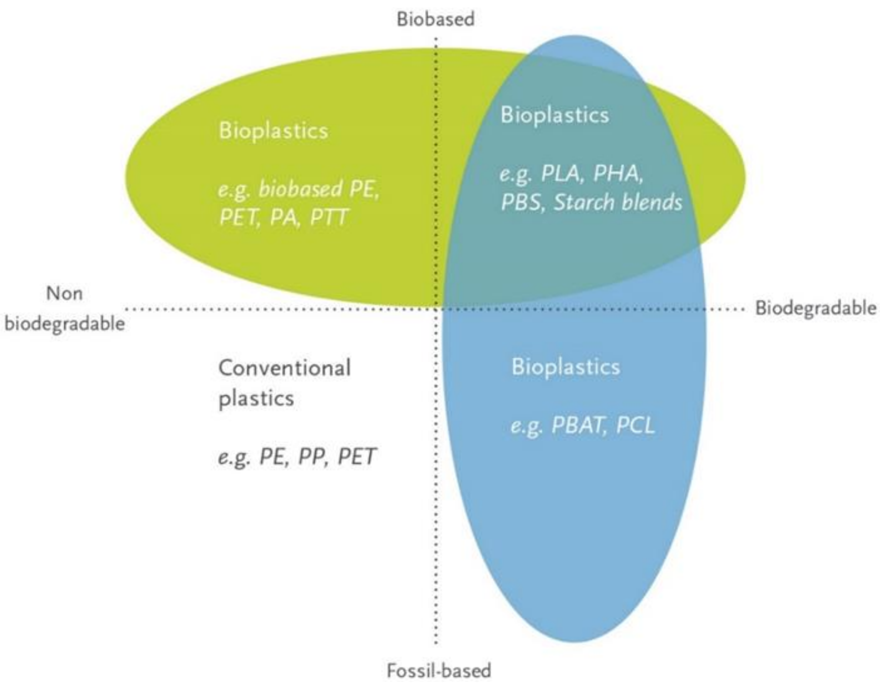

Figure 2.2: Classification of plastics [35].

2.2 Global Production and Applications of Bioplastics

The amount of global production of bioplastics in 2018 was around 2.11 million tones which represents almost one percent of global plastics production. The global production volume of bioplastics in 2018 is shown in Figure 2.3 according to material type. Today, those bioplastics are commercially used in several industries such as packaging, agriculture, consumer electronics, automotive, and household appliances. Among these areas packaging industry used 65% of the global production in 2018. Well-known automotive brands also use bioplastics in different applications. As an example, bio-based polyesters, bio-based PET, and PLA blends are used in Toyota. Headliners, sun visors and floor mats of Pirius and SAI models are bioplastics [2, 3].

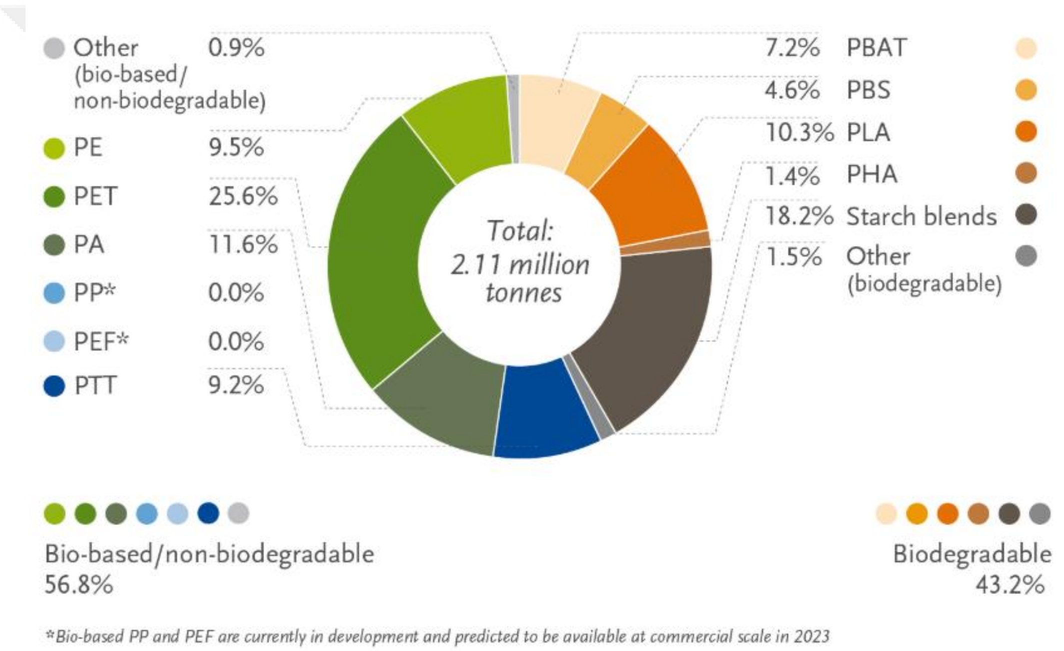

Figure 2.3: Global bioplastics production, 2018 [36].

Among those bioplastics, PLA (polylactic acid) as being both Bio-based and biodegradable becomes prominent as a driver for growth. Since PLA has comparable mechanical and barrier properties and it is considered as a candidate to be replaced with PS (polystyrene), PP (polypropylene), and ABS (acrylonitrile butadiene styrene). Thus, 60% of growth is expected for its production from 2018 to 2023 [1].

Last decades, PLA has been commercially used in various applications. The automotive industry uses PLA-based parts in automobiles as shown in Figure 2.4a. PLA-based packages are used in Europe and North America since PLA is suitable for

EU and USA’s food-grade requirements due to its Bio-based and biodegradable characteristics. A commercial example of PLA based water bottle is shown in Figure

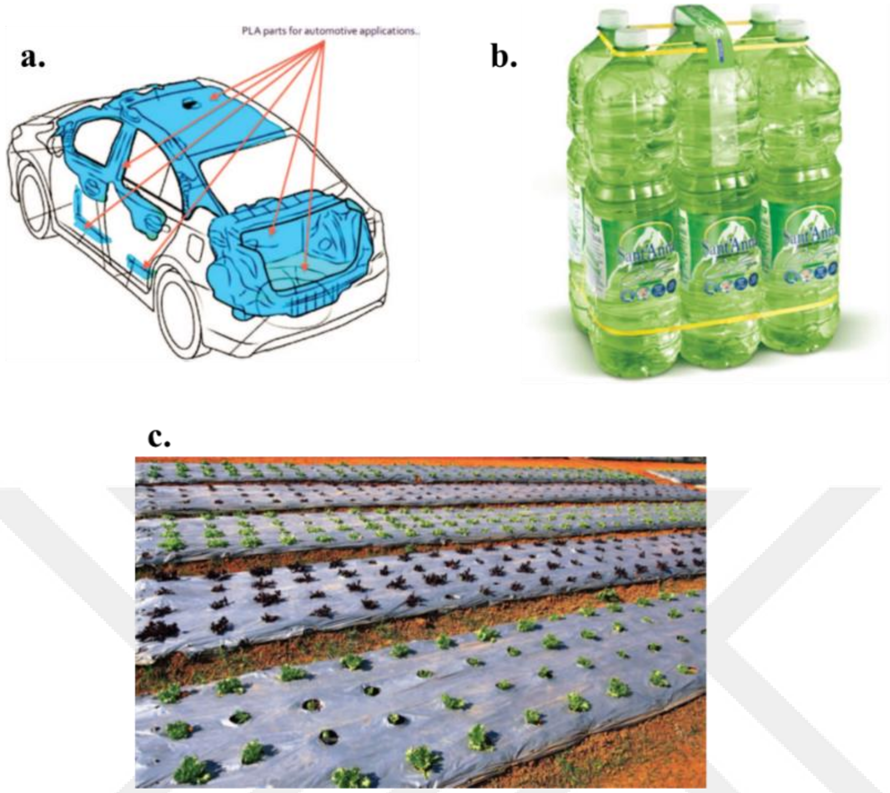

Figure 2.4: Examples of PLA-based products in different industries: a. automotive industry, b. packaging, and c. agriculture as mulch films [7].

2.4b. PLA products also utilized in agriculture as mulch films which are thin plastic films to escalate the ripening of crops, conserve moisture and protect corps from fungus and insects. An example of mulch film is shown in Figure 2.4c. Well-known brands used PLA products in electronic devices such as external Shell of Walkman (Sony, 2001), case of remote control and phone (Samsung and Toshiba), CD/DVDs case (Sanyo), Notebook case (Fujitsu and PEGA) and also some interior parts of copying machines (Fuji-Xerox) [7].

3. POLYLACTIDE (PLA)

Poly(lactic acid), poly(lactide) or PLA is a bioplastic that is both biodegradable and bio-based aliphatic polyester. Monomers of PLA could be lactic acid or lactide which can be produced from non-toxic and annually renewable sources such as corn sugar, potato, and sugar cane [4, 5]. PLA has many advantages over other bioplastics. It is not only bio-based but also biodegradable, recyclable, and compostable. The biocompatibility of PLA is another outstanding feature, especially for biomedical applications. Degradation products of PLA are non-toxic which makes it a good candidate for the biomedical application and food packaging industry. It can be processed with injection molding, film extrusion, blow molding, thermoforming, fiber spinning, and film-forming [5, 35]. Moreover, from cradle to grave amount of CO_2 emission of PLA production is negative which means it consumes more CO_2 than the amount it emits during the production. That is because the plants used as a source of lactic acid consume CO_2 during the cultivation process. It is also stated that the net amount of carbon dioxide emission including the emission from the composting process will be still less than the emission number of others [35].

3.1 Synthesis and Molecular Structure

PLA is produced from the polymerization of lactic acid which is an elementary form of hydroxyl acid. Repeating unit of PLA, lactic acid, occurs in two optically configurations which are L(+) and D(-) isomers with an asymmetric carbon that is shown in Figure 3.1. Lactide dimer is also shown in figure 3.1 in the form of DD-lactide, LL-lactide, or LD-lactide (meso lactide). There are two different production methods for PLA which are shown in Figure 3.2. Polycondensation from a lactic acid monomer or ring-opening polymerization (ROP) from lactide dimer. The ones produced by polycondensation of lactic acid are called poly(lactic acid) while the ones obtained by ROP of lactide are called poly(lactide) still, they are commonly referred to as PLA. When it was discovered in 1932 by Carothers (at Dupont), PLA was produced by exposing lactic acid to high temperatures under vacuum meanwhile evacuating the condensed water. However, that process has only enabled the production of low molecular weight PLA. Today, although the polycondensation method is less expensive, commercial high molecular weight PLA is produced by ring-opening polymerization of lactide dimer, since water is formed as a by-product and it is difficult to obtain a solvent-free product by polycondensation [5, 6, 15, 36].

It is possible to obtain homopolymers of PLA through polycondensation from L-lactic acid or D-lactic acid, which are stated as PLLA (poly(L-lactic acid)) and PDLA (poly(D-lactic acid)), respectively. Those homopolymers could also be produced by ring-opening polymerization of LL- or DD-dimers. Nonetheless, since it is hard to obtain pure PLLA and PDLA homopolymers and production is much expensive, copolymer PLAs based on L- and D-lactide are commercially used. Commercial PLA is obtained by the ring-opening polymerization of L-lactide and LD-lactide dimers which are also shown in the same figure [14, 37].

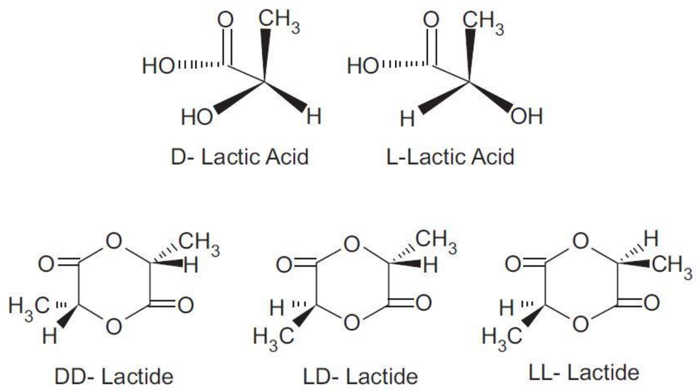

Figure 3.1: Stereochemistry of Lactic Acid and Lactide [6].

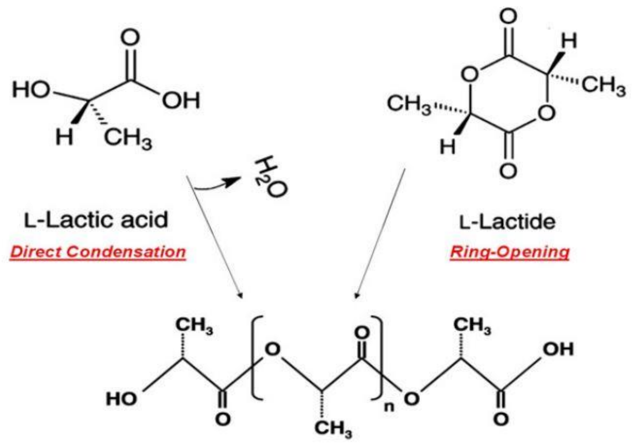

Figure 3.2: Polymerization of PLA through polycondensation from Lactic acid and ring-opening polymerization from Lactide dimer [6].

3.2 Mechanical Properties

PLA stands out among the other biopolymers with its remarkable mechanical and physical properties. In addition to its eco-friendly and biocompatible characteristics, PLA has comparable properties to those of polystyrene (PS) and polyethylene terephthalate (PET) and it is considered as a candidate to be replaced with fossil-based polymers. It is widely used in film and packaging, textile, fiber, and biomedical application. Table 3.1 shows a comparison of the properties of PLA versus PS and PET. On the other hand, poor ductility value (elongation at break) and poor impact strength of PLA limits its further use in different areas, especially in engineering applications [6].

Table 3.1: Comparison of PLA properties versus PS and PET [6].

Properties	PLA	PS	PET
Density (kg/m^3)	1.26	1.05	1.40
Tensile strength (MPa)	59	45	57
Stiffness (GPa)	3.8	3.2	2.8-4.1
Elongation at break (%)	4.7	3	300
Impact strength (J/m)	26	21	59
Heat deflection temperature (^oC)	55	75	67

3.3 Thermal Properties and Crystallization Behavior

Transition temperatures influence the mechanical and physical properties, service temperature, and temperature window for processability. Glass transition temperature (T_g) of PLA is around 60-70^oC and the melting point of PLAs is in the range of 170-180^oC [9-12]. Crystallization kinetics of semicrystalline PLA is slow and depending on the process PLA cannot fully crystallize upon cooling. As a result, PLA exhibits cold crystallization (T_{cc}) during heating which is the crystallization of crystallites that could not crystallize upon cooling. Cold crystallization occurs beyond the Tg where molecular mobility is high enough. Figure 3.3 shows the heating and cooling DSC thermograms of PLA with two different cooling rates. Heating thermogram (solid line) shows the cold crystallization and melting of all crystals around 150^oC. Cooling thermogram (solid line) with a rate of 10^oC/min has revealed no crystallization at all while cooling with a rate of 2^oC/min enabled formation of some crystals [6].

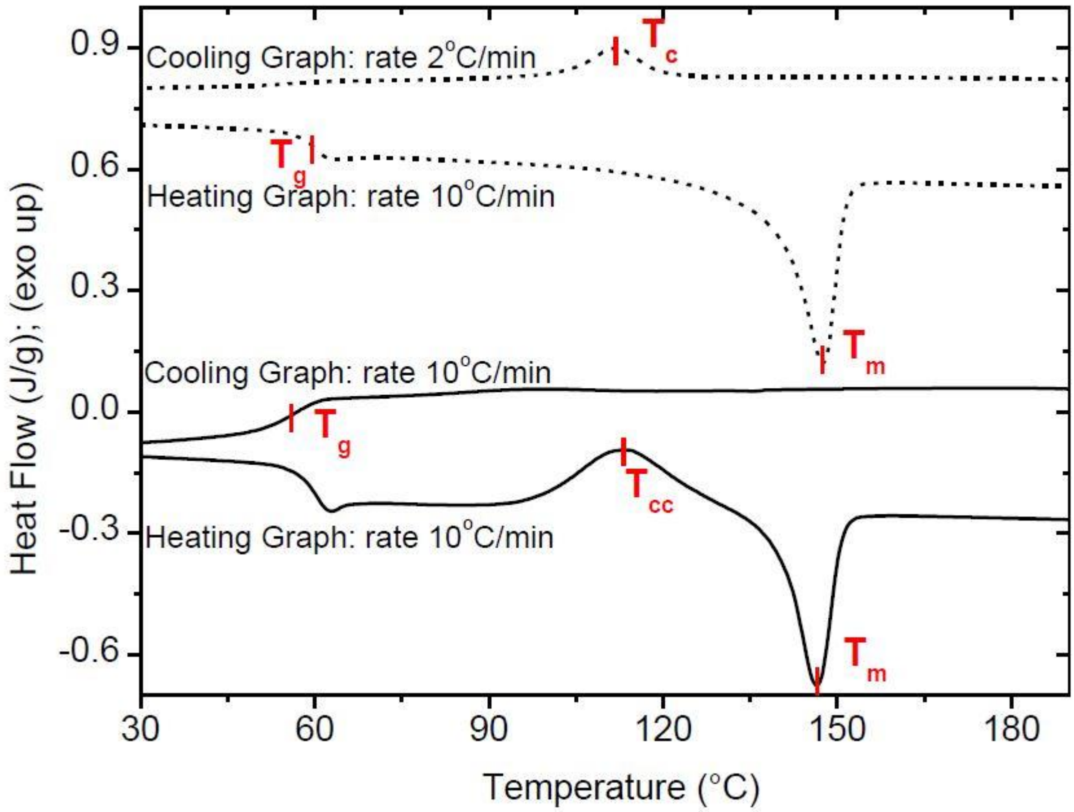

Figure 3.3: DSC thermograms of PLA with two different cooling rates [6].

Transition temperatures of PLA vary as a function of D-lactide content. The change in the transition temperature of PLAs with different isomer content is given in Table 3.2. The increase in L-content results in an increase in crystallinity and transition temperature. It is shown that transition temperature increases with increasing L-content. Also, PLAs having L-lactide more than 90% are semi-crystalline while an increase in D-content results in an amorphous structure. As an example, PLA with high L-content is semi-crystalline while the ones with higher D-content are amorphous and they can be used in heat seal applications. In the end, PLAs with very low D-content are preferred due to their higher melting temperature and a higher amount of crystallinity [4, 15].

Table 3.2: Effect of isomer content on the transition temperature.

Copolymer ratio	Glass transition temperature (°C)	Melting temperature (°C)
100/0 (L/D,L)-PLA	63	178
95/5 (L/D,L)-PLA	59	164
90/10 (L/D,L)-PLA	56	150
85/15 (L/D,L)-PLA	56	140
80/20 (L/D,L)-PLA	56	125

Crystal structure of PLA varies according to the process parameters. The α-form is the most common crystal conformation obtained through melt and solution crystallization. A less ordered α'-form is formed under crystallization temperatures below 100^{o}C which results in lower modulus, lower barrier properties, and higher ductility due to its loose and less ordered structure compared to α-form. Another crystal structure of PLA, which is β-form, is obtained through the stretching of α-form at high temperature or through solution spun with a high draw ratio. The melting temperature of the β structure is lower and thermally less stable. A more ordered crystal structure of PLA, γ-form, is also obtained through epitaxial crystallization of PLA in hexamethyl benzene [12].

Various methods such as the use of chain extenders [38, 39], plasticizers [40, 41], blending [42], and making nanocomposites have been employed to improve thermal properties and crytallisation kinetics of PLA. Nofar et al. [38] compared non-isothermal cold crystallization and isothermal melt crystallization of linear PLA (Ingeo 8051D) and commercially available long-chain branched (LCB) PLA (reactive extruded 8051D with Joncryl ADR-4368C). Non-isothermal measurements showed that branching of PLA resulted in a higher degree of crystallinity since branches act as crystal nucleation points. Through isothermal measurements, it was found that branched PLAs had much higher crytallisation kinetics compared to linear PLA.

Some of the studies reported the incorporation of plasticizers into PLA and blending PLA with other polymers could improve the crytallisation kinetics of PLA. Sungsanit et al. [41] incorporated PEG as a plasticizer in PLA and reported increased final crystallinity and improved impact properties. However, the use of plasticizers also negatively affected the rheological properties of PLA. Jiang et al. [42] blended PLA and PBAT with a twin-screw extruder to prepare biodegradable and immiscible PLA/PBAT blends. They observed that PBAT increased the crystallization rate of PLA.

Studies have shown that the use of nanosized reinforcements at low concentrations affects the crytallisation kinetics of PLA. Najafi et al. [43] studied the crytallisation kinetics of PLA nanocomposites containing 2% organoclay. They also searched the effect of different chain extenders on these nanocomposites. They reported increased crystallinity (from 6.3 to 8.7%) since clay nanoparticles acted as nucleating agents. However, the amount of crystallinity was more pronounced (15.4%) when TNPP used as a chain extender for PLA clay nanocomposites. Trifol et al. [44] compared the effect of CNC, CNF, and nanoclay (C30B) on the crystallization of PLA. Faster isothermal (at 120°C) crystallization kinetics were reported for PLA/C30B nanocomposites. However, cellulose fibers and cellulose nanocrystals resulted in a higher amount of final crystallinity since the higher aspect ratio of C30B hindered the PLA's molecular mobility and restricted the crystal growth. Kamal and Khoshkava [45] prepared PLA/CNC nanocomposites and reported improved isothermal crystallization kinetics (at 100°C) by using 3wt.% spray-dried CNC. Several other studies about PLA/CNC nanocomposites showed that homogeneously dispersed CNC improved the crystallization kinetics of PLA as shown in Figure 3.4.

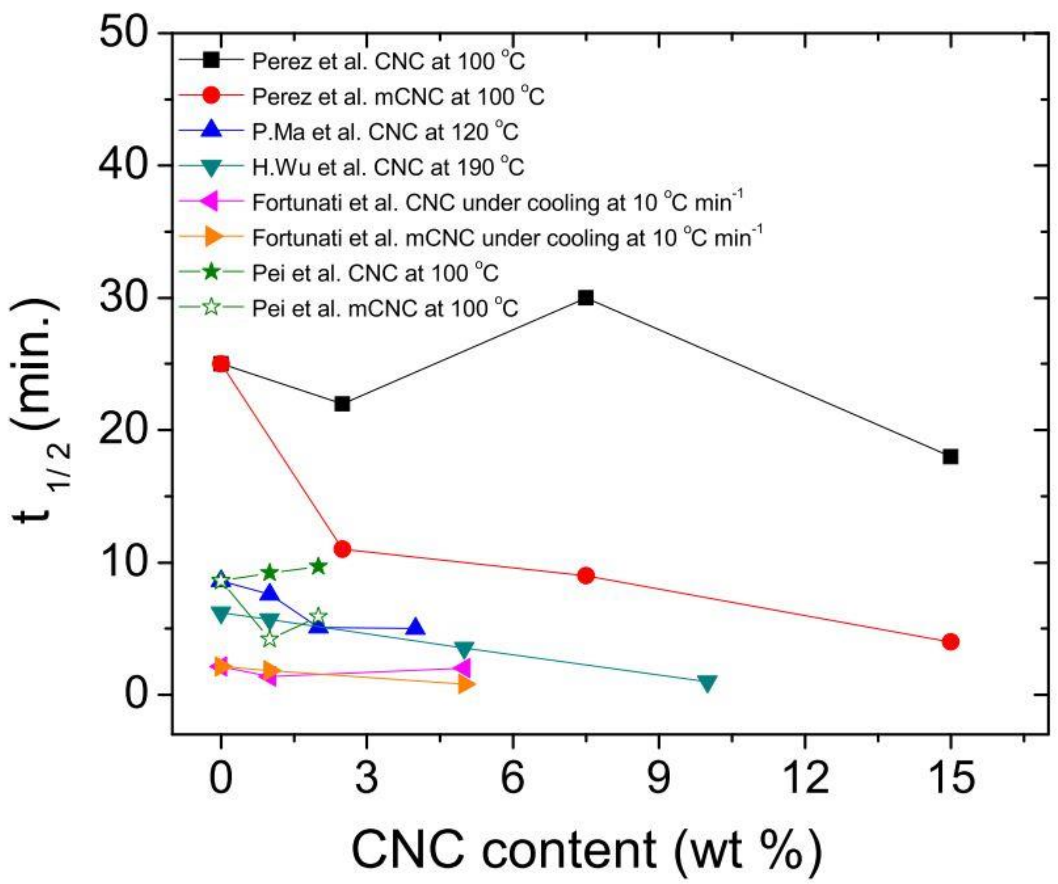

Figure 3.4: The relation between CNC content and crystallization half-time of PLA (mCNC refers surface modified) [16].

3.4 Rheological Properties

The study of melt rheological properties of polymers, in which viscosity, temperature, and shear rate are strongly linked to each other, plays a key role to determine the processability of polymer, quality of the shape of the final product meanwhile influencing the crystallization mechanism. Moreover, the rheological analysis can be effectively used to analyze the dispersion quality of reinforcement in nanocomposites [14, 17, 46, 47]. The rheological behavior of polymers highly depends on intrinsic properties such as molecular weight, molecular configuration and process parameters such as temperature, and shear rate. Figure 3.5 compares the change of viscosity curves versus the shear rate of commercially used high molecular weight polymers acrylonitrile butadiene styrene (ABS), polycarbonate (PC), and polyamide (PA6) at different temperatures. As the shear rate increased, due to gradual disentanglement of polymer molecules, melt viscosity decreased. Such behavior is called shear-thinning and observed in pseudoplastic non-Newtonian fluids such as polymers [9, 48-50].

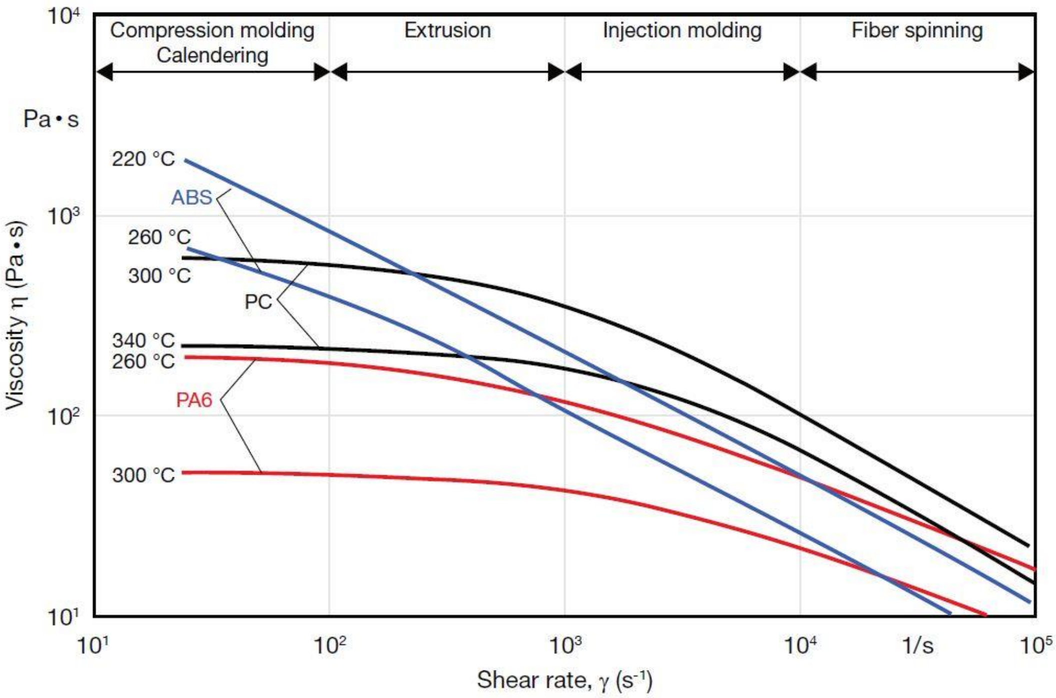

Figure 3.5: Viscosity of ABS, PC, and PA6 according to the shear rate at different temperatures [53].

Unfortunately, melt strength (which is influenced by zero shear viscosity and crystallization kinetics) and rheological properties of PLAs are reported to be low which limits their processability and applications [13, 14]. It has been reported that at shear rates corresponding to film extrusion, melt viscosity of low molecular PLAs (~40,000 Da) shows Newtonian-like behavior (negligible shear-thinning) while high molecular weight PLAs (100,000-300,000 Da) exhibits shear-thinning which is typical behavior of non-Newtonian fluids [9, 48-50]. Various attempts have done to improve the rheological properties of PLA accordingly to improve its processability. The use of chain extenders, making blends of PLA and making composites of PLA are some of those methods with their challenges and achievements.

Use of chain extenders such as Joncryl [51, 52], tris(nony1- phenyl) phosphite (TNPP) [53, 54], and CesaExtend [55] to modify PLA chain structure has been extensively studied to improve the melt strength and rheological properties of PLA. It has been shown that longer or branched chains resulted in improved melt strength and viscoelastic properties. Najafi et.al. [52] melt compounded PLA (3001D, Natureworks) with different amounts of chain extender (Joncryl® ADR-4368 F) using an internal mixer. They aimed to improve the foamability of PLA by introducing long-chain branching (LCB) to enhance its viscoelastic properties. Figure 3.6 shows the steady-shear viscosity (η) versus shear rate ($\dot{\gamma}$) and complex viscosity (η*) versus frequency (ω) of neat PLA and PLA with different Joncryl concentrations. Complex viscosity (η*) is measured by applying oscillatory shear to sample and it is the ratio of shear stress amplitude to the strain rate. For viscoelastic materials, it is not in phase and defined with real and imaginary components [56]. As can be seen, neat PLA has the lowest viscosity and wide Newtonian region with a slight shear thinning at high frequencies. It also has a low shear viscosity and shear sensitivity. The addition of chain extender increased the shear and complex viscosity by two orders of magnitude. Moreover, shear-thinning is observed at lower frequencies or shear rate suggesting that chain extension and branching improved the viscoelastic properties.

Another approach to improve the rheological properties of PLA is by blending it with other polymers. Several studies investigated the rheological properties of PLA-based blends. In the case of miscible blends [57], it was found that the viscoelastic properties of the final product are in between that of two polymers. On the other hand, in the case of immiscible blends [58-61]: composition, morphology, and the interfacial interactions between phases influence the rheological properties. As an example, Hao et al. prepared miscible blends of PLA (Ingeo 4032D) and PMMA (Plexiglas 7N) by melt mixing. Frequency sweep results of PLA/PMMA blends with different compositions are shown in Figure 3.7. It can be said that preparing miscible blends of PLA with another polymer having better viscoelastic properties resulted in a final blend with viscoelastic properties in between that of two polymers. As shown in the figure, the Newtonian plateau of neat PLA becomes narrower with an increased amount of PMMA.

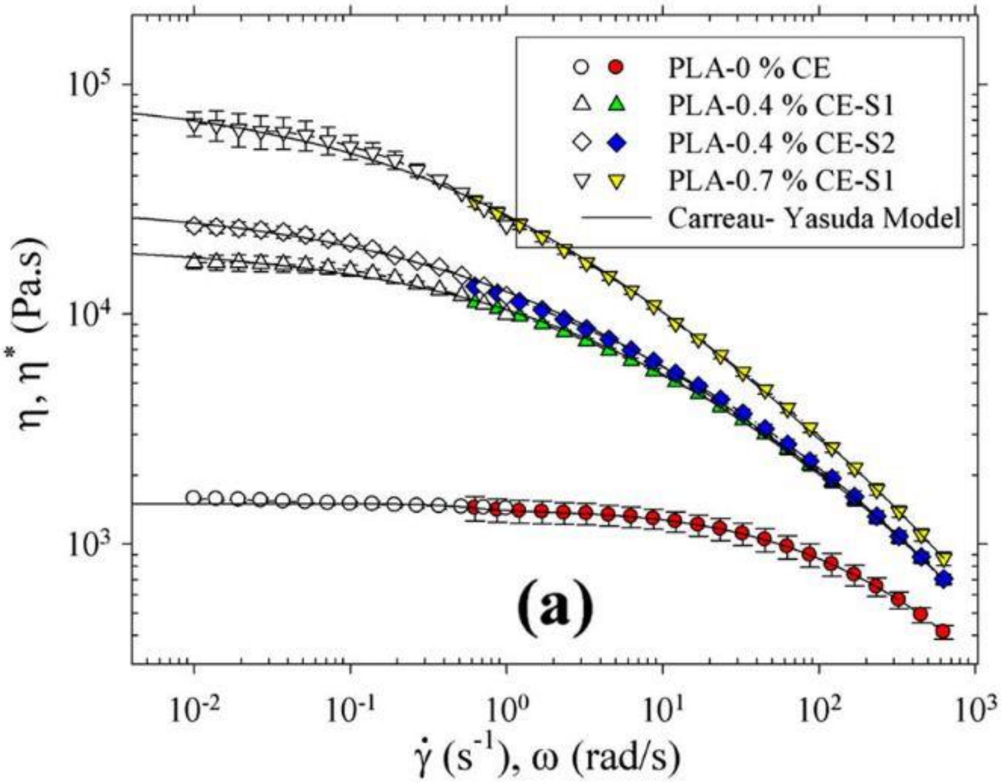

Figure 3.6: Shear (open symbols) and complex viscosity (filled symbols) of neat PLA and PLA with different CE concentrations [55].

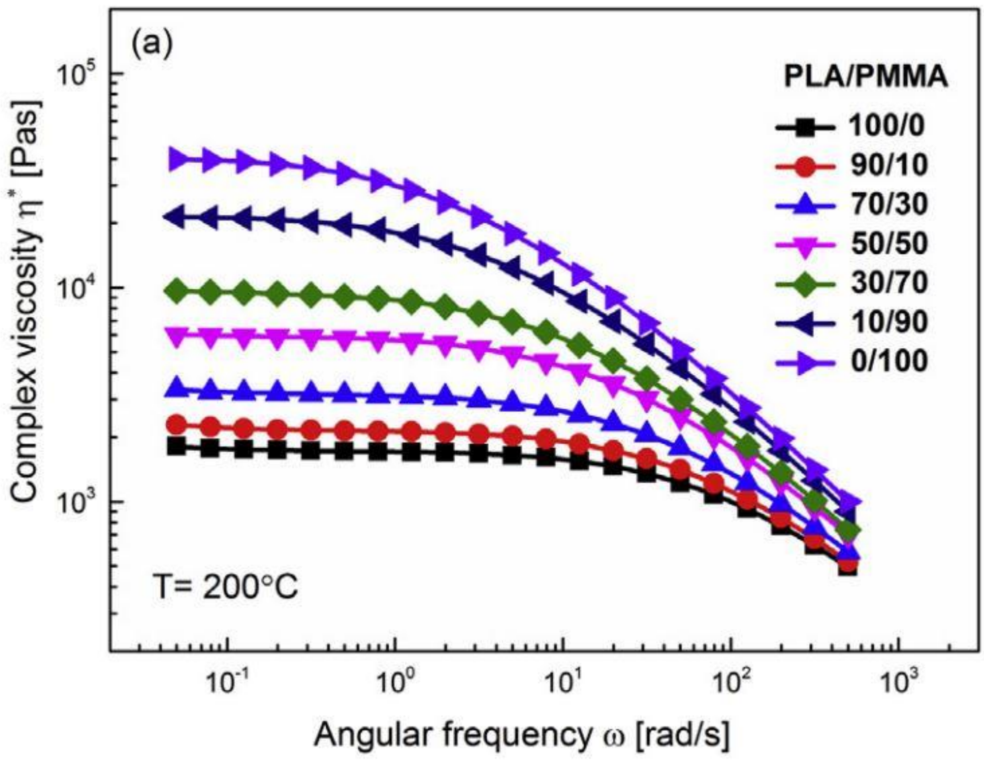

Figure 3.7: Complex viscosity of PLA/PMMA blends with various compositions [60].

Making nanocomposites of PLA is another method to enhance its rheological properties. Studies have shown that commonly used additives such as talc, short fibers, silk, and graphite are also successful to improve the rheological properties thus the processability of PLA. However, it is possible to obtain similar or better improvements by using nano-additives in much lower amounts [14]. Significant achievements made by using nanoclay [62], nano-silica [63], carbon nanotube [21], graphene [64], cellulose nanofiber [65, 66], and cellulose nanocrystals (CNC) [28, 33]. Bagheriasl et al. [28] prepared nanocomposites of PLA (Ingeo 3251D) and CNC (FPInnovations) using the solution casting method. Complex viscosity and storage modulus of nanocomposites with different CNC loadings are shown in Figure 3.8. Complex viscosity of neat PLA exhibits a wide Newtonian plateau with negligible shear thinning at high frequencies. With the incorporation of CNC, with such small amounts, complex viscosity profoundly increases at low frequencies. The increase in rheological properties indicate the strong network formation between PLA molecules and CNC at molecular level.

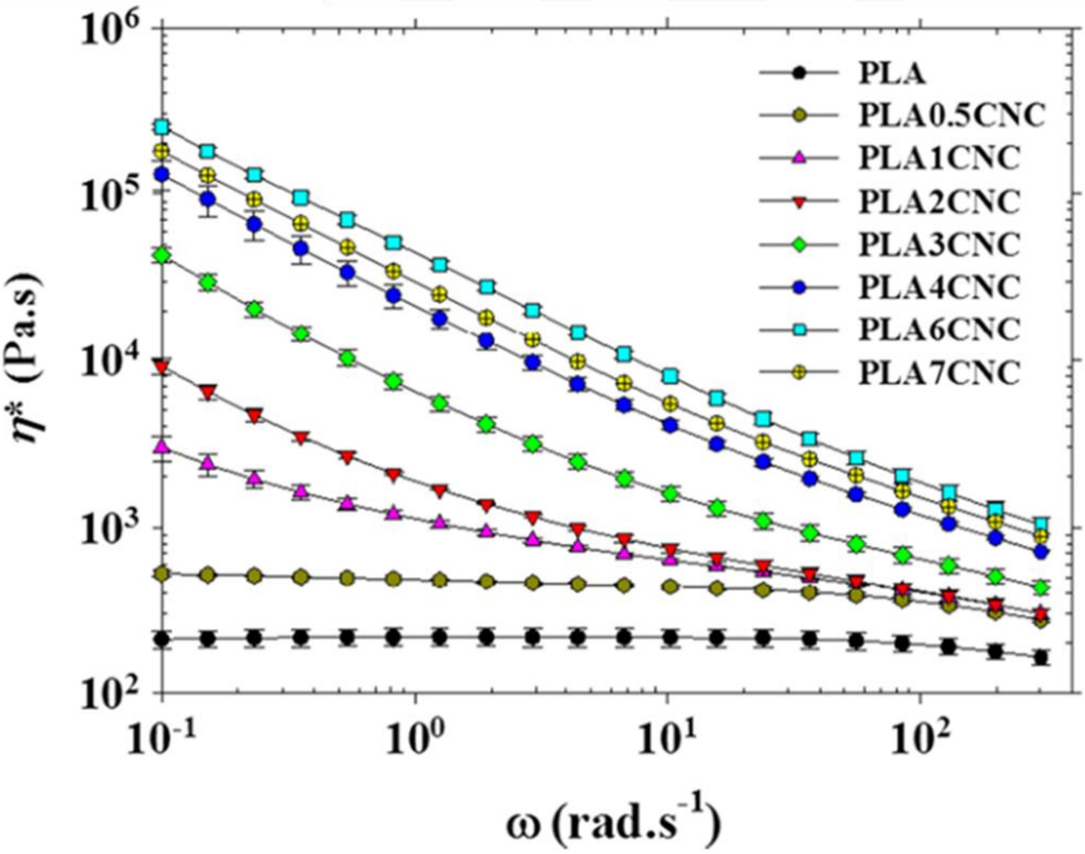

Figure 3.8: Complex viscosity of PLA/CNC nanocomposites with different CNC loadings (frequency sweep test was conducted at 170 °C with a strain amplitude of 5%) [28].

3.5 Efforts to Improve Properties of PLA

It was shown that PLA is a Bio-based, biodegradable, and biocompatible polymer [4, 5, 35]. Moreover, its comparable mechanical properties to that of commercially used petroleum-based polymers make it a candidate to be replaced in the industry with petroleum-based counterparts [6]. PLA-based articles are already used in various applications and it is assumed that PLAs production rate will continue to increase [7, 8]. However, PLA has some drawbacks that limit its processability and applications. Those limitations could be listed as:

1. Low T_g (or low transition temperatures): limits its service temperature and result in narrow processing window [9-12],

2. Slow crystallization kinetics: limits processability (notably in productions with fast cycles), results in a low amount of crystallinity (negatively affects mechanical, thermal and barrier properties), and poor melt strength (which greatly influence the processability) [6],

3. Poor rheological (or viscoelastic) properties: limits processability and application, result in poor melt strength [13, 14].

There are different approaches to overcome the aforementioned drawbacks of PLA, such as copolymerization, blending with other polymers, plasticizing, chemical modification, use of chain extender, and composite making [5, 6, 14, 15]. Some of those methods were explained in previous sections with their advantages and disadvantages. Among those methods, making nanocomposites of PLA by using nanosized particles as reinforcement proved to be an effective way which enables to tailor the properties of PLA for a wide range of applications [14, 16]. Studies have shown that the use of nanosized reinforcements not only improves mechanical, thermal, and barrier properties but also enhance crystallization kinetics by acting as nucleating points, improves the rheological properties, and melt strength which at the end, improves the processability and application of PLA [5, 14, 17]. Different kinds of nanosized fillers have been widely incorporated into PLA and some of them could be listed as:

1. Clay-based nanofillers [18, 19]: sepiolites, layered silicates (montmorillonite), and halloysite nanotube (HNT),

2. Carbonaceous nanofillers [20, 21]: carbon nanotubes (CNT), carbon nanofiber (CNF), and graphene,

3. Silicon-based nanoparticles [14, 22]: nano-silica and POSS,

4. Some metal and metal oxide nanoparticles [23]: silver, titanium dioxide, etc.,

5. Cellulose-based nanofillers [16, 23, 24]: cellulose nanocrystals (CNC), cellulose nanofibers (CNF), and bacterial cellulose (BC).

Clay-based nanofillers widely used to make PLA nanocomposites. Layered silicates extensively studied and it has been shown that in comparatively low amounts they successfully improved crystallization kinetics of PLA thus, the barrier properties and the processability of PLA. Moreover, layered silicates also improve the thermomechanical and flame retardancy of PLA. To obtain a homogeneous dispersion of those clay-based nanofillers, surface modification is necessarily applied to obtain surface affinity between PLA and layered silicates [18, 19]. It is also worth mentioning that during melt mixing clay nanofillers result in degradation of PLA thus chain extenders are used to prevent degradation during the process [43, 67].

Carbonaceous nanofillers are preferred as reinforcement due to their electrical properties, in terms of conductivity, and remarkable physical properties. CNT are extensively studied to make PLA nanocomposites due to their physical properties, high electrical, and thermal conductivity. However, the incompatible nature of PLA and those carbonaceous fillers results in poor dispersion of CNT in the PLA matrix which results in poor mechanical, thermal, and electrical properties; and prevents obtaining percolation level at a lower amount. As a result, surface modification of CNT can be required [20, 21].

Silicon-based nanofillers are generally preferred due to their thermal resistance, natural abundance, and low cost. However, silicon-based nanofillers possess a low surface area/volume ratio thus, they don’t successfully improve the processability of PLA in terms of rheological properties [14, 22].

Metal and metallic oxide nanofillers have been incorporated into PLA due to their optical, magnetic, and electrical properties. Moreover, those nanoparticles can provide antimicrobial properties to PLA nanocomposites [23].

Cellulose-based nanofillers can be listed as cellulose nanofibers (CNF), bacterial cellulose (BC), and cellulose nanocrystals (CNC). Cellulose-based nanofillers enable us to obtain fully bio-based, biodegradable, biocompatible, and non-toxic PLA nanocomposites. Among those cellulose-based nanofillers, thanks to their commercialization in recent years, CNC received a remarkable interest to produce PLA-based fully biodegradable and Bio-based nanocomposites [16, 23, 24, 68, 69]. As a result, by using CNC, it is possible to improve the crystallization kinetics and melt strength of PLA without sacrificing its Bio-based and biodegradable properties. As well as being Bio-based and biodegradable, CNC stands out with its remarkable properties. Table 3.3 compares the CNC with some other materials. It has low density, comparable tensile strength, and elastic modulus value comparable to that of steel. Other remarkable features of CNC are low thermal expansion coefficient, optical transparency and anisotropy, negative diamagnetic anisotropy, and flexible surface chemistry [27].

Thus, PLA/CNC nanocomposites enable us to increase the mechanical properties, crystallization kinetics, thermal stability, and rheological properties of PLA without compromising PLA's biodegradable characteristics. Accordingly, PLA/CNC nanocomposites are intensively studied to deeply understand the parameters affecting the incorporation of CNC into the PLA matrix and to further enhance their properties.

Table 3.3: Comparison of density, tensile strength, and modulus of CNC to some other materials [25].

Materials	Density (g/cm^3)	Tensile Strength (GPa)	Modulus (longitudinal) (GPa)	Modulus (transverse) (GPa)
Steel wire	7.8	41	210 - 369	-
Nanoclay	1.8 - 2.2	-	120 - 180	-
Kevlar	1.4	3.5	124 - 130	2.5
Carbon fiber	1.8	1.5 - 5.5	150 - 500	-
CNT	1.5 - 2	10 - 60	300 - 1000	-
CNC	1.6	7.5 - 7.7	130 - 250	10 - 50

4. PLA/CELLULOSE NANOCRYSTAL NANOCOMPOSITES

As previously mentioned, PLA considered as a candidate to be replaced with fossil-based conventional polymers thanks to its both bio-based and biodegradable characteristics combined with comparable mechanical properties. However, slow crystallization kinetics and low melt strength characteristics limit the production PLA. Nanocomposite making is a versatile method to overcome those drawbacks which also enables the tailoring of properties of the final product. Moreover, nano-sized fillers, with at least one dimension smaller than 100 nm, have high surface area and aspect ratio thus, it is possible to obtain better or comparable reinforcement effect with nanofillers with lower volume fraction [18, 19, 23]. CNC as being both bio-based and biodegradable has comparable mechanical properties to that of commonly used petroleum-based fibers. Several studies have shown that making PLA/CNC nanocomposites by incorporating CNC into the PLA matrix had improved the mechanical, rheological, and thermal properties of PLA which will be explained in the following sections in detail.

4.1 Cellulose Nanocrystal (CNC)

Cellulose is a high molecular weight biopolymer whose chains consist of amorphous and crystalline parts. Figure 4.1 shows the cellulose polymer from tree to its monomer (1,4-anhydro-D-glucopyranose: $(C_6H_{10}O_5)_n$). Cellulose nanocrystals (CNC) are produced through the acid hydrolysis of the amorphous regions in the cellulose chains. CNC stands out among other filler with its higher mechanical properties, low density, the potential for surface modification meanwhile being renewable, Bio-based, and biodegradable [25, 26].

Cellulose nanocrystals have a high aspect ratio (11-32) with a diameter of 7 ± 3 nm and length of 120 ± 8 nm [25]. The rod-like morphology of CNC is shown in Figure 4.2.

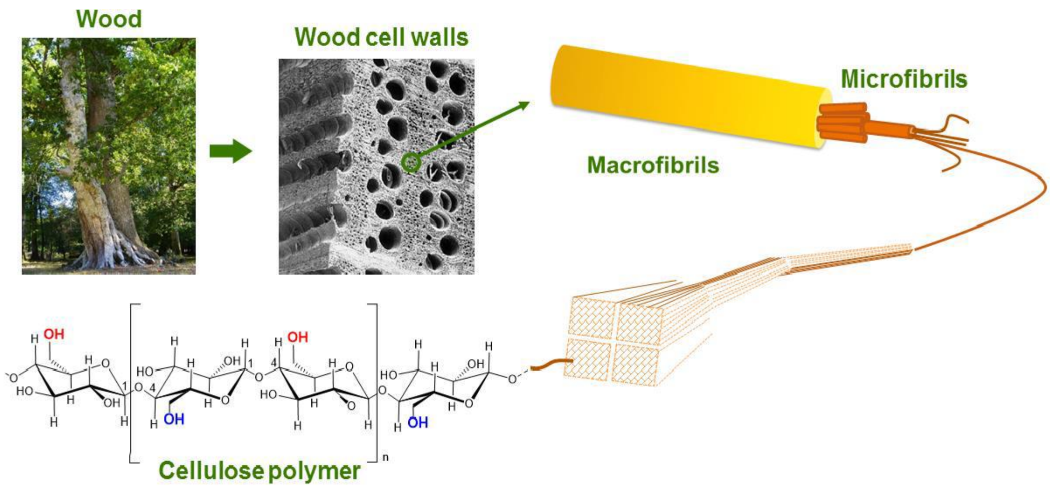

Figure 4.1: The chemical structure of the cellulose components from tree to the anhydroglucose molecule [25].

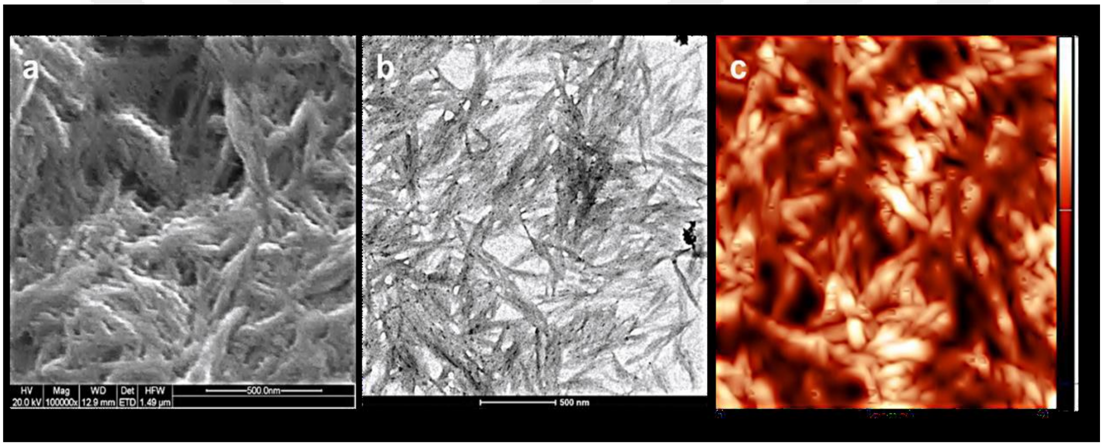

Figure 4.2: (a) Scanning electron microscopy (SEM); (b) transmission electron microscopy (TEM); (c) Atomic Force Microscopy (AFM) images of CNC [25].

4.1.1 Production and the chemical structure of CNC

Cellulose nanocrystals are produced through the acid hydrolysis of amorphous domains in the cellulose microfibrils which is schematically represented in Figure 4.3. Acid hydrolysis can be achieved through the use of hydrochloric acid (HCl) or sulphuric acid (H_2SO_4). As shown in Figure 4.4, during HCl hydrolysis hydroxyl groups remain on surface which results in week surface charge and poor colloidal stability. The colloidal stability of HCl hydrolyzed CNC was increased by introducing carboxyl groups on surface through post treatment with TEMPO (2,2,6,6-Tetramethyl-1-piperidinyloxy) which also increases the thermal stability. On the other hand, sulfate half ester groups ($O\text{-}SO_3^-$) are introduced on CNC surface during H_2SO_4 hydrolysis. Those groups make the CNC surface negatively charged thereby, increase the dispersion or deagglomeration of CNC due to electrostatic repulsion. However, those groups also make the CNC hydrophilic which result in poor compatibility between hydrophilic CNC and hydrophobic polymer matrix [25, 27].

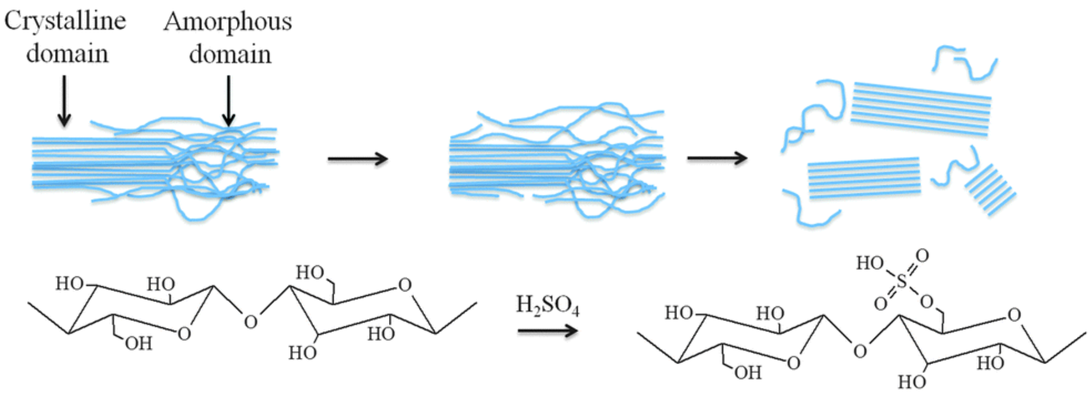

Figure 4.3: The isolation of cellulose nanocrystals through sulfuric acid hydrolysis [25].

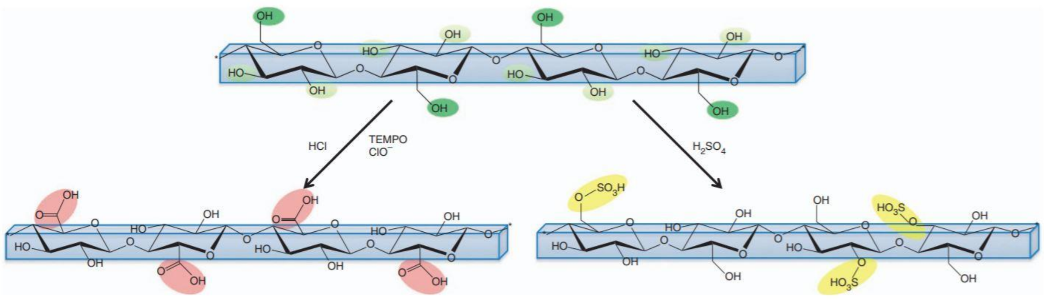

Figure 4.4: Production of CNCs through acid hydrolysis: HCl (left) and H_2SO_4 (right) [27].

4.1.2 Thermal and mechanical properties of CNC

Degradation of CNC starts around 280°C and the sulfate groups on the CNC surface affect its thermal stability. As previously stated, CNC produced through H_2SO_4 hydrolysis is thermally less stable and degradation temperature is lower compared to ones produced by HCl hydrolysis due to the presence of sulfate half groups that are introduced during hydrolysis. Still, sulfuric acid hydrolysis is commercially used since negatively charged half ester groups provide the deagglomeration of CNC by electrostatic repulsion. In addition to its bio-based, biodegradable, and sustainable characteristics, CNCs with tensile strength of 7.5 to 7.7 GPa and axial modulus of 100 to 220 GPa possess significant mechanical properties that make them comparable to other nanofillers [25]. Rigidity and strength of CNC makes it a good candidate to be used as fillers for especially for polymers.

4.1.3 Drying method of CNC

As explained before CNCs are produced from the acid hydrolysis of cellulose which result in a final product as an aqueous suspension. However, it is not favorable to use aqueous suspension with hydrophobic media especially in polymer nanocomposite production since the residual water from the suspension will affect the process. As a result, CNC aqueous suspension is objected to a drying step to obtain dry CNC powders. There are two main methods, commercially used, to obtain dry powders: spray drying and freeze drying. Drying steps of these two methods are indicated in the phase diagram of water and shown in Figure 4.5. Spray drying process proceeds through the evaporation of water inside the CNC-water droplet. On the other contrary, freeze drying takes place in two steps: first water inside the suspension is frozen then removed by sublimation. Details of these methods and morphology of the final powders are explained in the following sections.

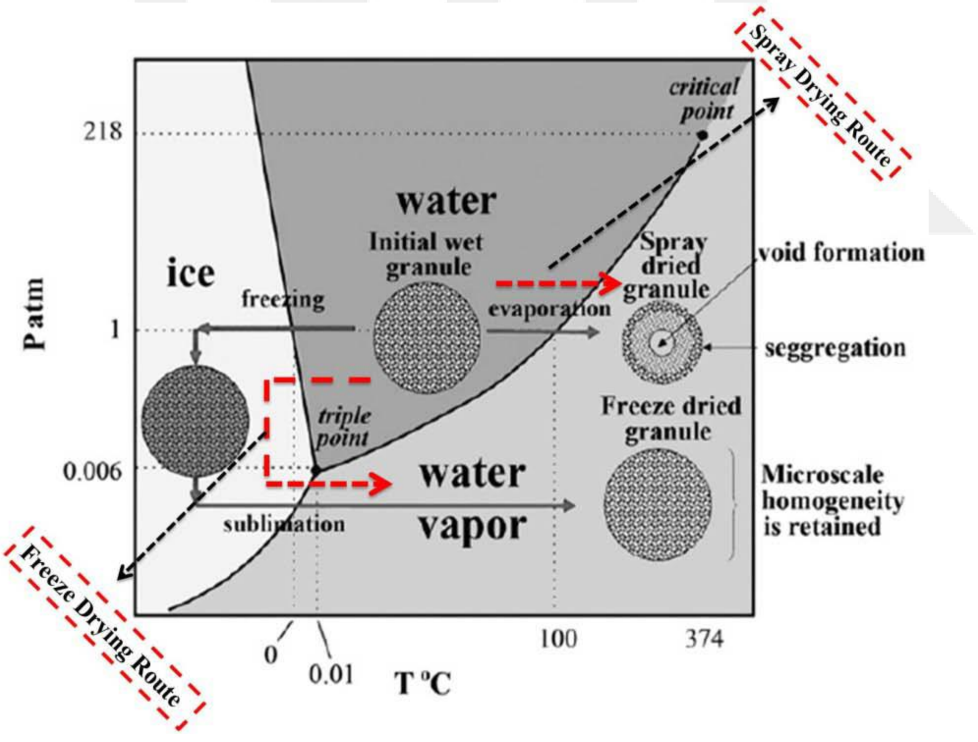

Figure 4.5: Spray and freeze-drying steps on water phase diagram [26].

Khoshkava and Kamal [43] studied the effect of drying method of CNC on dispersion and rheological properties of polypropylene (PP)/CNC nanocomposites. They compared spray dried CNC and freeze-dried CNC, which are commercially available methods to dry CNC, with spray freeze dried CNC which is a method they developed. Nanocomposites were prepared through melt mixing method (190ºC, 60 rpm, 10 min) by using an internal mixer. Morphological analysis of CNCSD, CNCFD, neat PP, and nanocomposites are shown in Figure 4.6. Large and spherical agglomerates are seen in Figure 4.6d. Those agglomerates of spray dried CNC resulted from the capillary, hydrogen bonding, and van der Waals forces between CNC particles. As shown in Figure 4.6b freeze dried CNC has a lamellar morphology since water crystallization is the driving mechanism for CNC aggregation during freeze drying. As a result, sheet like CNC particles are seen in Figure 4.6e. However, there are no significant particle deagglomeration (or size reduction) which means polymer infiltration into CNC agglomerates was hardly successful. The red holes and arrows in the figure indicate particles of CNC detached from large aggregates.

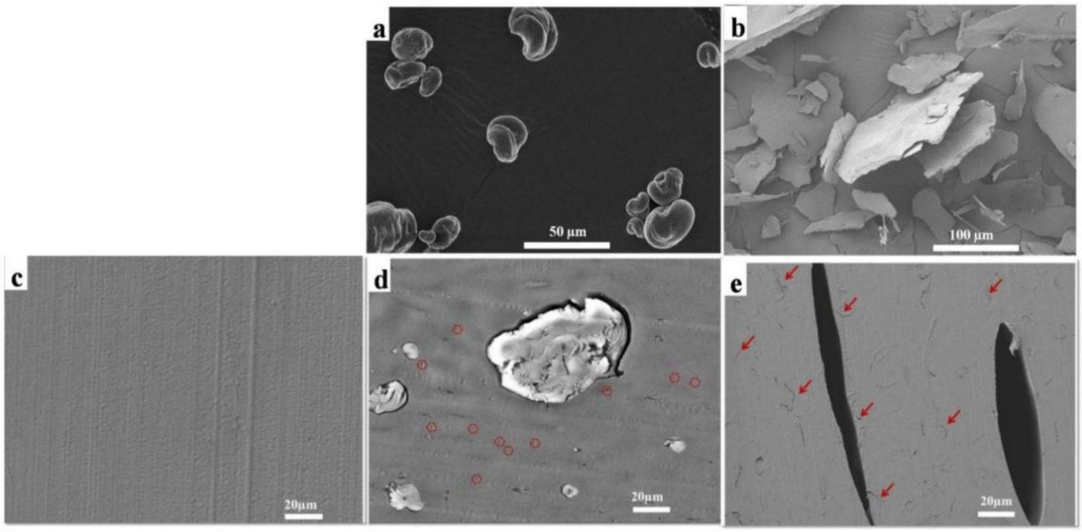

Figure 4.6: SEM images of nanocomposites (a) spray dried CNC (CNCSD), (b) freeze dried CNC (CNCFD), (c) neat PP, (d) PP-CNCSD, and (e) PP-CNCFD (nanocomposites contains 5wt.% of CNC) [43].

4.1.3.1 Spray dried CNC

Spray drying chamber is shown in Figure 4.7. Aqueous CNC suspension is atomized through spraying inside the chamber which is filled with hot air with a temperature higher than 100^{o}C. The water on the surface of the droplet evaporates first when introduced with hot air. The water at the interior of the droplet first diffuse toward the surface then evaporates. Since the diffusion kinetic of the interior water is slower than the evaporation from the surface, structure of the final powder will be different in radial direction.

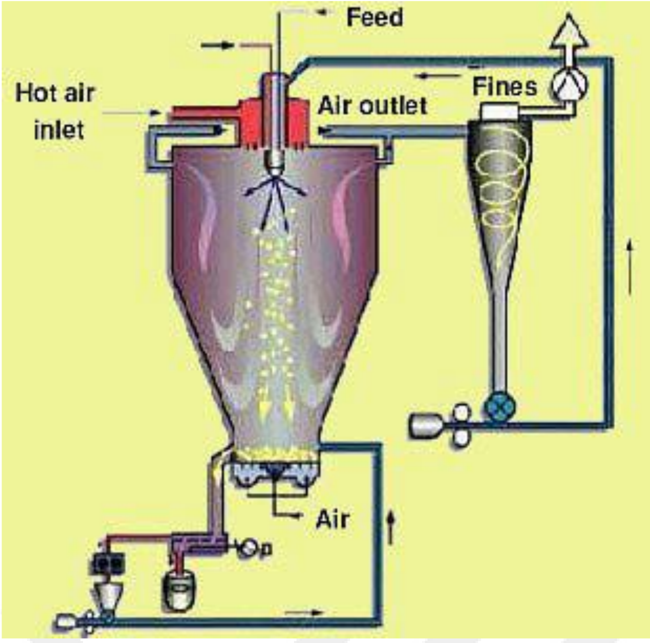

Figure 4.7: Spray drying chamber [26].

At the end, powders or CNC agglomerates in size of micron range (5-30 µm) are obtained. Figure 4.8 shows the SEM and PLM images of spray dried CNCs. As shown in SEM images the CNC agglomerates are not in sphericall shape due to shrinkage of aggregates.

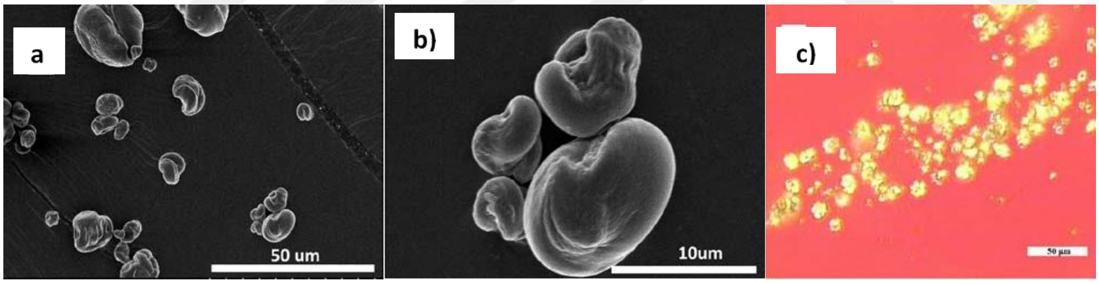

Figure 4.8: SEM image of spray dried CNC a) low magnification, b) high magnification and c) PLM image (20X magnification) [26].

During spray dying process capillary, Van der Waals, hydrogen bonding and electrostatic repulsion forces control the shape of the agglomerates. While the electrostatic repulsion force facilitates the deagglomeration, the other three forces facilitate the agglomeration and thanks to the competition between the forces CNC particles do not agglomerate rapidly instead they find time to minimize their energy. As a result, compact and dense CNC agglomerates in powder form is obtained [26].

4.1.3.2 Freeze dried CNC

As explained before, freeze drying method takes place through the first freezing of suspension then sublimation of the water. The freeze-drying unit is shown in figure 4.9. The aqueous CNC suspension is frozen inside the freeze dryer unit equipped with a condenser and a vacuum pump. Vacuum is applied to drop the pressure below the triple point to enable the sublimation process. After pressure drop, the residual frozen water is evaporated through heating.

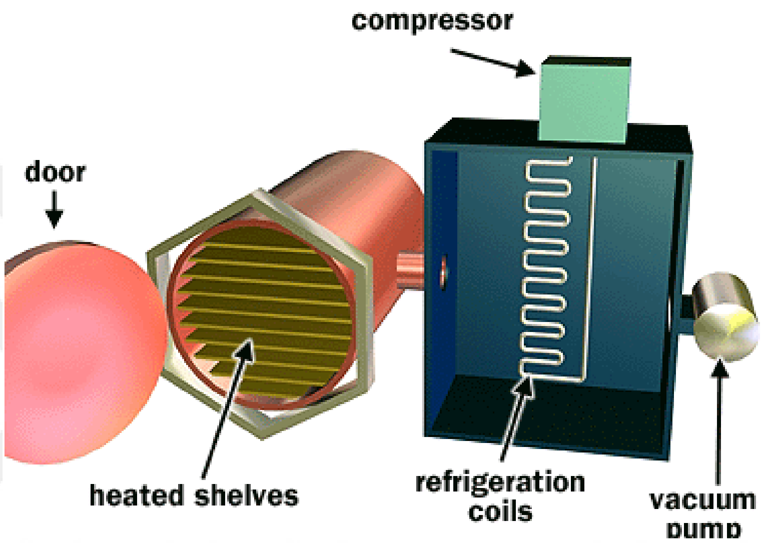

Figure 4.9: Schematic of a commercial freeze dryer [26].

SEM and PLM images of freeze dried CNCs are shown in Figure 4.10 and 4.11, respectively. Different from the spray-dried CNC, freeze-dried CNC has a flake-like shape. That is because, during the freezing step, water crystals form and push the CNC particles to each other resulting in a flake-shaped dense CNC agglomerates.

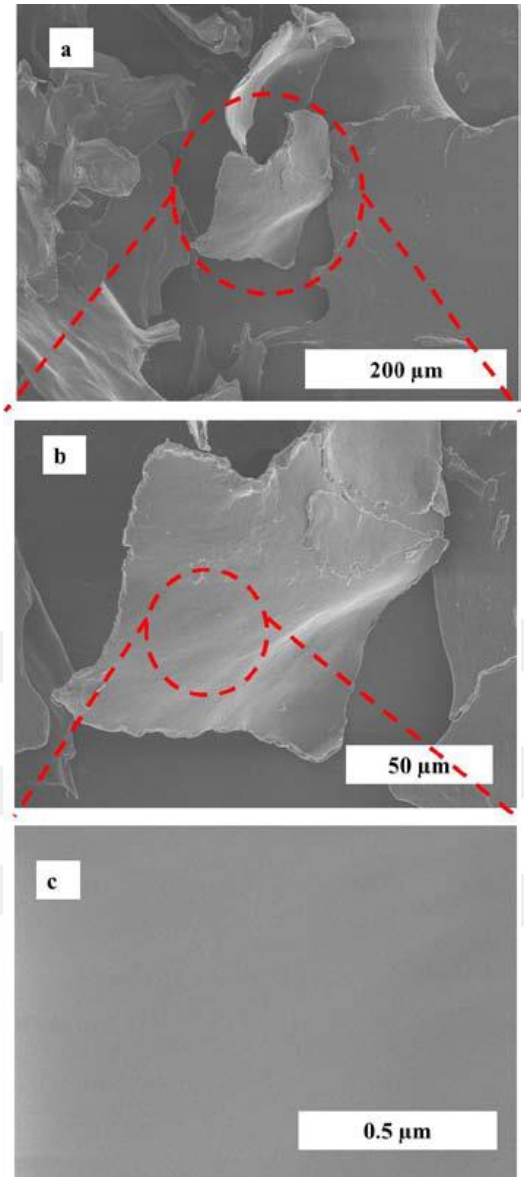

Figure 4.10: SEM image of 4 wt.% CNC suspension frozen at -50ºC in a refrigerator at a) low, b) medium, and c) high magnification [26].

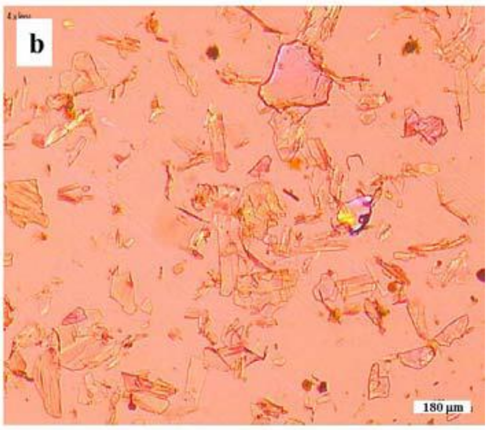

Figure 4.11: PLM image of freeze-dried CNC at 10X magnification [26].

4.2 Mechanical Properties of PLA/CNC Nanocomposites

Incorporation of nanoparticles into polymer results in nanocomposite with better mechanical properties compared to that neat polymer. The reinforcement mechanism takes place by the stress transfer through the matrix to the nanofillers. As a result, a good level of interface between polymer matrix and nanofiller, and a homogeneous dispersion of nanoparticles are key factors to obtain enhanced mechanical properties. Studies have shown that due to poor interfacial interaction between PLA and CNC results in slightly improved mechanical properties due to non-uniform stress transfer. As a result, to obtain pronounced mechanical properties surface chemistry of CNC is modified [70-72]. However, there still some studies that obtained improved mechanical properties especially at low amounts of CNC (less than 5wt.%) [17]. Figure 4.12 shows the mechanical properties of unmodified PLA/CNC nanocomposites prepared by Bagheriasl et al. [29]. They reported a 23% increase in Young modulus which can be resulted from the high stiffness of CNC. The change in tensile strength was insignificant and attributed to the poor stress transfer between matrix and filler having different polarities.

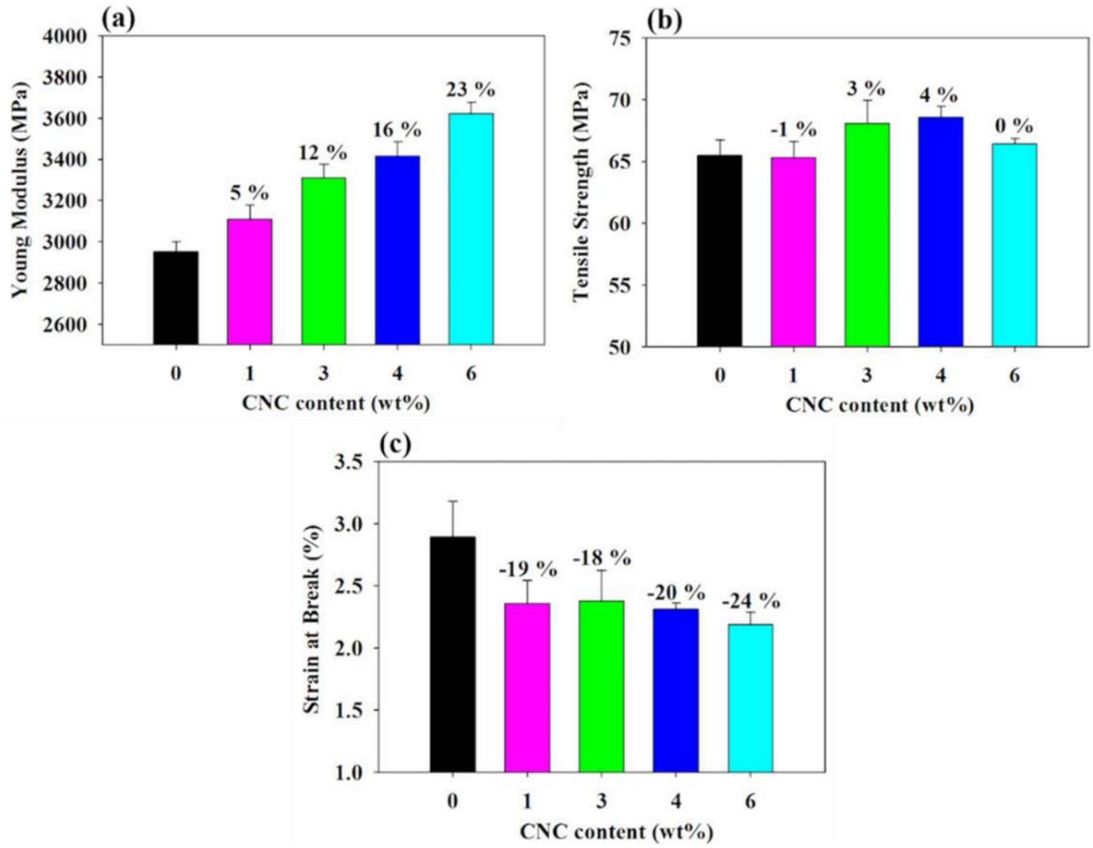

Figure 4.12: Mechanical properties of unmodified PLA/CNC nanocomposites [29].

4.3 Rheological Properties of PLA/CNC Nanocomposites

It was previously mentioned that PLA suffers from poor rheological properties which limit its processability. Different studies have shown that PLA/CNC composites have successfully improved the rheological properties of PLA through a network formation of CNC in the PLA matrix. A rheological analysis is one of the most effective methods to see network formation accordingly to the dispersion level [73]. The change in complex viscosity and storage modulus versus shear rate clearly shows the effect of the CNC network and dispersion on the rheological properties of PLA. The increase in complex viscosity at lower shear rates reveals the interaction of CNC and PLA at the molecular level.

Bagheriasl et al. [28] prepared PLA/CNC nanocomposites, without any surface modification, by solution casting method. First, freeze-dried CNC was dispersed in DMF through bath sonicator (2 hours) and magnetic stirrer was used (150 min) to dissolve PLA in CNC-DMF mixture which was followed by drying in a vacuum oven at 80^{o}C for 36 hours. The rheological analysis is shown in Figure 4.13. The increase in complex viscosity and storage modulus of PLA/CNC nanocomposites is an indication of CNC network formation and that reveals the success of their method to finely disperse CNC in PLA. The imaginary part of the complex viscosity is the storage modulus (G') and defines the energy stored in material for a half cycle [56]. The storage modulus of neat PLA has a terminal zone slope equal to 2 on the log-log scale which is typical for molten polymers while PLA/CNC nanocomposites exhibited higher storage modulus values. Those improvements in rheological properties indicate the strong network formation between PLA molecules and CNC at a molecular level. The calculated percolation threshold of rheological properties was found to be 0.68 or 0.55%.

Bagheriasl et al. [29] prepared PLA/CNC nanocomposites by the same solution casting method as previously mentioned without the use of any surface modification or compatibilizer. Storage modulus (G'), loss modulus (G''), and loss tangent (tan δ) versus frequency of neat PLA and PLA/CNC nanocomposites at different loadings are shown in Figure 4.14. G' and G'' of nanocomposites increased by 4 and 1 orders of magnitude compared to neat PLA and the increase is more pronounced for highly loaded nanocomposites (Figure 4.14a). Loss tangent (loss factor or damping factor) is a dimensionless factor and defined as tan δ = G''/G'. The phase angle (δ) is equal to

0º for ideally elastic materials that doesn't have a viscous property (G'' = 0) and equal to 90º ideal viscous fluids (G' = 0) [74]. The loss tangent (tan δ) as a function of frequency is shown in Figure 14b. The neat PLAs tan δ increases with the decreasing frequency which is an indication of the Newtonian character of PLA. On the other hand, tan δ of nanocomposites decreases in a whole frequency range which indicates that nanocomposites behave elastically. It was reported that the decrease in tan δ and plateau regions in G'' and G' at low frequencies indicate the behavior of PLA turned from liquid to solid-like resulted from CNC network formation.

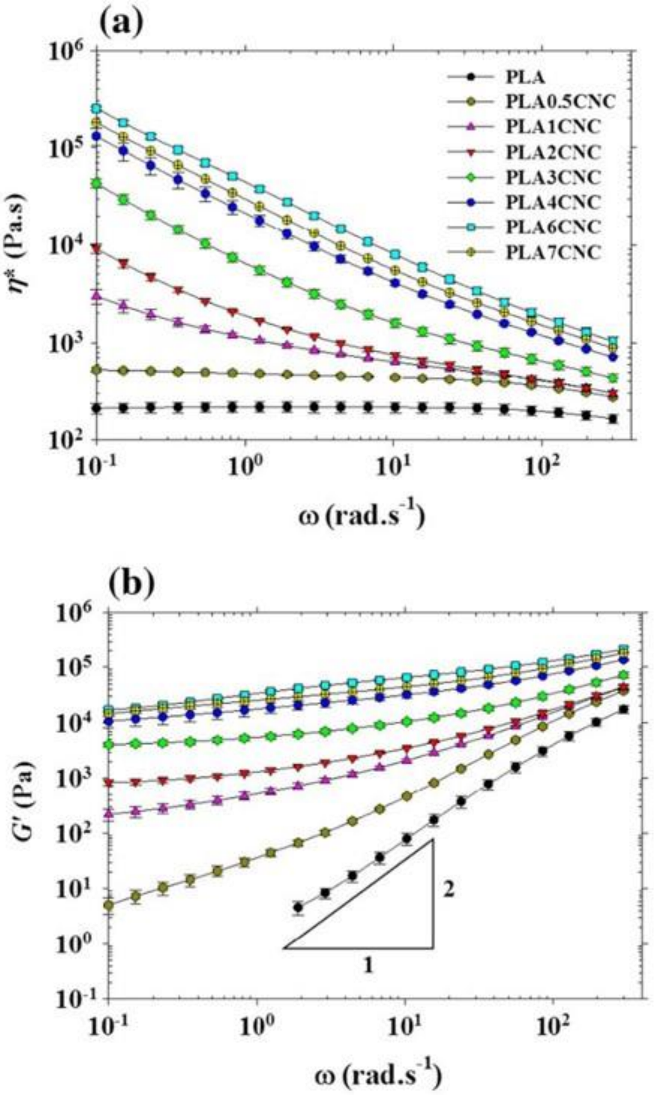

Figure 4.13: Complex viscosity (a) and storage modulus, G',(b) versus frequency, of the neat PLA and PLA–CNC nanocomposites at 170 °C (strain = 5%) [28].

Heshmati et al. [30] studied the dispersion of CNC in PLA/PA11 blends. To prepare CNC incorporated blends they first prepared PLA/CNC or PA11/CNC nanocomposites as masterbatches. To do that CNC was dispersed in DMF using a bath sonicator for then, PLA is added to this mixture by further mixing with a magnetic stirrer for 2 hours. Later on, those masterbatches are diluted with two polymers by using the melt mixing method. They also studied the rheological properties of nanocomposites used as masterbatches and the results of PLA/CNC nanocomposites are shown in Figure 4.15. For the neat PLA complex viscosity versus frequency is almost Newtonian with a slight shear thinning at high frequency. Meanwhile, nanocomposites revealed shear thinning behavior at lower frequencies which became more pronounced with increasing CNC loading. The slope of the storage modulus of nanocomposites decreased to 0.12 which was 1.5 for neat PLA. Again the tend of storage modulus to the plateau is an indication of network formation.

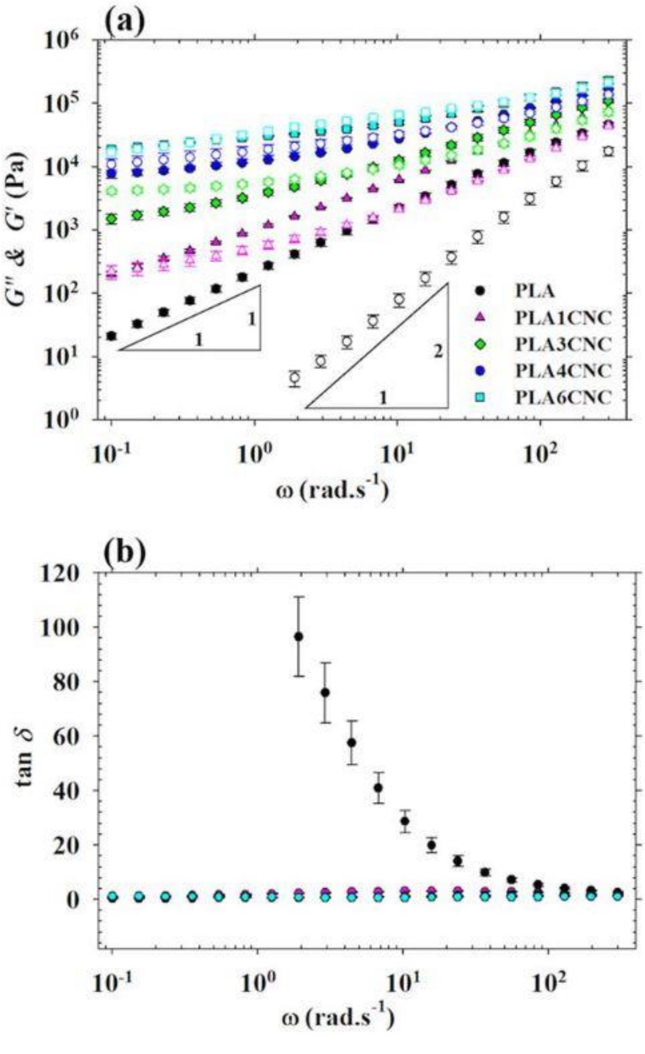

Figure 4.14: Loss modulus (G'', filled symbols) and storage modulus (G', filled symbols) versus frequency (a) and loss tangent (tan δ) versus frequency (b) at 170°C with strain amplitude of 0.55 [29].

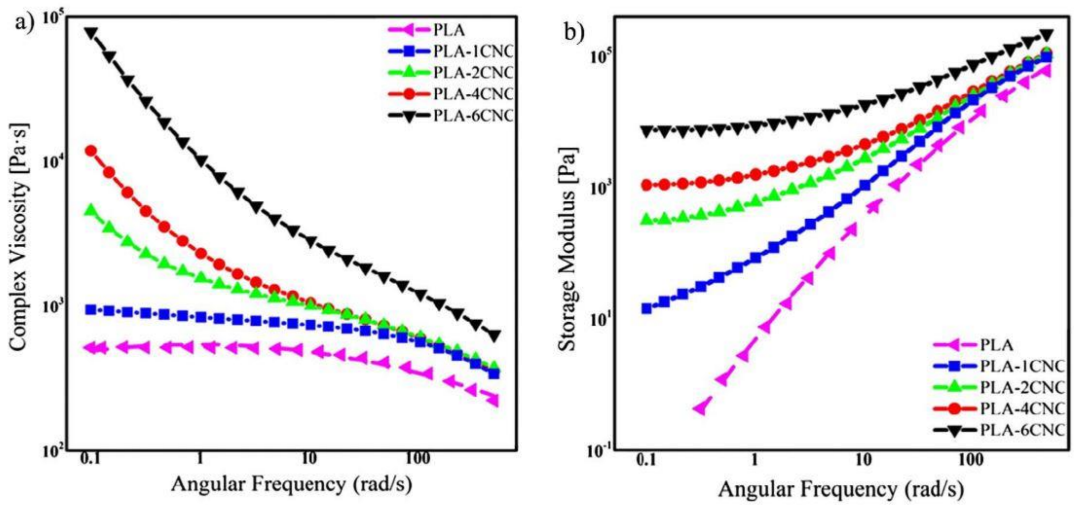

Figure 4.15: Complex viscosity (a) and storage modulus (b) versus frequency of PLA/CNC nanocomposites loaded with different amounts of CNC [30].

4.4 Thermal Properties and Crystallization behavior of PLA/CNC Nanocomposites

Crystallinity is one of the key factors to control various final properties such as degradation rate, thermal stability, optical, barrier, and mechanical properties of PLA [75]. However, compared to many other thermoplastics, PLA has a slow crystallization rate thus, PLA may not undergo crystallization during fast or even moderate cooling rates [12]. The presence of homogeneously distributed CNC nanoparticles within PLA can affect the crystalline morphology and crystallization kinetics of PLA by served as nucleating sites to initiate the crystallization. These effects are usually more pronounced for low filler loading levels since above certain amount rigid particles may hinder the PLA's chain mobility and act as obstacles for the chain folding and the growth of lamellar crystals [76, 77].

The majority of the literature studies confirmed that during the isothermal or non-isothermal melt crystallization process, the presence of CNC within the PLA matrix leads to enhanced PLA's crystallization rate [78-81]. Kamal and Khoshkava [33] reported an isothermal melt crystallization (100^{o}C) half-time of 2.2 min for 3wt.% CNC loaded PLA/CNC nanocomposites which was 16.5 min for neat PLA. Trifol et al. [82] prepared nanocomposites of PLA (2003D) with CNC, CNF (partially acetylated), and clay (C30B) through solution casting method. They dispersed the CNC in DMF with magnetic stirrer (24h, at room temperature) meanwhile separately dissolved the PLA in DMF with magnetic stirrer (2h, 70^{o}C). Then, the mixture of

CNC-DMF and PLA-DMF were mixed and sonicated for 10 min followed by casting and drying. The isothermal crystallization thermogram is shown in Figure 4.16. Faster crystallization kinetics for all nanocomposites were reported. Moreover, the degree of crystallinity of nanocomposites found to be higher especially for PLA/CNC nanocomposites and results are shown in figure 4.17.

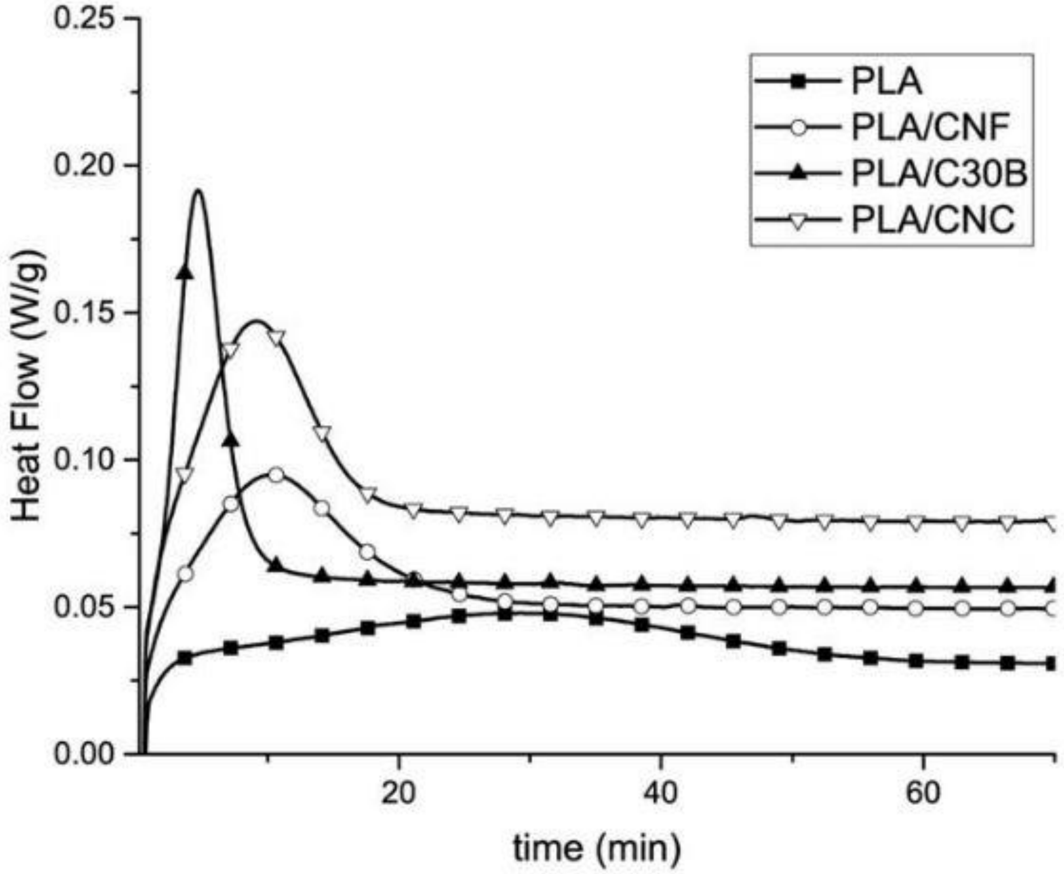

Figure 4.16: Isothermal crystallization of the nanocomposites (1wt.% - best dispersion) at 120^{o}C [85].

Bagheriasl et al. [29] studied the crystal content and crystallization temperatures of PLA/CNC nanocomposites prepared by solution casting. The results are shown in Figure 4.17. In polymer nanocomposites crystallization takes place with the competition of two phenomena. While nanoparticles act as nucleation points to increase crystal amount polymer, they also restrain the chain mobility. The final crystal content of the polymer is a result of those two competing factors. Here in Figure 4.18a, the crystal content was increased to 45 and 49% for PLA loaded with 1 and 6 wt.%. The onset of crystallization time from the cooling cycle of nanocomposites are also shown in Figure 4.18b. The crystallization temperature was shifted to higher temperatures even with the addition of CNC in small amounts.

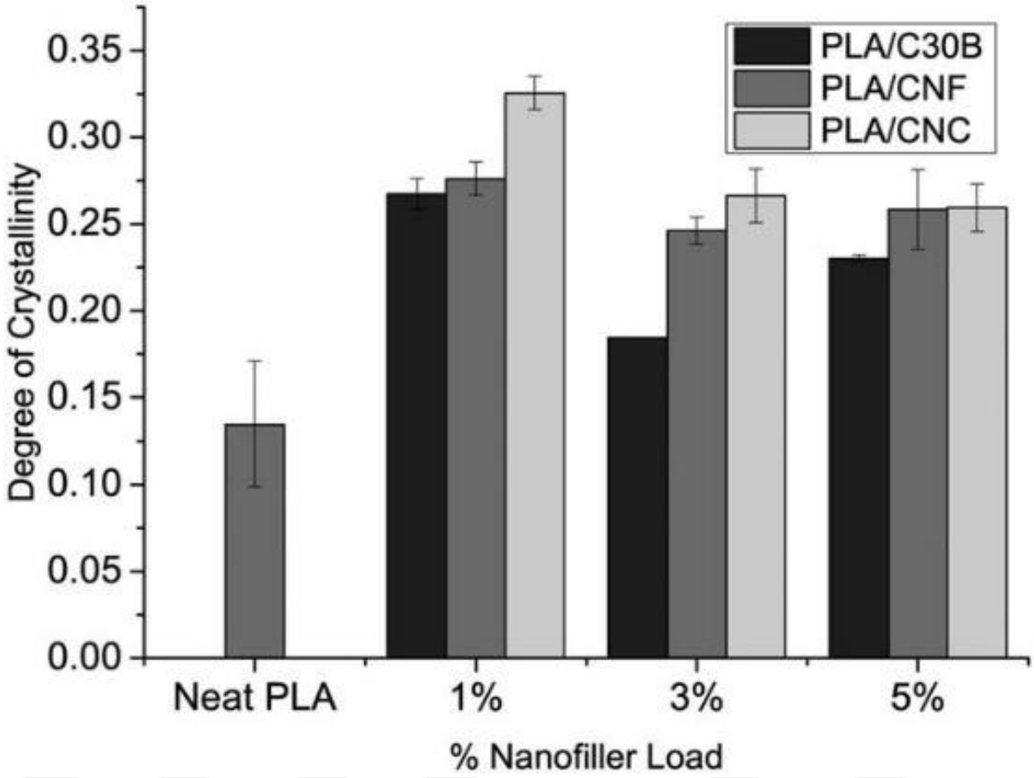

Figure 4.17: Degree of crystallinity of PLA nanocomposites with C30B, CNF, and CNC calculated from the 1st heating cycle (heat-cool-heat cycle between 0 and 200^{o}C with heating and cooling rate of 10^{o}C/min) [85].

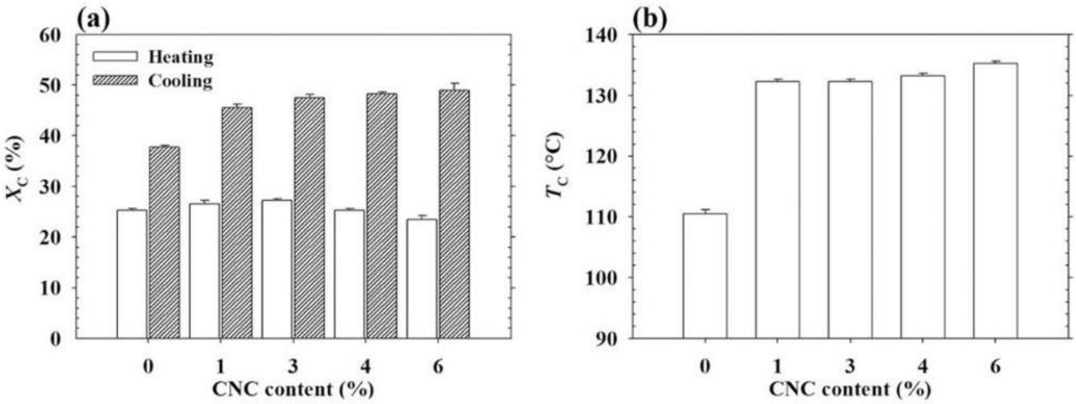

Figure 4.18: Degree of crystallinity of PLA nanocomposites with C30B, CNF, and CNC calculated from the 1st heating cycle (heat-cool-heat cycle between 0 and 200^{o}C with heating and cooling rate of 10^{o}C/min) [29].

4.5 Production of PLA/CNC Nanocomposites

One of the major concerns about PLA/CNC nanocomposite making is the achievement of a good dispersion of CNC in the PLA matrix which is very important to obtain better mechanical, thermal, crystallization, and rheological properties. However, the achievement of a good dispersion of hydrophilic CNC in non-polar PLA medium is challenging. Several studies have shown that the preparation method of PLA/CNC nanocomposite significantly affects the dispersion of CNC in PLA accordingly, the final properties of the nanocomposite. Thus, it is really important to choose a production method to obtain finely dispersed PLA/CNC nanocomposite systems. There are two main methods for making nanocomposites: melt mixing and solution casting. Those methods are extensively used to prepare PLA/CNC nanocomposites and each method results in different nanocomposite properties.

Melt mixing achieved through heating the material above its melting temperature to give the desired shape which is followed by cooling to obtain the final product. Melt mixing mainly employs the use of the twin-screw extruder (TSE) or internal mixer which are highly viable to be applied in the industrial scale. During the extrusion process required heat is externally applied to the polymer through the heaters around the barrel meanwhile the frictional force caused by the applied shear also provides heat. To completely melt the crystal structure and to obtain suitable viscosity processing temperature is set 40-50°C above the melting temperature of the material. As previously stated melt rheological properties are crucial for the melting process of PLA through TSE. However, due to the slow crystallization rate of PLA and short cycle time of melt mixing processes, PLA processed with melt mixing suffers from low crystallinity [4]. In case of the production of PLA/CNC nanocomposites through melt mixing, hydrophilic CNC should be homogeneously dispersed in nonpolar PLA media. However, researches have shown that the shear or elongational force of melt mixing is not enough to deagglomerate hydrophilic CNC particles and disperse them in the non-polar PLA matrix [16].

The solution casting process is applied through the dissolution of PLA and dispersion of CNC particles in an appropriate solvent then casting which is followed by evaporation of the solvent. To dissolve PLA, a solvent with a solubility parameter close to that of PLA will be used with heat if necessary. On the other hand, the same solvent should be suitable to disperse polar and hydrophilic CNC or CNC will be separately dispersed in another suitable solvent. The studies have shown that although solution casting is not industrially viable as melt mixing, it is successful to deagglomerate the CNC to develop a network inside PLA medium. Bagheriasl et al. [28] compared the effect of melt mixing and solution casting on CNC dispersion. Solution cast PLA/CNC nanocomposites were prepared by first dispersing the freeze-dried CNC in DMF using a bath sonicator (2 hours) and then using a magnetic stirrer (150 min) to dissolve PLA in CNC-DMF mixture which was followed by drying in a vacuum oven at 80°C for 36 hours. Melt mixing was employed by using an internal mixer where PLA and CNC are added to the internal mixer and melt-processed at 180 °C with 100 rpm (7 min, under N_2 atmosphere). The rheological analysis of PLA/CNC nanocomposites produced with melt mixing and solution casting methods are shown in Figure 4.19. Although two nanocomposites have the same amount of CNC content, the one processed with melt mixing exhibits a complex viscosity behavior similar to that of neat PLA. The wide plateau indicates the melt mixing was not successful to disperse CNC. On the other hand, the complex viscosity and storage modulus of solution cast nanocomposite gradually increases as the shear rate decreases. This increase at low shear rate resulted from the network formation of CNC and indicates the molecular interaction between PLA and CNC. Moreover, through these rheological analyses, the success of solution casting to finely disperse CNC could be interpreted.

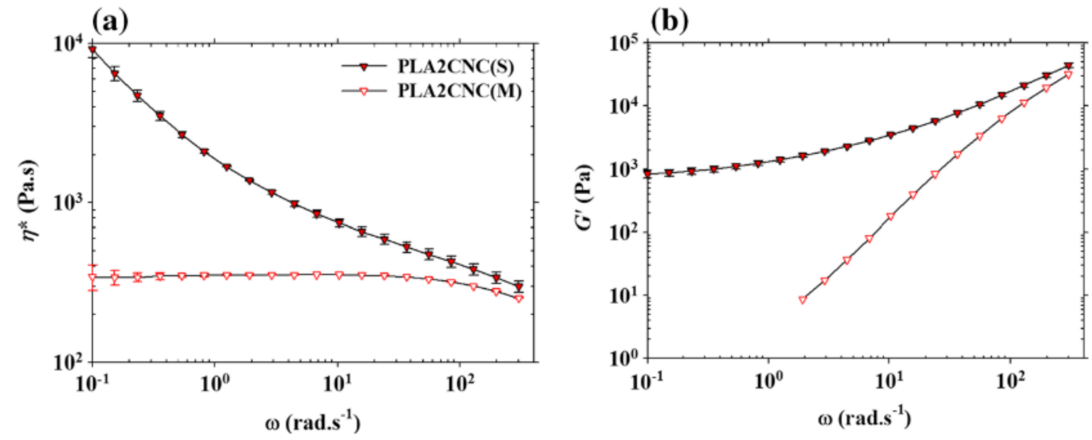

Figure 4.19: Complex viscosity (a) and storage modulus (b) of two different PLA/CNC nanocomposites with same amount of CNC content one produced with solution casting (S) and the other produced with melt mixing (M) [28].

4.6 Achievements in Development of PLA/CNC Nanocomposites

It was clearly shown that the solution casting method is more successful to develop a well-dispersed PLA/CNC nanocomposite which is crucial for mechanical, thermal, and crystallization properties of the material. Accordingly, the solution casting method has been extensively studied for PLA/CNC nanocomposites. Different studies searched the effects of various parameters. This study focuse on the studies about PLA/CNC nanocomposites without any additive or surface treatment for a better understanding of the effect of solution casting parameters and drying type of CNC on dispersion kinetics of CNC and crystallization behavior, thermal properties, and rheological properties of the nanocomposite. Important achievements about PLA/CNC nanocomposites that reveals key factors about preparation are listed below. These studies are significant since they don't employ surface modification, the addition of chain extender, or compatibilizer.

Bagheriasl et al. [31] prepared PLA/CNC nanocomposites by first preparing masterbatches through solution casting then diluting with TSE. Direct melt mixing resulted in fibrillar shaped CNC agglomerates while the combined method achieved smaller agglomerates. They also studied the rheological behavior of two different nanocomposites and an increase in complex viscosity at low shear rates for nanocomposites diluted from masterbatch was reported which is an indication of CNC network development. Arslan et al. [83] comprehensively compared the efficiency of solution casting, direct melt mixing, and a combination of solution casting with TSE to produce PLA/CNC nanocomposites. TEM and SEM images in Figure 4.20 show the morphological analysis of nanocomposites with 5wt.%CNC. TEM images indicate that the solution casting method resulted in much better CNC dispersion and the mTSE method resulted in some level of agglomeration. This was attributed to the fact that strong hydrogen bonds between CNC particles in solution cast masterbatch caused re-agglomeration during TSE process. However, the success of mTSE method was found to be much higher than the direct melt mixing method. SEM images of directly melt mixed nanocomposite with 5wt.% indicate large CNC agglomerates in Figure 4.20.

The effect of PLAs molecular weight and crystallinity on rheological and crystallization properties of PLA was extensively studied by Vatansever et al. [17]. Four different PLAs was used as a matrix: semi-crystalline high and low molecular weight PLA and amorphous high and low molecular weight PLA. The rheological analysis revealed that the dispersion of CNC in crystalline PLA was the best in semi-crystalline low molecular weight PLA. It was explained that since CNC act as nucleating points for semi-crystalline PLA, the formation of crystalline regions locks the CNC particles thereby prevent their re-agglomeration. The rheological percolation threshold was reported to be 2.8%.

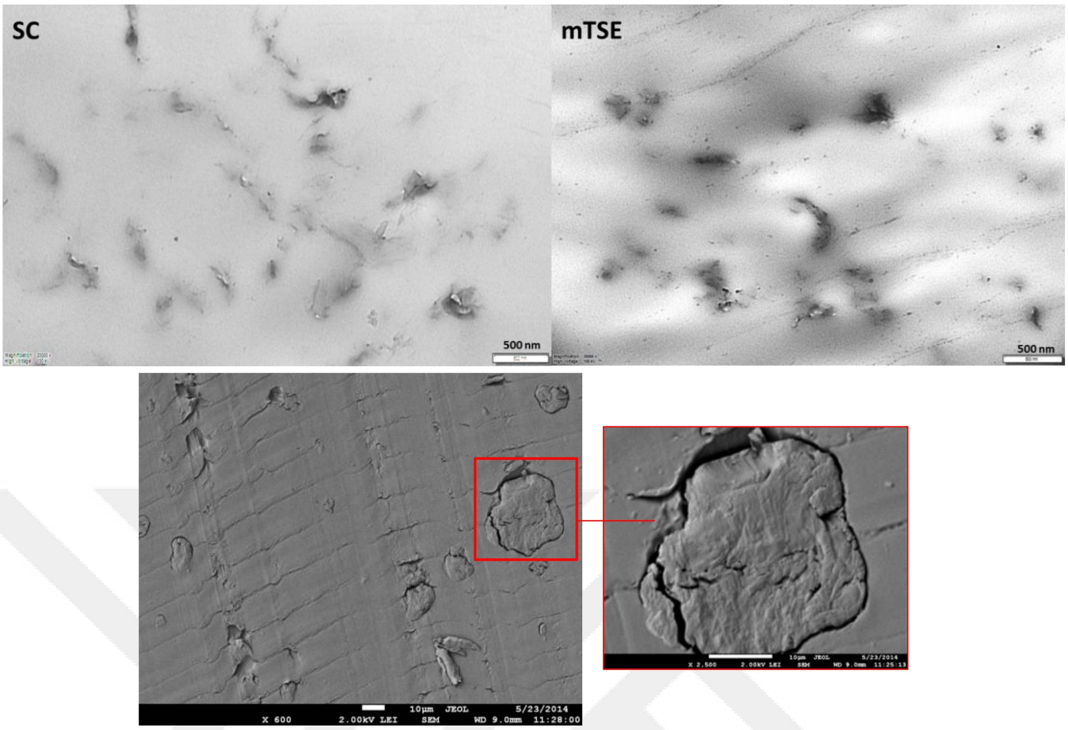

Figure 4.20: TEM images of solution casted (SC) and masterbatch diluted (mTSE) PLA nanocomposites with 5 wt% CNC (top row) and SEM images of the directly melt mixed PLA with 5 wt% CNC through a TSE (bottom row) [83].

As previously explained spray drying involves the atomization of the CNC suspension into a hot (>100°C) chamber which results in micron-sized powder form. The agglomeration during spray drying is governed by capillary, hydrogen-bonding, and van der Waals forces. Spray freeze drying method is commercially used in ceramic, food and pharmaceutical industries. Studies have shown that due to porous structure of spray freeze dried CNC (CNCSFD), a good level of dispersion of spray freeze dried CNC by melt mixing in polymer melts was possible [32]. Khoshkava and Kamal [33] compared the dispersion of the spray dried (CNCSD) and CNCSFD in PLA matrix using melt mixing method. SEM micrographs of PLACNCSD, and PLACNCSFD and TEM images of PLACNCSFD3 (7wt.%) and CNC particles are shown in Figure 4.21. The agglomerates of spray-dried CNC were observed in PLA (Figure 4.21a) since polymer couldn't infiltrate into compact CNCSD particles. Well dispersion of CNCSFD3 in PLA was achieved (Figure 4.21 b and c) due to the porous structure of CNCSFD3 enabled polymer infiltration into CNC particles. TEM image of PLA/CNCSFD3 and individual CNC (Figure 4.21d and e) shows that deagglomeration took place. The storage modulus versus strain graph of nanocomposites with different loadings for PLACNCSFD3 is shown in Figure 4.22. The narrowing in linear viscoelastic regions of samples with increasing CNC loading indicates network formation resulted from the deagglomeration of CNCSFD3.

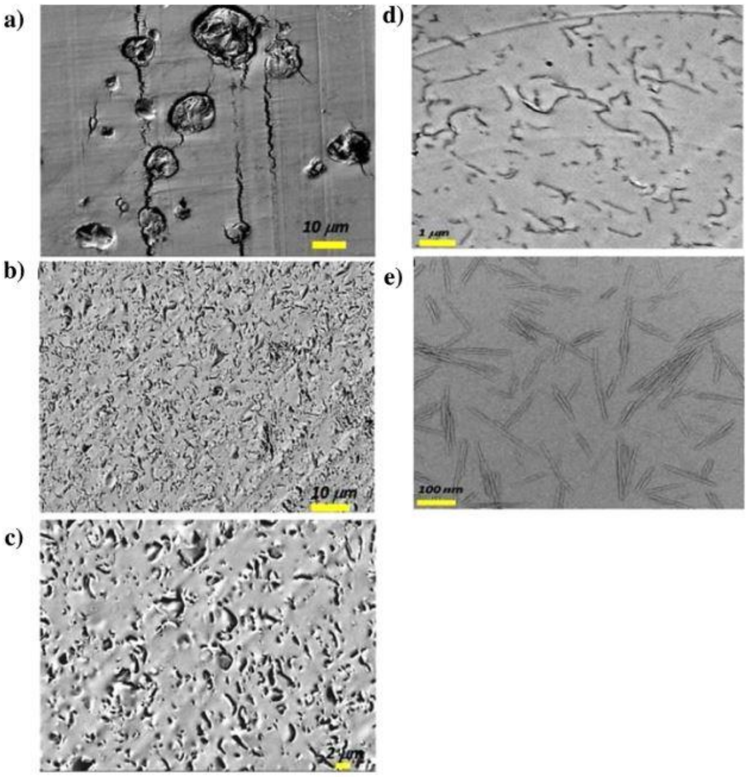

Figure 4.21: SEM micrographs of PLACNCSD (a), PLACNCSFD3 (b), and higher mag. of b (c) with 7wt.% loading. TEM images of PLACNCSFD3 (d) with 7wt.% loading and individual CNC (e) [33].

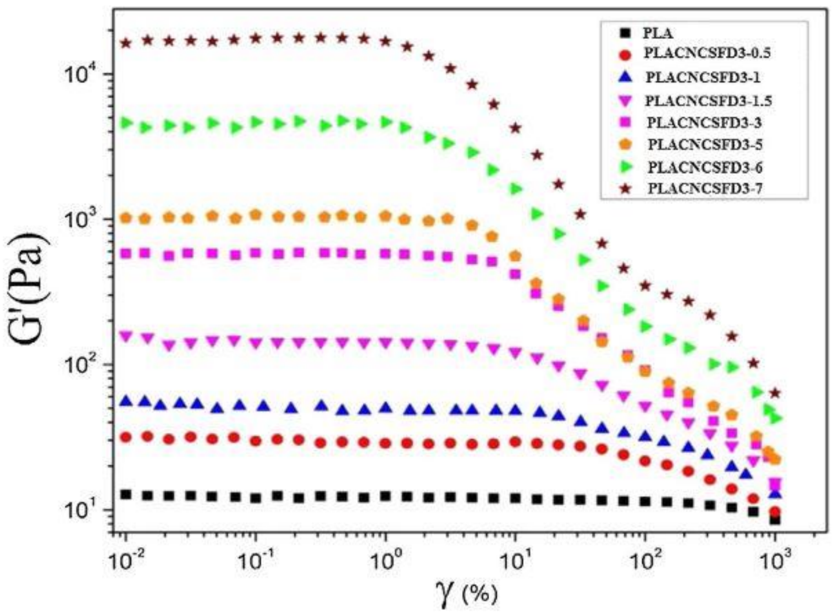

Figure 4.22: Strain sweep graph of neat PLA and PLACNCSFD3 with different CNC loading [33].

5. EFFECT OF SOLUTION CASTING PARAMETERS ON CNC DISPERSION

The outstanding success of the solvent casting method to obtain well dispersion of CNC in PLA without the use of any treatment or additive was proved by different researches [17, 28, 30]. However, strong interparticle interactions of CNCs still challenge its dispersion in hydrophobic PLA media [14, 16, 17]. Thus, the parameters of the solution casting process strongly influence the dispersion quality of the CNCs. A summary of the studies that employed the solution casting method to prepare PLA/CNC nanocomposites without the use of any additional treatment is given in Table 5.1. However, the literature of solution cast PLA/CNC nanocomposites varies in terms of instruments (tip sonicator or bath sonicator), duration and sequence of the applied process, type of PLA and CNC, and type of solvent.

The solvent to be used must be suitable to dissolve PLA and to disperse CNC. However, due to their electrostatic character (surface charges) and strong hydrogen bonding between CNC particles, cellulose nanocrystals tend to agglomerate in nonpolar solvents. Thus, their dispersion is possible in aqueous suspensions or organic solvents with high dielectric constant [84]. As a result, to choose the most suitable solvent, the characteristics of both PLA and CNC must be considered to obtain effective dispersion without CNC surface modification or compatibilizer. Some of the solvents commonly used to prepare PLA/CNC nanocomposites are tetrahydrofuran (THF), chloroform (CHL), dimethylformamide (DMF), and dimethyl sulfoxide (DMSO). The solubility parameters of these solvents are close to that of PLA which is 10 $(cal/cm^3)^{1/2}$ [85]. Hildebrand solubility parameter, δ, is an important solvent property that defines the work that is needed to separate the solvent molecules to form a cavity that is large enough to incorporate the solute. The solubility parameter of the gas phase is equal to zero while the value of δ is much higher for highly ordered solvents. To determine the suitable solvent for a non-electrolyte material, the δ values should be similar. The polarity of solvents which is a qualitative parameter is also an important factor. THF, DMF, and DMSO are polar aprotic solvents. Polar aprotic solvents accept hydrogen bonds and characterized by their high dielectric constant and high dipole moments. Among the polar aprotic solvents listed in Table 5.2, DMSO has the highest dielectric constant. DMF also has a high dielectric constant but, the value is much lower for THF. Chloroform is a nonpolar aprotic solvent which means molecules have a net dipole moment of zero. Another important characteristic of solvents is the dielectric constant which defines its ability to separate negative charges. DMSO and DMF have the highest dielectric constants among those four solvents [86]. The other important physical properties of those solvents are also listed in Table 5.2.

As shown almost all of the study differs in terms of the type of material, type of instrument (magnetic stirrer, bath sonicator, and tip sonicator), duration, and temperature. The situation makes it impossible to compare the effect of solvent, process parameters, or type of CNC. This study aims to investigate the effects of solvent and the preparation method on the dispersion of both SCNC and FCNC in PLA. Moreover, the rheological and thermal properties of nanocomposites are also aimed to be studied.

Table 5.1: A review of studies employed solution casting to prepare PLA/CNC nanocomposites without use of any treatment or additive.

Study	PLA	CNC	Method	Results
Pei et al.[71]	Biomer L9000 (PLLA)	CNC and partially surface silylated CNC (SCNC)	PLLA Chloroform (MS, RT) CNC Chloroform PLLA-CNC Chloroform (MS, 4h) Vacuum drying (RT, 48h)	agglomeration of CNC, deagglomeration of SCNC, 16.4% crystallinity in CNC1, 30.4% crystallinity in SCNC
Khoo et al.[87]	Ingeo 3051D	CNC (in suspension)	CNC Chloroform (MS) PLA Chloroform (MS) PLA-CNC Chloroform (MS) Drying (RT, 24h)	27.7% crystallinity in CNC1, 34.5% crystallinity in CNC5, 30.9% crystallinity in neat PLA
Trifol et al.[82]	Ingeo 2003D	CNC (in suspension)	CNC DMF (MS, RT, 24h) CNC DMF (CF, 1500rpm, 10min)* PLA DMF (MS, 70ºC, 2h) PLA-CNC DMF (SC, 200W, 10min) Drying (80ºC, 15h) Vacuum Drying (50ºC, 24h)	~32% crystallinity in CNC1, ~13% crystallinity in neat PLA, shorter isothermal crystallization time, improved storage modulus (DMA)
Bagheriasl et al.[28]	Ingeo 3251D	Freeze-dried CNC	CNC DMF (WS, 100 Watts, 2h) PLA CNC-DMF (MS, 70ºC, 150min) Vacuum drying (80ºC, 36h)	Improved rheological properties, percolation conc. of 0.68wt.% CNC
Bagheriasl et al.[29]	Ingeo 3251D	Freeze-dried CNC	CNC DMF (WS, 100 Watts, 2h) PLA CNC-DMF (MS, 70ºC, 150min) Vacuum drying (80ºC, 36h)	Improved rheological properties, 23% enhancement in Young modulus, 74% increase in storage modulus
Heshmati et al.[30]	Ingeo 3001D	Spray-dried CNC	CNC DMF (WS, 100 Watts) PLA-DMF CNC-DMF (MS, 50ºC, 2h) Vacuum drying of film (80ºC, 48h) Vacuum drying of powder (60ºC, 48h)	Improved rheological properties in PLA/CNC nanocomposites
Vatansever et al.[17]	CH 2500HP CL 3001D AH 4060D AL 8321D	Spray-dried CNC	CNC DMF (WS, 2h) PLA CNC-DMF (MS, 70ºC, 150min) Vacuum drying of film (85ºC, 36h) Vacuum drying of powder (85ºC, 48h)	Low molecular PLA enhance crystallization and decrease percolation treahold, better CNC dispersion in CL PLA. Percolation con. of 2.8wt.% in CL PLA

*to seperate aggregates, MS: magnetic stirrer, WS: water sonicator, SC:Tip sonicator, CH: semicrystalline high M_w, CL: semicrystalline low M_w, AH: amorphous high M_w, AL: amorphous low M_w,

Table 5.2: Some of the important properties of solvents commonly used to dissolve PLA [85, 88]

Solvent	Molecular Formula	Solubility Parameter δ, $(Cal/cm^3)^{1/2}$	Polarity	Dielectric constant, ε	Boiling Point (ºC)	Viscosity, η (mPa.s)	Electrical conductivity $(\mu S.cm^{-1})$	Surface Tension, σ (mN/m)
DMF	C_3H_7NO or $HCON(CH_3)_2$	12.1	Polar Aprotic	36.7	153	0.92	6.00E-02	35
CHL	$CHCl_3$	9.3	Apolar Aprotic	4.8	61	0.563	1.00E-04	27.2
THF	C_4H_8O or $(CH_2)_3CH_2O$	9.1	Polar Aprotic	7.6	66	0.48	4.50E+01	28
DMSO	C_2H_6OS or $(CH_3)_2SO$	13	Polar Aprotic	48.9	189	2.47	3.00E-08	43.54

6. EXPERIMENTAL PROCEDURE

6.1 Materials

The PLA used in this study was supplied by NatureWorks® IngeoTM (3251D Injection Molding Grade) with a D-content of 1.4 mol% and MFR of 80g/min (210^{o}C) [14]. PLA 3251D was chosen due to its low molecular weight and low D-content which enables high crystallization ability to obtain enhanced CNC dispersion and final crystallinity [17]. Spray-dried cellulose nanocrystals (SCNC) and freeze-dried cellulose nanocrystals (FCNC) were kindly provided by Cellular Force (Canada) and FPInnovations (Pointe Claire, Canada), respectively. Tetrahydrofuran (THF) with 99%, Chloroform (CHL), Dimethylformamide (DMF) with 99 %, and Dimethyl Sulfoxide (DMSO) with 99% purity as the solvents were purchased from Sigma-Aldrich.

6.2 Preparation of PLA/CNC Nanocomposites

Preparation methods are summarized in Table 6.1. Preparation of PLA/CNC nanocomposites with different solvents done by first dispersing CNC in the solvent by using a bath sonicator at room temperature. Then, PLA was added to the CNC solvent mixture and further mixed with a magnetic stirrer. Bath sonication was conducted at room temperature for all samples while magnetic stirring was achieved at proper temperatures according to the type of solvent. The magnetic stirring temperature was 55^{o}C for CHL and THF since PLA is soluble in them. Since PLA isn't soluble in DMF and DMSO, the temperature was above the T_g of PLA. It was 75^{o}C for DMF and 95^{o}C for DMSO. After magnetic stirring, PLA and CNC mixtures poured into petri dishes and left to dry under fume hood for 2 days followed by 2 days (5 days in case of DMSO) of vacuum drying at 85^{o}C. Then, the dried films peeled from petri dishes and ground with a coffee grinder. Powders were further vacuum dried at 85^{o}C for 2 days.

The disk shape rheological samples (25mm diameter and 1.5mm thickness) of nanocomposites were prepared through the compression molding of powders. Before compression molding, the powders were vacuum dried overnight at 55ºC. The molding was conducted at 190°C for 5 minutes by gradually increasing the pressure up to 1.5 tons. After 5 minutes, the samples were fast cooled with water circulation before being taken out from the mold.

The effect of the solvent was compared by considering the methods labeled with 1, 2, 3, and 4 in Table 6.1. The most successful solvent in terms of CNC dispersion was select to compare the effect of preparation method especially the effect of bath sonication. Thus, three more different preparation methods with varying bath sonication time and sequence were used labeled as 5, 6, and 7. To see the effect of drying type of CNC, PLA/CNC nanocomposites with both SCNC and FCNC with a fixed 3 wt.% CNC content were prepared with each seven methods. After the selection of best solvent, and preparation method, CNC nanocomposites with varying loadings were prepared.

Table 6.1: Preparation methods.

	Solvent	Preparation		Temperature	Drying
1	Chloroform	CNC + Chloroform	WS, 2h	RT	Drying under fume hood (RT 2D), Vacuum drying of film (85ºC, 2D), Vacuum drying of powder (85ºC, 2D)
		PLA + CNC Chl. Mixture	MS, 2.5h	55ºC	
2	THF	CNC + THF	WS, 2h	RT	
		PLA + CNC THF Mixture	MS, 2.5h	55ºC	
3	DMF	CNC + DMF	WS, 2h	RT	
		PLA + CNC DMF Mixture	MS, 2.5h	75ºC	
4	DMSO	CNC + DMSO	WS, 2h	RT	Drying under fume hood (RT 2D), Vacuum drying of film (85ºC, 5D), Vacuum drying of powder (85ºC, 2D)
		PLA + CNC DMSO Mixture	MS, 4h	95ºC	
5	DMSO	CNC + DMSO	WS, 0h	-	
		PLA + CNC DMSO Mixture	MS, 4h	95ºC	
6	DMSO	CNC + DMSO	WS, 4h	RT	
		PLA + CNC DMSO Mixture	MS, 4h	95ºC	
7	DMSO	CNC + DMSO	WS, 2h	RT	
		PLA + CNC DMSO Mixture	MS, 4h	95ºC	
		PLA CNC DMSO Mixture	WS, 2h	RT	

6.3 Characterization

6.3.1 Rheological Analysis

Rheological properties of nanocomposites were determined in small amplitude oscillatory shear (SAOS) by using an MCR-301 rotational rheometer (Anton Paar, Austria) (Fig. 6.1) equipped with a parallel-plate geometry (plate diameter 25mm) with a gap of 1 mm. All of the rheological experiments were conducted at 190^{o}C under the nitrogen atmosphere.

The linear viscoelastic region of sample nanocomposites determined with small amplitude oscillatory shear (SAOS) experiments in which strain sweep from 0.01 to 100% was applied with a constant frequency of 1rad/s. The linear viscoelastic region is defined by a 5% decrease in the viscoelastic properties (storage modulus, G'). To be in the LVR for all nanocomposites strain amplitude of 0.3% (0.003) was selected to conduct a frequency sweep experiment. Frequency sweep experiments were conducted from 668 to 0.1 rad/s. The strain amplitudes were 5% for neat PLAs and 0.3% for nanocomposites.

Time sweep experiments were conducted to investigate the thermal stability of samples at constant angular frequency of 1 rad/s. The strain amplitude was 5% for neat PLAs and 0.3% for NCs.

Figure 6.1: Anton Paar MCR 302 Rheometer.

6.3.2 FTIR analysis

FTIR spectra of the neat PLA prepared with different solvents were recorded at room temperature in the mid-IR range (400 – 4000 cm^{-1}) by using a Bruker FTIR spectrometer equipped with a Bruker Platinum ATR accessory. All of the measurements were conducted on dry, powder films obtained after vacuum drying of ground powders. Each spectrum was taken over 12 scans with a resolution of 2 cm^{-1}. The results were analyzed using OPUS Software (Bruker Optics).

6.3.3 Differential scanning calorimetry (DSC)

After selecting the best solvent, preparation method, and CNC the non-isothermal crystallization kinetics were analyzed using a TA Instruments Q1000 series DSC under nitrogen. The heating steps were as followed: the nanocomposites were first heated from room temperature to 200°C at a heating rate of 10^{o}C/min and remained for 5 min to remove the thermal history of the samples Then, the samples were then cooled to 25 °C at a cooling rate of 2^{o}C/min. The samples were again reheated to 200 ^{o}C at a heating rate of 10^{o}C/min.

7. RESULTS AND DISCUSSION

The rheological properties of nanocomposites studied to understand the effect of nanoparticles on the viscoelastic properties of polymer accordingly, its processability. Moreover, rheological analysis has been extensively used to study the dispersion of CNC in the PLA matrix since the direct microscopic analysis of organic nanoparticles in organic PLA medium is challenging [14, 17, 28, 32].

To be consistent in each rheological test in terms of eliminating the effect of strain or stress, at first, the linear viscoelastic region (LVR) should be determined which is defined as where 5% reduction in viscoelastic properties occurs [32, 33]. The LVR of nanocomposites were determined using strain sweep tests with strain sweep from 0.01 to 100% at a constant frequency of 1 rad/s and it was determined as 0.3% of strain amplitude for nanocomposites and as 5% for neat PLAs.

The nonisothermal crystallization on nanocomposites were also characterized to see the effect of SCNC, FCNC, and amount of SCNC on crystallisation kinetics.

7.1 The effect of solvent

To investigate the effect of solvent on CNC dispersion, the amount of CNC was fixed at 3wt.%. Moreover, each nanocomposite was prepared with both SCNC and FCNC to see the effect of the CNC drying method on dispersion.

Complex viscosity as a function of neat PLA and nanocomposites prepared with different solvents are presented in Figure 7.1. The complex viscosity of the nanocomposites prepared with THF, slightly increased in total compared to neat PLA. However, they revealed linear behavior over the whole strain range which is a characteristic of liquids. Although THF is a polar solvent due to its low dielectric constant it was not much effective to disperse CNC. Complex viscosities of nanocomposites prepared with CHL is much lower compared to that of neat PLA. CHL as being both apolar and having low dielectric constant can not deagglomerate the CNC thus, agglomerates in the structure resulted in poor viscoelastic properties than that of neat PLA. Nanocomposites prepared with DMF and DMSO revealed significant improvements. The nanocomposites prepared with DMF revealed higher complex viscosity in total compared to neat PLA, with a slightly narrow down in plateau region. The narrow linear region in viscoelastic properties in strain sweep experiments is an indication of solid-like behavior and an indication of CNC network formation [33]. The complex viscosity of nanocomposites prepared with DMSO is greatly increased and the plateau region becomes narrower. For the following rheological experiments, the strain amplitude is determined as 0.3% for nanocomposites and as 5% for PLA which are in the linear viscoelastic region.

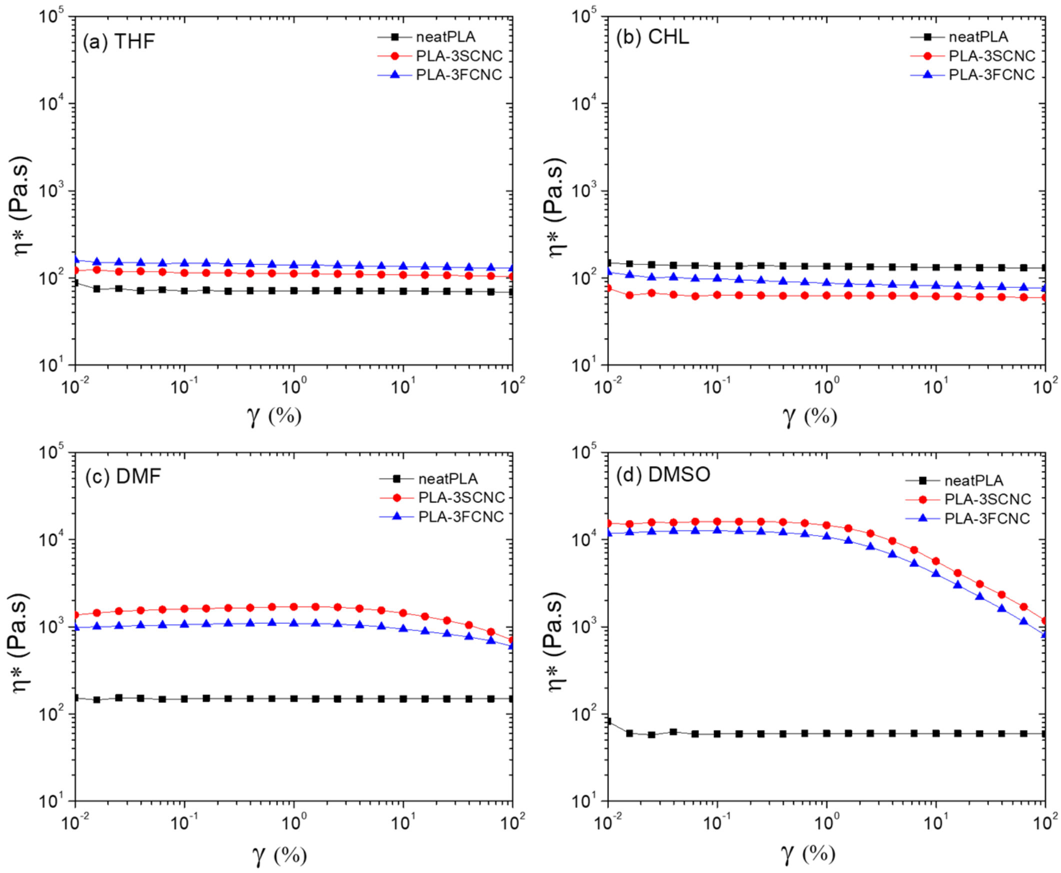

Figure 7.1: Complex viscosity as a function of strain for neat PLA, PLA3SCNC and PLA3FCNC prepared with (a) THF, (b) CHL, (c) DMF, and (d) DMSO.

The frequency sweep experiments were conducted with a strain amplitude of 0.3% for nanocomposites and 5% for neat PLAs. Results of frequency sweep experiments of neat PLAs and nanocomposites prepared with different solvents are presented in Figure 7.2. All the four neat PLAs prepared with different solvents revealed Newtonian behavior over a wide range of frequency (the change in complex viscosities of PLAs prepared with different solvents is discussed under the section 7.1.1). The complex viscosities of nanocomposites prepared with THF are slightly increased in total compared to neat PLA. However, the nanocomposites revealed Newtonian behavior over a wide range of frequency and slight shear thinning at high frequencies. Which is consistent with strain sweep experiments. Although THF is a polar solvent due to its low dielectric constant it resulted in a poor level of dispersion. The complex viscosity of NCs prepared with CHL is much lower since the apolar CHL having low dielectric constant can not deagglomerate the CNCs. Thus, the CNC network on a molecular level can not be obtained. Figure 7.3 presents the visual appearance of PLA/SCNC and PLA/FCNC NCs prepared with CHL. The huge aggregates are visible with the naked eye exist in both PLASCNC and PLAFCNC. It is clear evidence that the deagglomeration of CNC couldn't be achieved with chloroform.

The overall complex viscosities of nanocomposites prepared with DMF and DMSO increased compared to that of neat PLAs. Moreover, complex viscosity of NCs prepared with DMF and DMSO sharply increased at low frequencies and revealed a strong shear-thinning behavior without the plateau region. In nanocomposites, the increase in complex viscosity at lower frequencies indicates the increased interfacial interactions of molecules of matrix and nanoparticles resulted from the homogeneous dispersion of nanoparticles [14]. With consistency with the polar nature of DMSO and highest dielectric constant compared to other solvents, it was successfully deagglomerate the polar CNC and revealed the highest improvement.

The difference between PLA/SCNC and PLA/FCNC nanocomposites is insignificant in THF and CHL while PLA/SCNC nanocomposites have slightly higher viscoelastic properties in NCs prepared with DMF and DMSO.

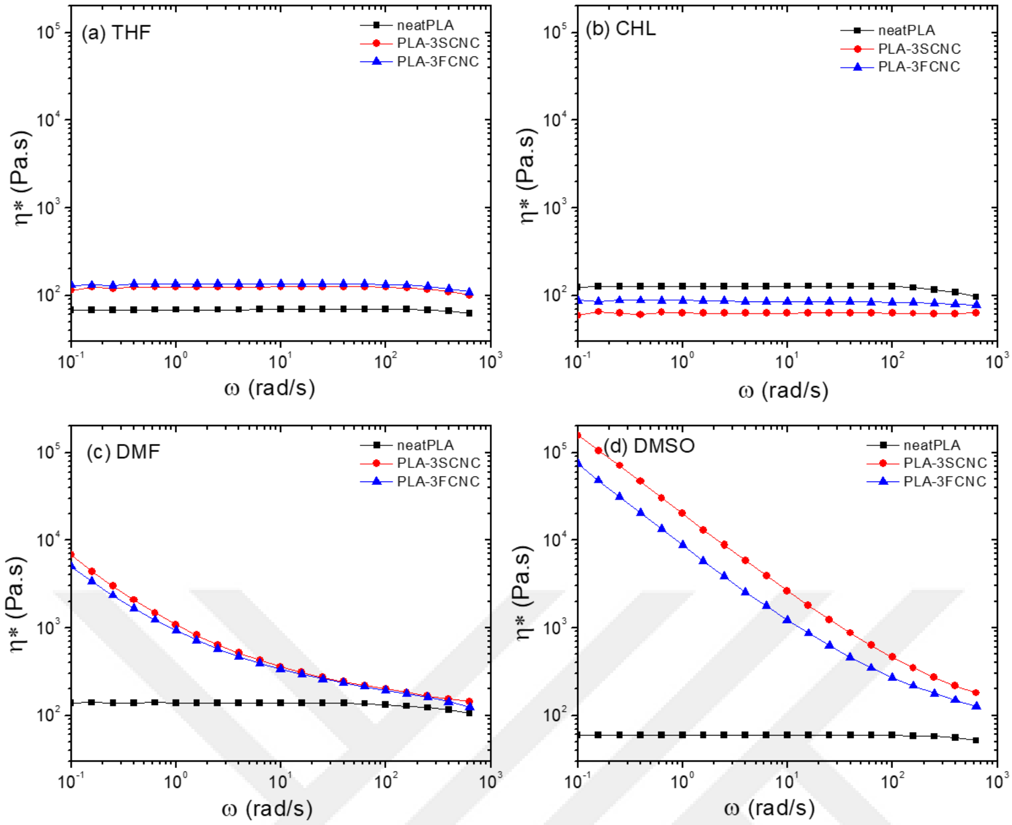

Figure 7.2: Complex viscosity as a function of frequency for neat PLAs and nanocomposites prepared with prepared with (a) THF, (b) CHL, (c) DMF, and (d) DMSO.

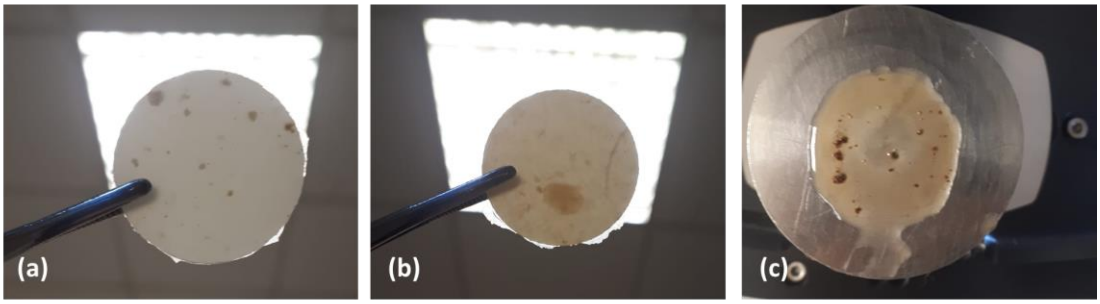

Figure 7.3: Visual appearance of nanocomposites prepared with CHL (a) PLA3SCNC, (b) PLA3FCNC, and (c) PLA3SCNC after frequency sweep test.

The visual appearance of the nanocomposites prepared with different solvents is shown in Figure 7.4. The ones on top rows show PLA3SCNC while the ones below show PLA3FCNC nanocomposites. Both PLA3SCNC and PLA3FCNC prepared with DMF and DMSO revealed a darker appearance. The nanocomposites prepared with chloroform contain agglomerates.

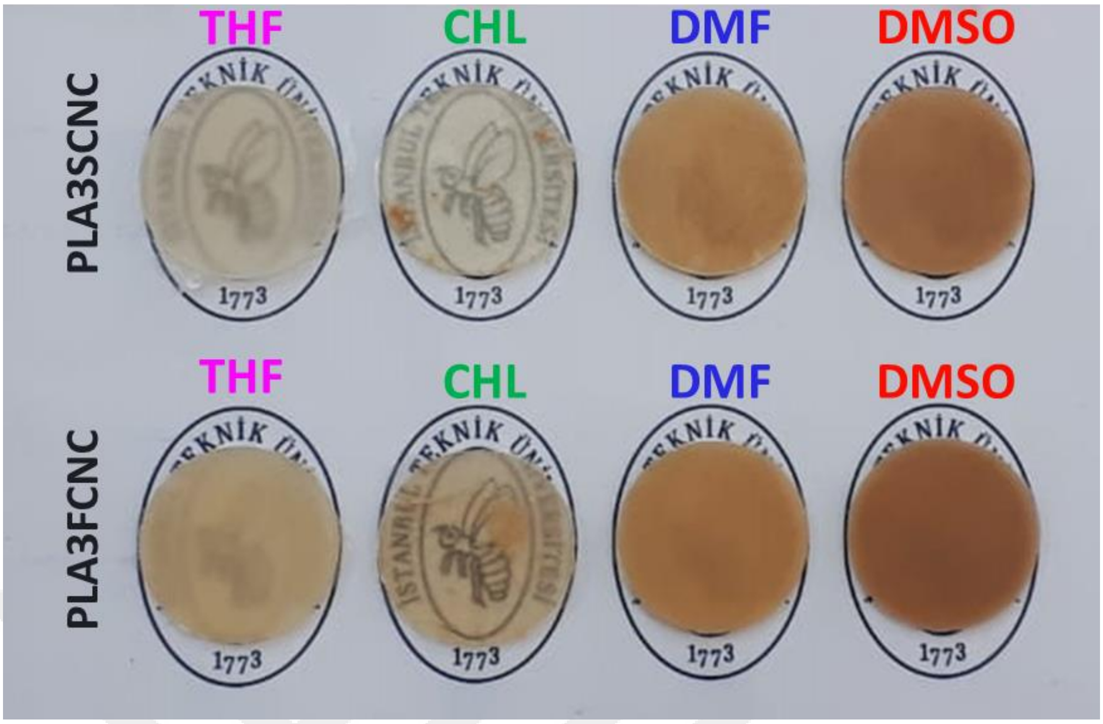

Figure 7.4: Visual appearance of nanocomposites prepared with different solvents. Upper row: PLA3SCNC and Lower row: PLA3FCNC

7.1.1 Time sweep experiment and thermal stability

The visiual appearance of NCs (Fig. 7.4) revealed a brownish appearance with increased CNC dispersion. To be sure whether this brownish colur is resulted from the CNC dispersion or thermal degradation the neat PLA and PLA-3SCNC samples prepared with DMF and DMSO were subjected to time sweep test. The time sweep experiments conducted at 190^{o}C for 20 min. To observe the color change the visual appearances of each samples are reported before and after the time sweep test. Figure 7.5 shows the change in complex viscosity versus time for neat PLAs and PLASCNC nanocomposites (3wt.%) prepared with DMF and DMSO. The changes in complex viscosity of samples are indicated on figure. The changes were found to be below 10% for all samples which are in acceptable range. The visual appearances of samples before (a) and after (b) the time sweep experiment are presented in Figure 7.6. The colors of the samples before and after the time sweep test seem to be same. The time sweep experiments were conducted at 190^{o}C for 20 min and the applied heat during production was much lower and during compression molding the duration is much lower (5 min). Thus, it could be said that the darker appearance of NCs resulted from the CNC dispersion and not from the thermal degradation of PLA or CNC.

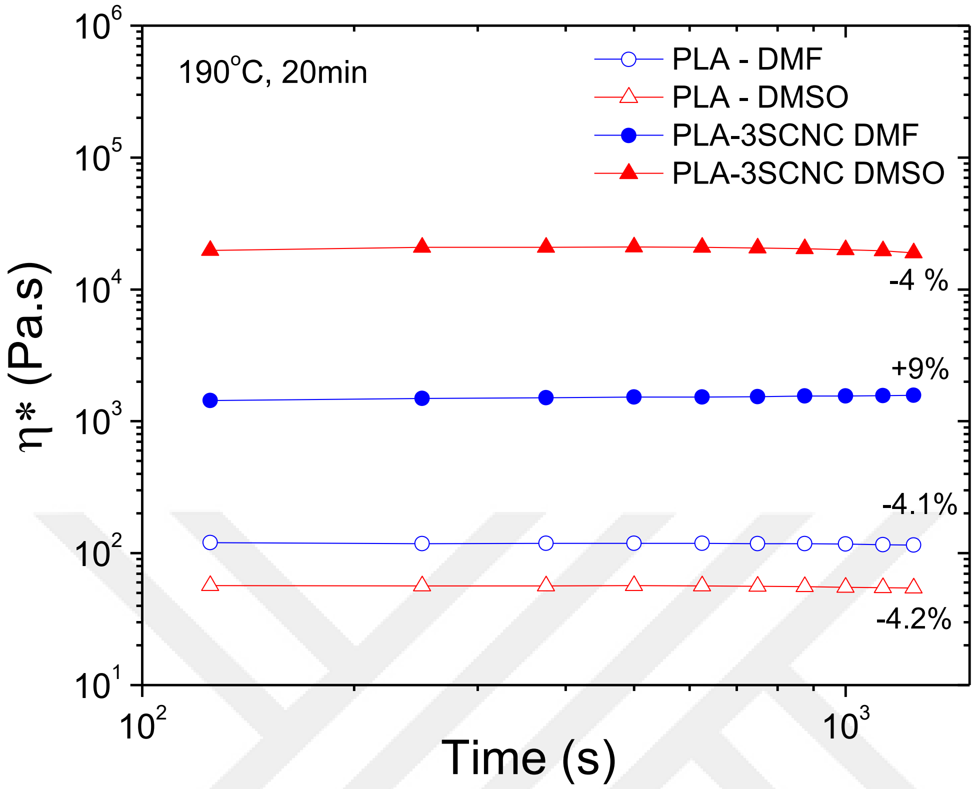

Figure 7.5: Time sweep results for neat PLAs and PLA-3SCNC NCs prepared with DMF and DMSO (angular frequency = 1 rad/s, strain amplitude = 5% for neat PLAs and 0.3% for NCs).

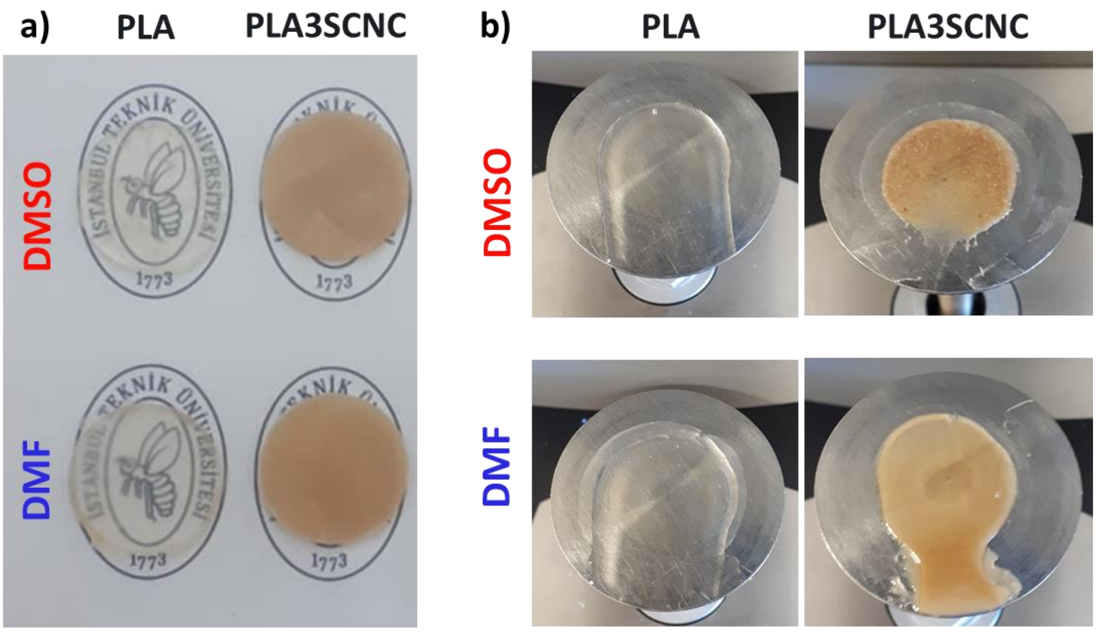

Figure 7.6: The visual appearances of neat PLA and PLASCNC NCs prepared by DMF and DMSO a) before and b) after the time sweep tests.

7.1.2 The decrease in rheological properties of neat PLAs and FTIR analysis

Figure 7.7 shows the complex viscosity of unprocessed PLA and neat PLAs prepared with different solvents. Although one type of PLA is used in this study, the rheological properties differ in neat PLAs. A decrease is observed in rheological properties of processed PLAs compared to the unprocessed PLA which could be attributed to the presence of solvent. To investigate the traces of solvent in PLA matrix, FTIR analysis was done and results are shown in Figure 7.8. The intensities were normalized to one with respect to the main peak of neat PLA at (~1083cm^{-1}). The main difference in spectra exists around ~2750 and ~3500. Figure 7.9 shows the intensities in the range of ~2750 and ~3200. The triple peaks of PLA at 2853, 2921, and 2998 are the C-H vibrations of PLA. CHL, THF, DMF, and DMSO also have C-H vibrations around 3000. The C-H triplet of PLA is shifted in PLAs prepared with different solvents and the weak vibration at 2853 seems to be disappeared or weakened. The shift in C-H vibrations could be attributed to the interaction of solvent molecules and PLA molecules. Thus, consistent with the rheological results (Figure 7.7) it could be concluded that solvents haven't completely removed. DMSO and DMF have high

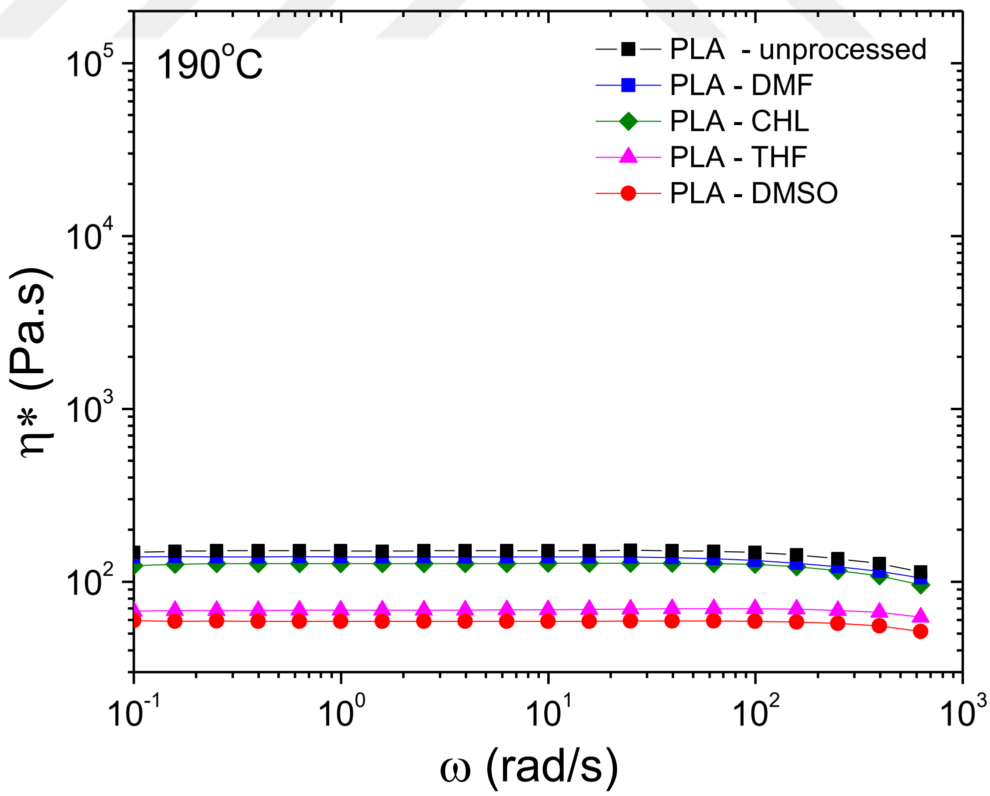

Figure 7.7: Complex viscosity of unprocessed PLA and neat PLAs processed with different solvents.

boiling points (189 and 153°C, respectively) which makes it hard to completely remove from the films. Although, THF have much lower boiling points (66 and 61°C respectively) due to good secondary interaction between THF and PLA, THF can not removed completely.

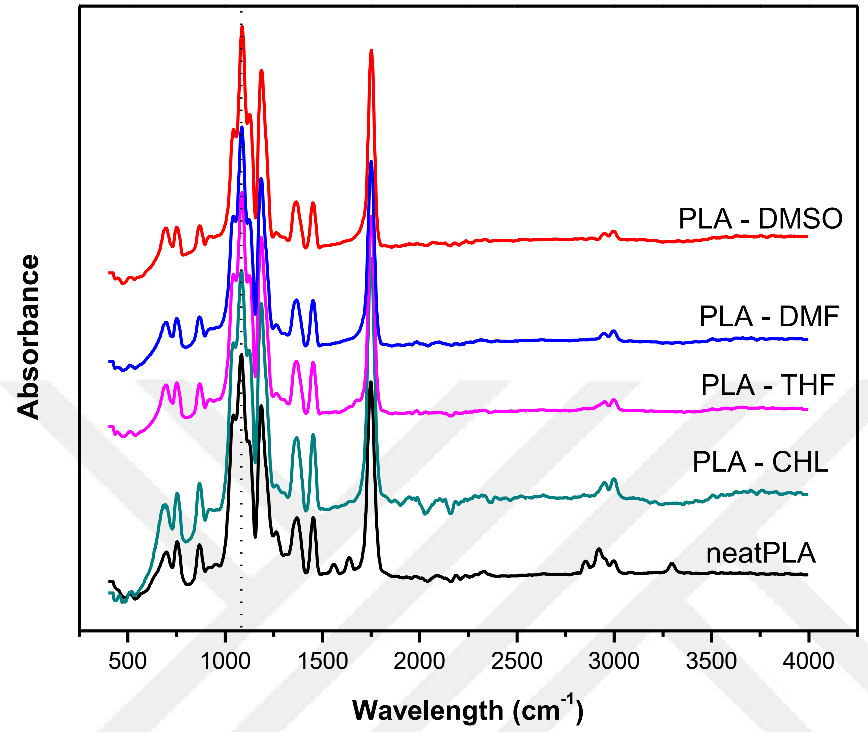

Figure 7.8: FTIR spectra of neat PLAs prepared with different solvents.

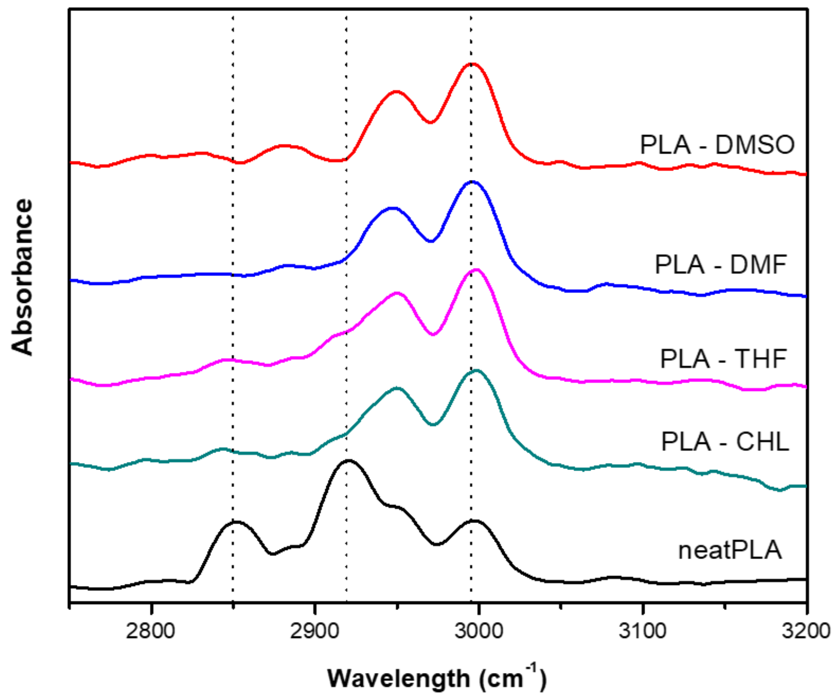

Figure 7.9: FTIR spectra of neat PLAs prepared with different solvents between 2800 and 3200 cm^{-1}.

7.2 The effect of preparation methods

To investigate the effect of preparation method, DMSO was chosen since it was found to be the most effective solvent for CNC dispersion. Both PLA/SCNC and PLA/FCNC nanocomposites were prepared with varying water sonication times and sequence. In total four different methods were compared: 0WS-4MS, 2WS-4MS, 4WS-4MS, and 2WS-4MS-2WS. The complex viscosity as a function of strain is shown in Figure 7.10. The narrow plateau region in complex viscosity of nanocomposites is an indication of improved CNC dispersion.

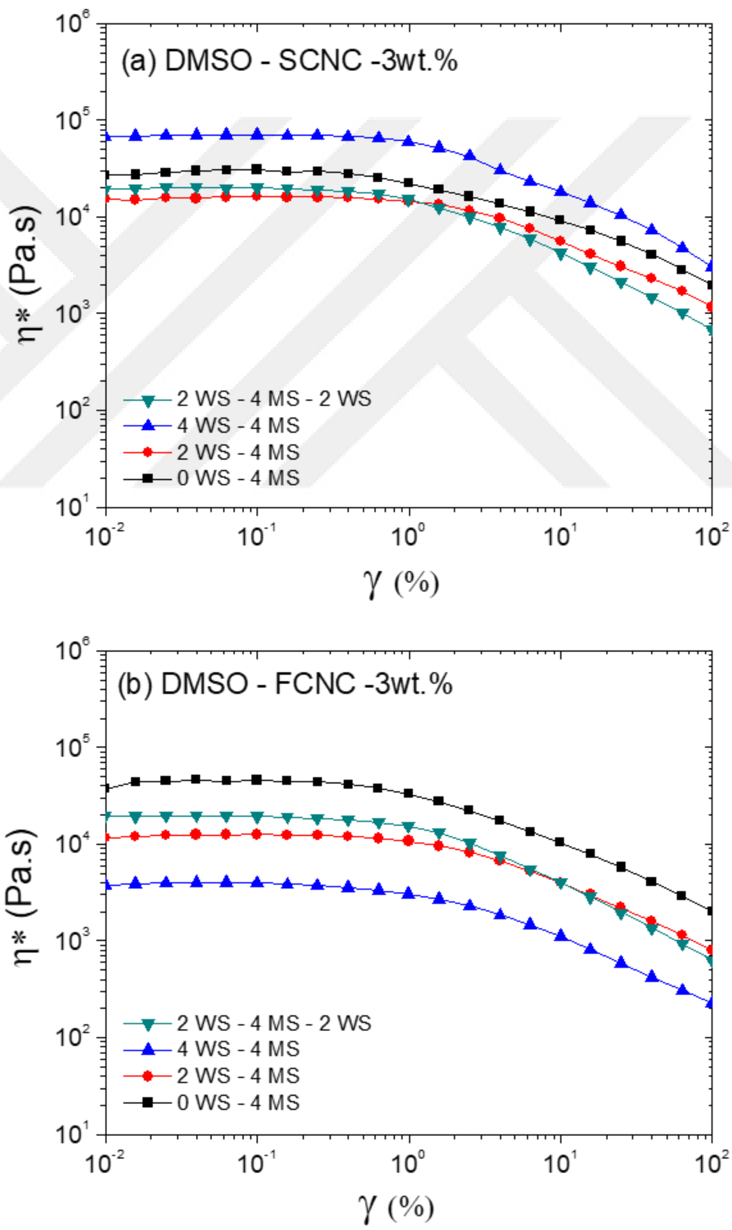

Figure 7.8: Complex viscosity as a function of strain for PLA/SCNC and PLA/FCNC nanocomposites prepared with different solution casting methods.

The results of the frequency sweep experiments are shown in Figure 7.11. The increase of complex viscosity in low frequency indicates the interaction of PLA and CNC interactions at a molecular level and network formation.

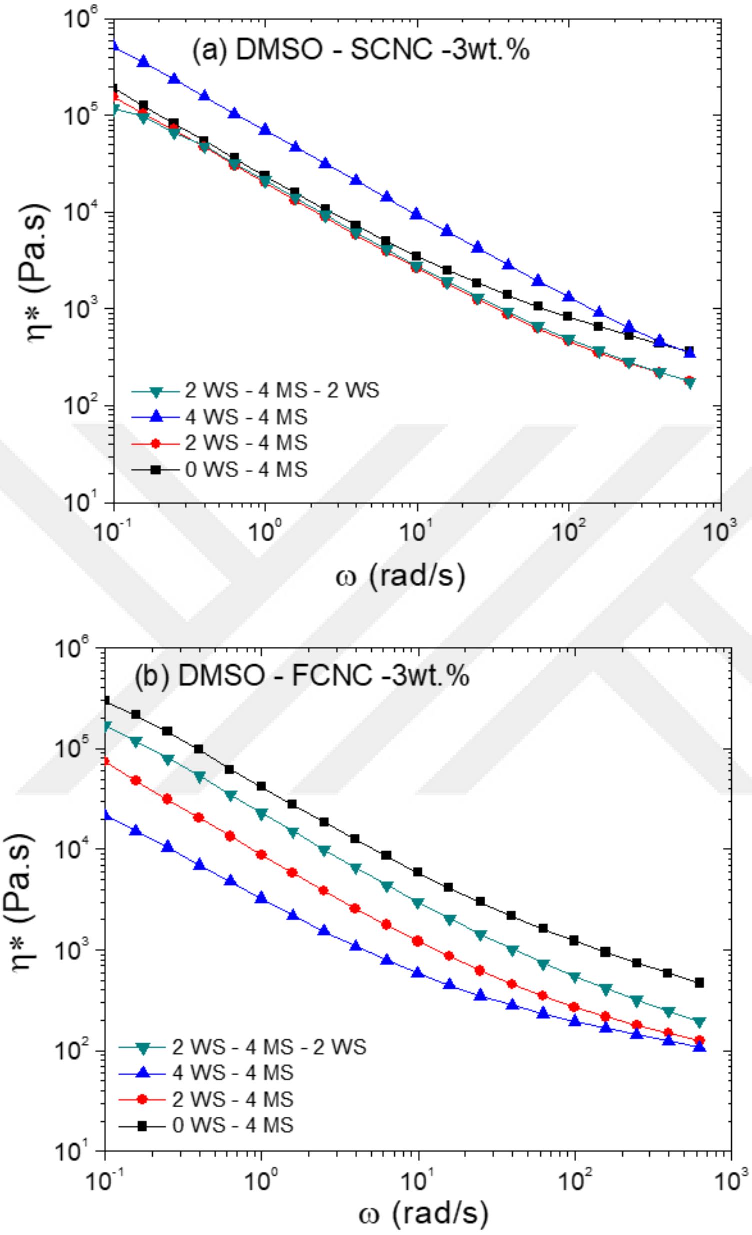

Figure 7.9: Complex viscosity as a function of frequency for PLA/SCNC and PLA/FCNC nanocomposites prepared with different solution casting methods.

The rheological experiments revealed the PLA/SCNC nanocomposite prepared with 4WS-4MS method has the highest improvement thus, the enhanced dispersion of CNC. It can be said that the increased water sonication time increased the dispersion of CNC however, the other methods displayed similar improvements. It could be also concluded that since the SCNC was in powder form only four hours of vigorous stirring at elevated temperature resulted similar improvement with other methods.

These results indicate the DMSO's much higher ability to disperse CNCs even without use of bath sonicator. In the case of PLA/FCNC, 0WS-4MS revealed the highest improvement. Since the FCNC is in flake form, the bath sonication at room temperature was not enough to disperse them. When the bath sonication time increased, nanocomposites revealed lower viscoelastic properties. The method 2WS-4MS-2WS revealed the second-best result and also better than 2WS-4MS method. In the 2WS-4MS-2WS method after 4 hours of magnetic stirring the PLA/FCNC and solvent mixture is placed in the bath sonicator when it was still hot. Thus, the high temperature could aid the solvent to further disperse the FCNC.

7.3 Investigation of CNC dispersion and percolation treshold

The results revealed that DMSO is the most effective solvent for CNC dispersion thus, nanocomposites prepared with DMSO revealed much higher improvements. SCNC also revealed higher and more consistent improvements in frequency sweep experiments due to easier dispersion of powder SCNC. Thus, PLA/SCNC nanocomposites with varying CNC amounts (0, 1, 2, 3, and 5 wt.%) were prepared with DMSO by using the 2WS-4MS method. For the sake of comparison, NCs with same amounts were also prepared with DMF by using the 2WS-2.5MS method. Although DMSO revealed the highest improvement in SCNC with 4WS-4MS method, the 2WS-4MS method was selected to compare the results with that of DMF.

7.3.1 Strain sweep results

Strain sweep results, complex viscosity as a function of strain, of PLASCNC NCs prepared with DMF and DMSO, are presented in Figure 7.12. The complex viscosities of NCs containing 2, 3, and 5 wt.% of CNC prepared with DMF increased compared to neat PLA. The PLA-SCNC5 and PLA-SCNC3 revealed similar results which could be due to agglomeration of CNC at higher content. Moreover, incorporation of CNC resulted in narrow plateau region at lower strains which is an indication of network formation [33]. However, PLA-SCNC1 revealed a wide linear behaviour similar to that of neat PLA which could be due to inefficiency of DMF to deagglomerate CNC at lower content. In the case of NCs prepared with DMSO, the complex viscosity greatly increased in all NCs even at such low amounts. Moreover, the deviations from linearity started at much lower strain values which indicates strong network formation resulted from the DMSO's higher ability to obtain better CNC dispersion.

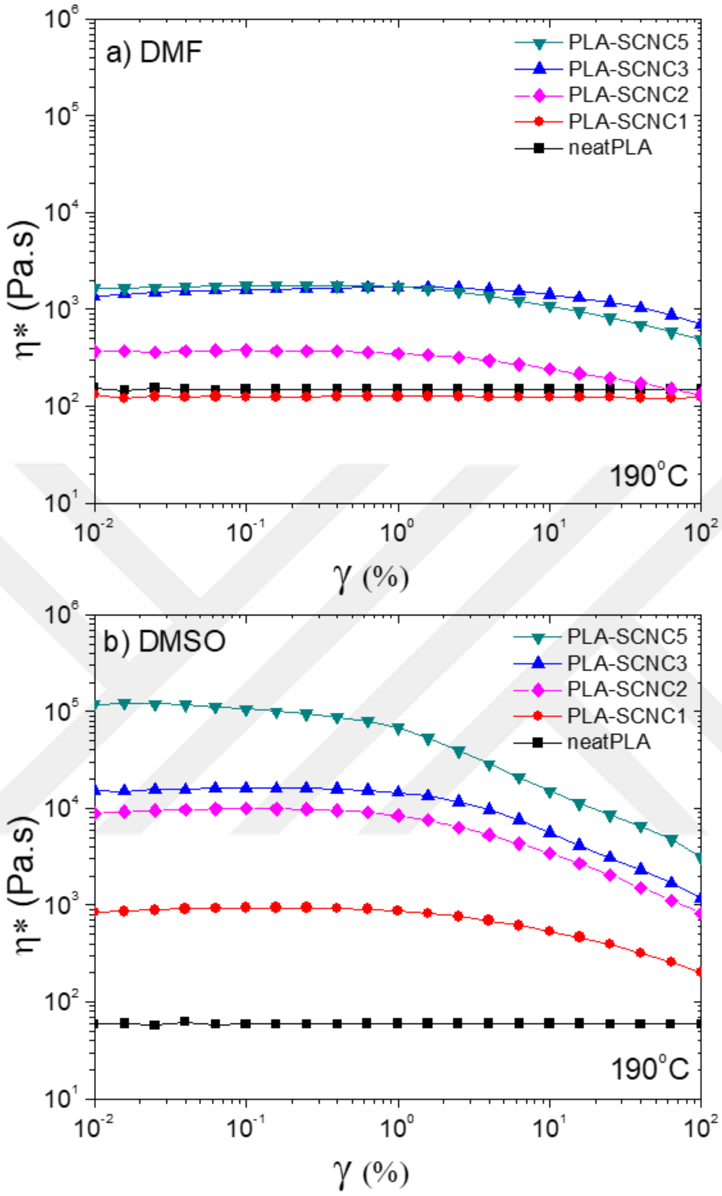

Figure 7.10: Complex viscosity versus strain for PLA/SCNC NCs prepared with DMF (a) and DMSO (b) with varying CNC content (angular frequency is 1 rad/s).

7.3.2 Frequency sweep results

The increase of complex viscosity with decreasing frequency is an indication of interaction between nanoparticles and polymer molecules. Thus, it is also an indication of good level of dispersion which results in increased interfacial interaction [13, 16, 17]. The complex viscosity as a function frequency for PLA-SCNC nanocomposites (1, 2, 3, and 5 wt.%) prepared with DMF (a) and DMSO (b) is shown in Figure 7.13.

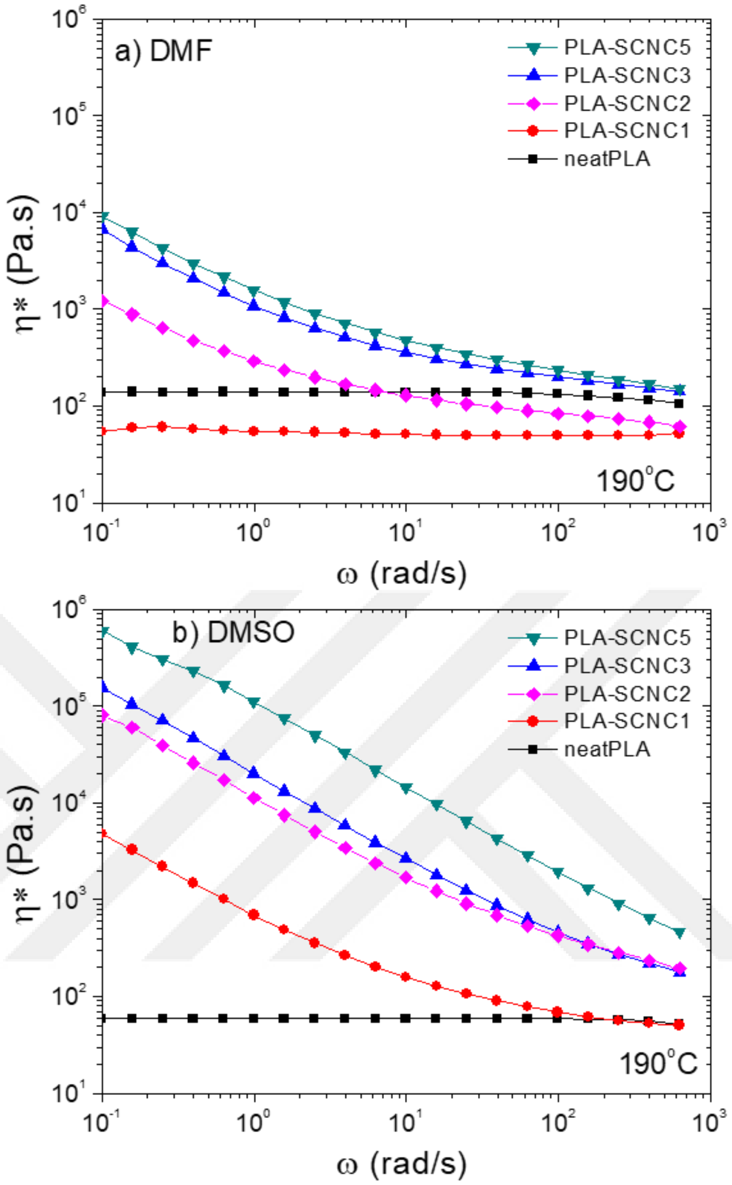

Figure 7.11: Complex viscosity versus frequency for PLA/SCNC NCs prepared with DMF (a) and DMSO (b) with varying CNC content (strain amplitude is 5% for neat PLAs and 0.3% for NCs).

Consistent with the strain sweep results, NCs prepared with DMF, except the PLA-SCNC1, revealed increased complex viscosity with decreasing frequency. NCs with 2, 3, and 5 wt.% of CNC revealed solid-like behavior while NC with 1 wt.% revealed Newtonian behaviour over the whole frequency region and lower complex viscosity compared to neat PLA. In the case of NCs prepared with DMSO all of the NCs revealed increased complex viscosity without a plateau region which is an indication of strong network formation and it increases with increasing CNC content. Moreover, the improvement of CNC dispersion with DMSO even with such small amount of CNC (1 wt.%) is more successful than that of obtained at 2 wt.% of CNC with DMF. The sharp increase in complex viscosity at low frequenct is an indication of strong network formation thus the percolation threshold is assumed to be in between 1-2 wt.% for NCs preapared with DMF and between 0-1 wt.% for DMSO.

Storage modules of NCs as a function of frequency is presented in Figure 7.14. Neat PLAs revealed a slope close to 2 on the log-log scale of storage modules versus frequency which is specific for molten polymers [28].

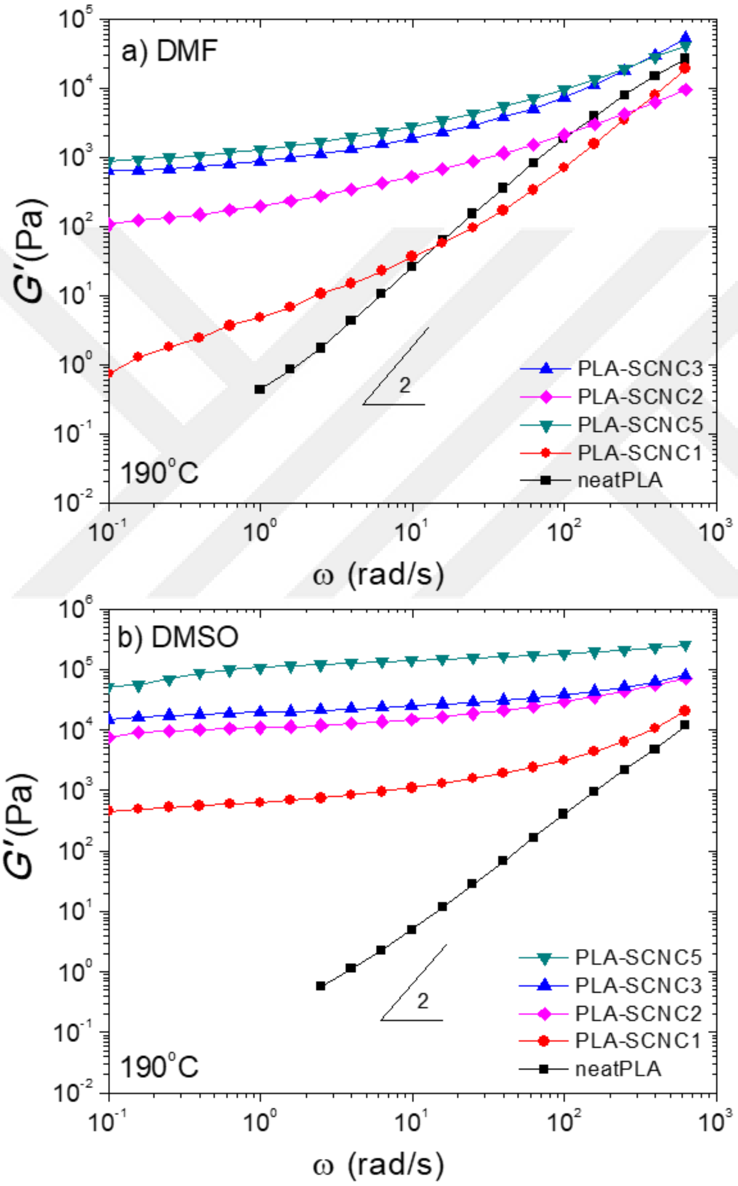

Figure 7.12: Storage modulus versus frequency for PLA/SCNC nanocomposites prepared with DMF (a) and DMSO (b).

For the all NCs prepared with DMF and DMSO, with increasing CNC content the slope decreased in other words the modulus increased with decreasing strain. The increase in G' of NCs was less pronounced at high frequency since at higher frequeinces polymer matrix dominates the viscoelastic properties while the terminal region is an indication of polymer and nanoparticle interaction. The decrease in the slope of NCs, or the increase in modulus at terminal region, is an indication of solid like behaviour. The decrease in the slope is much pronounced in NCs prepared with DMSO and the storage modulus of NCs become less frequency dependent.

As previously shown, with the homogeneous dispersion of nanoparticles in polymer matrix the rheological properties increase at low frequency (or strain) which is an indication of network formation. The concentration of amount of nanoparticles at which the sudden increase in rheological properties occur is the onset of percolation network concentration. With the increase in quality of the dispersion, the percolation network formation is obtained at smaller amount of nanoparticles [14]. It can be concluded that the percolation of solid-like behaviour is between 1-2 wt.% of CNC for NCs prepared with DMF and between 0-1 wt.% for DMSO.

The visual appearance of the nanocomposites is presented in Figure 7.15. As the amount of CNC increased the color of the nanocomposites turned into a brownish color. The NCs preapared with DMSO revealed darker appearance compared to DMF. That change in visual appearance is consistent with the time sweep results.

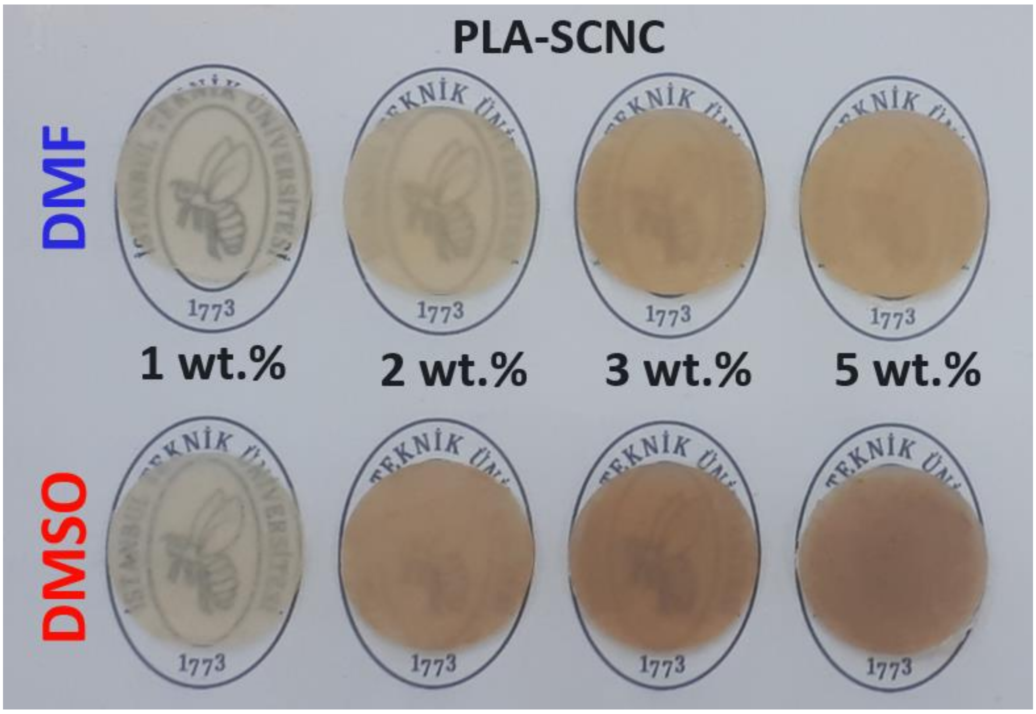

Figure 7.13: The visual appearance of PLA/SCNC nanocomposites containing varying amounts of CNC prepared with DMF (upper row) and DMSO (bottom row).

7.3.3 Modified Cole-Cole plot analysis

The incorporation of nanoparticles results in structural change in polymer matrix and this change can be investigated through modified cole-cole plot (or Han Plot) which reveals the frequency dependence of G' versus G'' [89-93]. The modified cole-cole plots of PLASCNC NCs prepared with DMF and DMSO are presented in Figure 7.16.

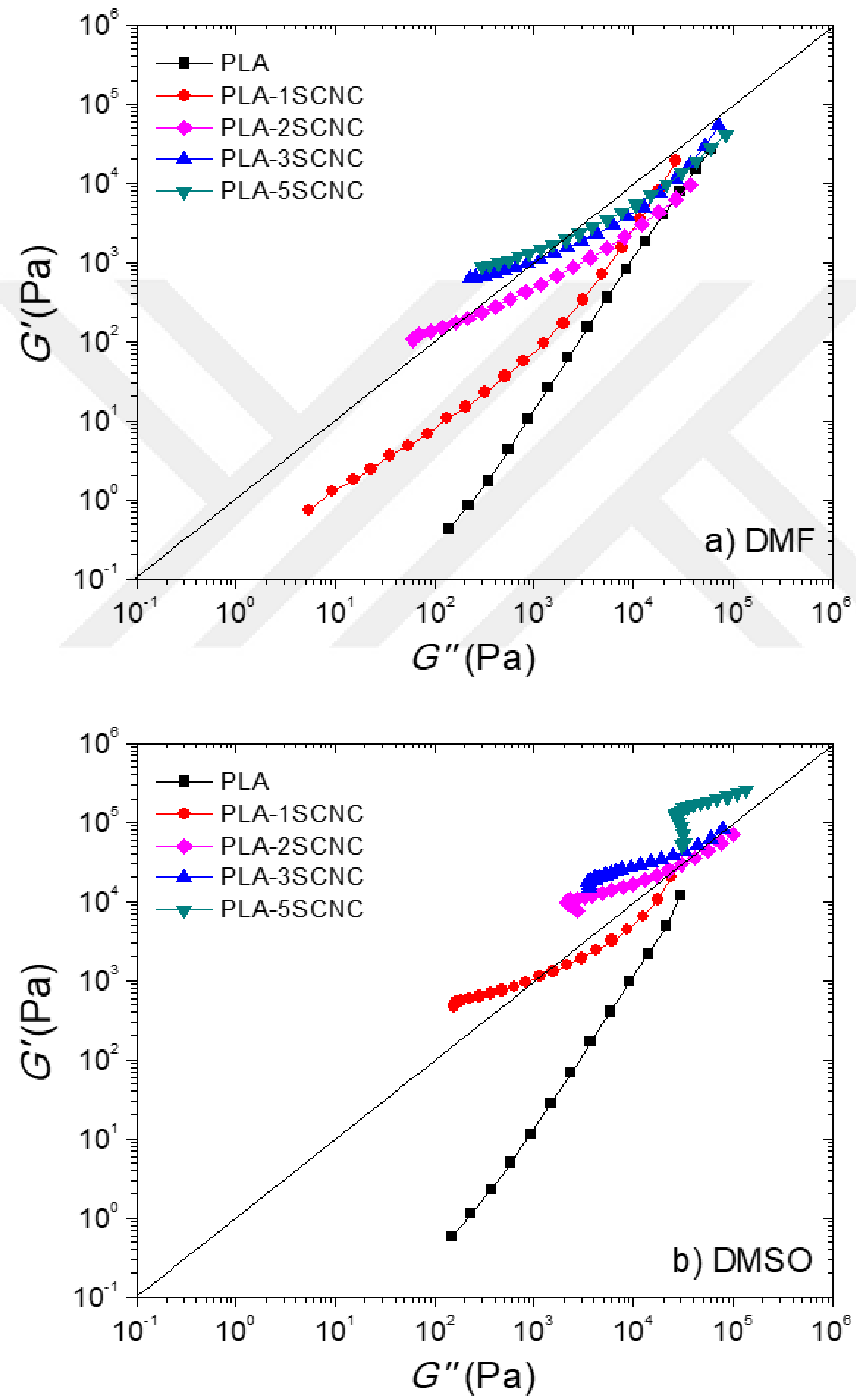

Figure 7.14: Modified cole-cole plots of PLASCNC NCs prepared by DMF (a) and DMSO (b).

The slopes of the neat PLAs are close to 2 which is a specific behaviour for homogeneous polymers and any deviation from this trend is an indication of heterogeneity [33]. Below the percolation threshold, the behavior of nanocomposites is very similar to that of neat PLA which could expleain the similar behaviour of PLA-SCNC1 DMF to that of neat PLA DMF [89]. However, as can be seen in figure the slope of $G' - G''$ curves of NCs dramatically decreased for nanocomposites prepared with DMF and DMSO with 2 wt.% and 1 wt.% of CNC respectively. This dramatic change indicates the onset of percolation concentration which resulted from the interaction between nanoparticles and polymer chains. As a result, consistent with the strain sweep and frequency sweep results, the percolation concentrations of NCs prepared with DMF and DMSO are estimated to be in between 1-2 wt.% and 0-1wt.% respectively.

7.3.4 Calculation of percolation threshold

The percolation network concentration could be calculated by fitting the empirical power-law equation into storage modulus (at 0.1 rad/s) versus CNC content graph obtained by rheological experiments. The empirical power-law equation is followed as:

$$G' = \beta_c G \left(\frac{m - m_c G}{m_c G}\right)^n \text{ for } m > m_c G \qquad (7.1)$$

where $\beta_c G$ and n are power law constants, m is the CNC concentration in wt.%, and $m_c G$ is the rheological percolation threshold in wt.% [17, 28, 94-96]. Figure 7.17 presents storage modulus (at 0.1 rad/s) versus CNC content obtained by rheological expriments for PLASCNC NCs preapared by DMF (a) and DMSO (b). The percolation threshold values were obtained by fitting the experimental results into equation 7.1 and and fitted curves (red curves) are presented in figure. For NCs prepared with DMF and DMSO, $m_c G$ values are calculated as 1.52 and 0.44 wt.% respectively. The calculated percolation concentration for NCs prepared with DMF is found to be better than the results obtained by Vatanser et.al. [17] in which the same preparation method and CNC was used. They reported percolation concentration of 2.8 wt.% for NCs with low molecular weight semicrystalline PLA matrix. As the PLA matrix, present study used comparatively low molecular weight and highly crystallizable PLA (3251D with a D content of 1.4%) which has higher ablity to obtain homogeneous CNC dispersion.

The percolation concentration obtained by using DMSO is found to be the lowest value and it is an indication of strong network formation even at such low concentration.

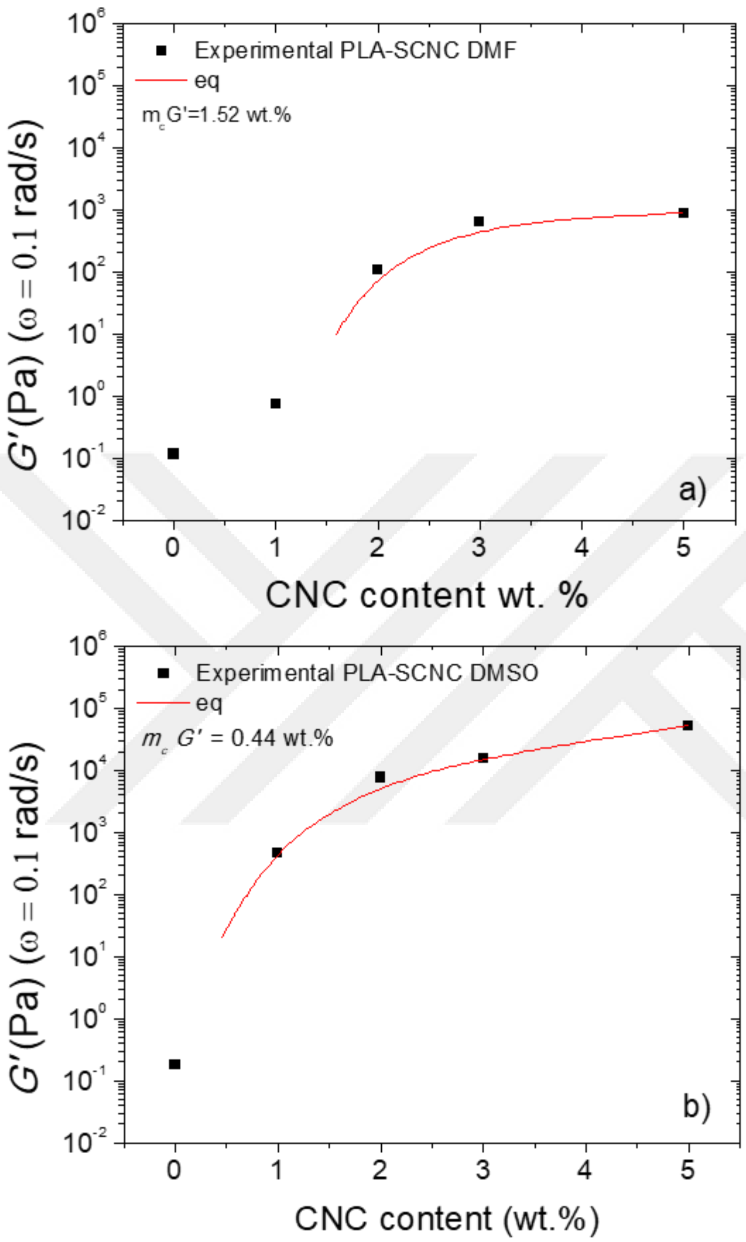

Figure 7.15: Storage modulus (at 0.1 rad/s) versus CNC content of PLASCNC NCs prepared with DMF (a) and DMSO (b). The red lines are fitted into empirical power-law equation (eq. 7.1).

7.3.5 Apparent yield stress

Incorporation of nanoparticles in polymer matrix results in an apparent yield stress. The yield stress defines the stress level at which flow initiates and it is highly dependent on the interaction of nanoparticles with polymer matrix which must be overcome for flow to initiate. The apparent yield stress is the yield stress determined by experimental method which is sensitive to the measurement method and parameters [28, 94]. Frequency and strain sweep results, increased complex viscosity at low frequency and narrow plateau region over strain sweep, revealed that with incorporation of nanoparticles solid-like behaviour was observed which is also an indication of yield stress. Apparent yield stress could be analysed by drawing complex viscosity versus complex modulus (G*) in log-log scale [17, 28, 94, 97]. Figure 7.18 presents the complex viscosity versus complex modulus of PLA-SCNC nanocomposites.

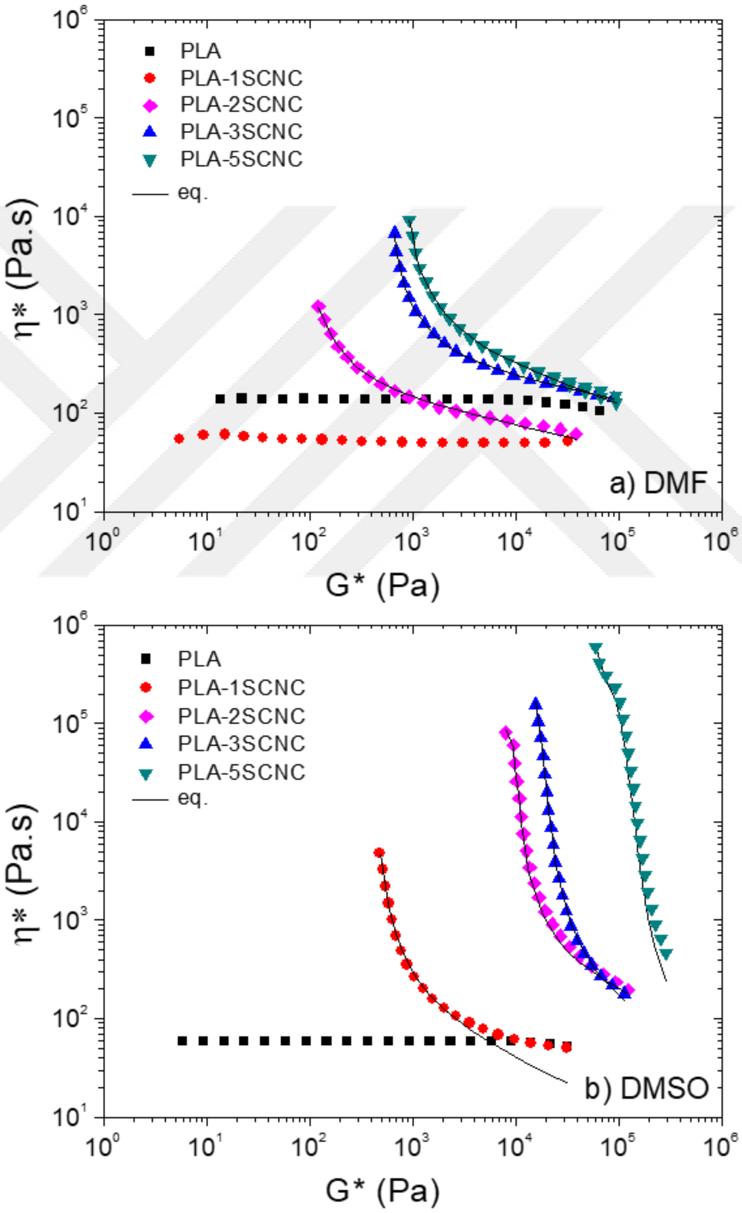

Figure 7.16: Complex viscosity versus complex modulus of PLASCNC NCs prepared with DMF (a) and DMSO (b). The black lines are fitted to modified Herschel–Bulkley equation (eqs. 7.2 and 7.3).

NCs revealed sudden increase in complex viscosity with decreasing complex modulus and at concentrations consistent with the previously calculated percolation concentration. This behaviour is a strong indication of network formation of CNC and it pronounces with increased amount of CNC.

The apparent yield stress of NCs could be determined by using the modified Herschel-Bulkley equation:

$$\eta^* = \frac{G_0^*}{\omega} + k\,(\gamma^0 \omega)^{n-1} \tag{7.2}$$

$$\sigma_0 = G_0^* \gamma^0 \tag{7.3}$$

where G_0^* is the magnitude of the complex modulus at the lowest frequency, γ^0 is the strain amplitude (0.05 for neat PLAs and 0.003 for NCs), k is a constant and n is the flow index. The solid lines in Figure 7.18 represents the calculated curves by fitting the experimental data to Equation 7.2 and 7.3. The fitting parameters and the calculated apparent yield stress of nanocomposites are given in Table 7.1. NCs revealed yield stress behaviour after the percolation concentration. NCs prepared with DMF revealed much lower yield stress compared to that of preapared with DMSO due to lower ability of DMF to CNC effectively. Vatansever et al. [17] could not obtained yield stress value below 3wt.% CNC with low molecular weight semicrystalline matrix. By using same method with highly crystallizable and much lower molecular weight PLA yield stress obtained at much lower concentration. However, Bagheriasl et al. [28] reported much higher yield stress at 3wt.% by using same PLA grade in this study and freeze-dried CNC. Although their method is similar, instead of water bath sonicator they used ultrasonicator to disperse CNC which is much more effective. NCs prepared with DMSO revealed much higher yield stress compared to ones prepared by DMF. Moreover, lowest CNC concentration at which yield stress obtained is 1wt.%. Thanks to much higher ability of DMSO to disperse CNC, pronounced yield stress obtained even at high concentrations. On the other hand, the results obtained by DMSO is still lower than the results obtained by Bagheriasl et al. [28]. This could be attributed to the used of sonicator and more importantly to the presence of solvent in NCs resulted from the inefficient solvent removal process. At the end, increased apparent yield stress resulted from the impediment of chain mobility resulted from particle-particle and polymer-nanoparticle interactions [17, 28]. The melt flow index (n) decreases with increased CNC content as expected with small deviations. The small deviations in the melt flow index could be resulted from the residual solvent.

Table 7.1: Yield stress and melt flow index of NCs calculated using the modified Herschel-Bulkley equation

DMF	σ^0 (Pa)	k (Pa s^n)	n	DMSO	σ^0 (Pa)	k (Pa s^n)	n
PLA	0	131.8	0.98	PLA	0	50.00	0.98
PLA-SCNC1	0	48.7	0.98	PLA-SCNC1	1.21	28.29	0.59
PLA-SCNC2	0.27	61.6	0.79	PLA-SCNC2	25.76	200	0.7
PLA-SCNC3	1.80	155.5	0.81	PLA-SCNC3	48.59	175	0.5
PLA-SCNC5	2.31	151	0.71	PLA-SCNC5	195.65	200	0.4

7.4 Differantial scanning calorimetry (DSC) analysis

Thermal and crystallisation behaviour PLA-SCNC and PLA-FCNC nanocomposites (3wt.% CNC) prepared with DMF and DMSO is presented in Figure 7.19. Thermal history of samples removed by heating from room temperature to 200^{o}C with a heating rate of 10^{o}C/min. Cooling thermograms revealed that crystallisation temperature and amount of crystallitinity of NCs prepared with DMSO increased. Rheological analysis revealed that DMSO provide better dispersion of CNCs. Since, CNC could act as nucleation points as crystallisation it promoted faster crystallisation. NCs filled with FCNC and SCNC revealed no significant difference however, PLA-FSCNC NCs prepare with DMF revealed a melting peak with a shoulder which could be due to nonhomogeneous dispersion of FCNC in DMF resulted in heterogenous crystallisation. Moreover, during the second heating NCs didn’t revealed any cold crystallisation which is an indication of completed crystallisation.

DSC thermograms of PLA-SCNC NCs with varying CNC content prepared with DMF and DMSO is shown in Figure 7.20. No cold crystallisation was observed during the second heating of NCs. At the end, except PLA-1SCNC no significant changes were observed. PLA-SCNC NCs prepared with DMSO revealed higher crystallisation temperatures compared to the ones prepared with DMF. Although DMSO enabled much better dispersion of CNC, presence of CNC especially at higher loadings could hinder the chain mobility of PLA which could be the reason of slower crystallisation. Morever, as presented previously in FTIR results, presence of solvent trace could also hindered the PLAs molecular mobility thus, crystallisation.

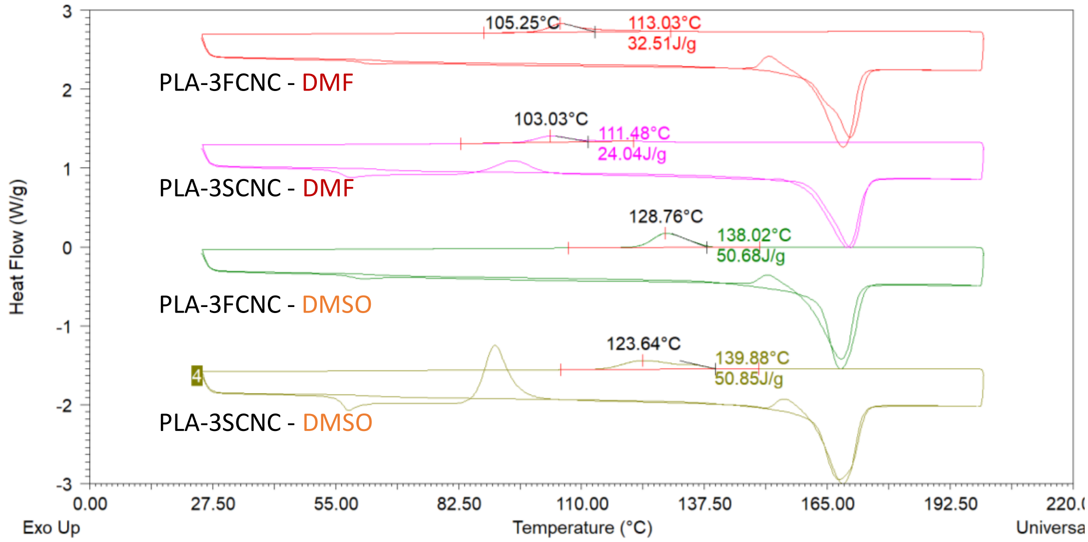

Figure 7.17: DSC heating-cooling-heating thermograms of PLA-SCNC and PLA-FCNC (3wt.%) prepared with DMF and DMSO (heating: 10^{o}C/min, cooling: 2^{o}C/min).

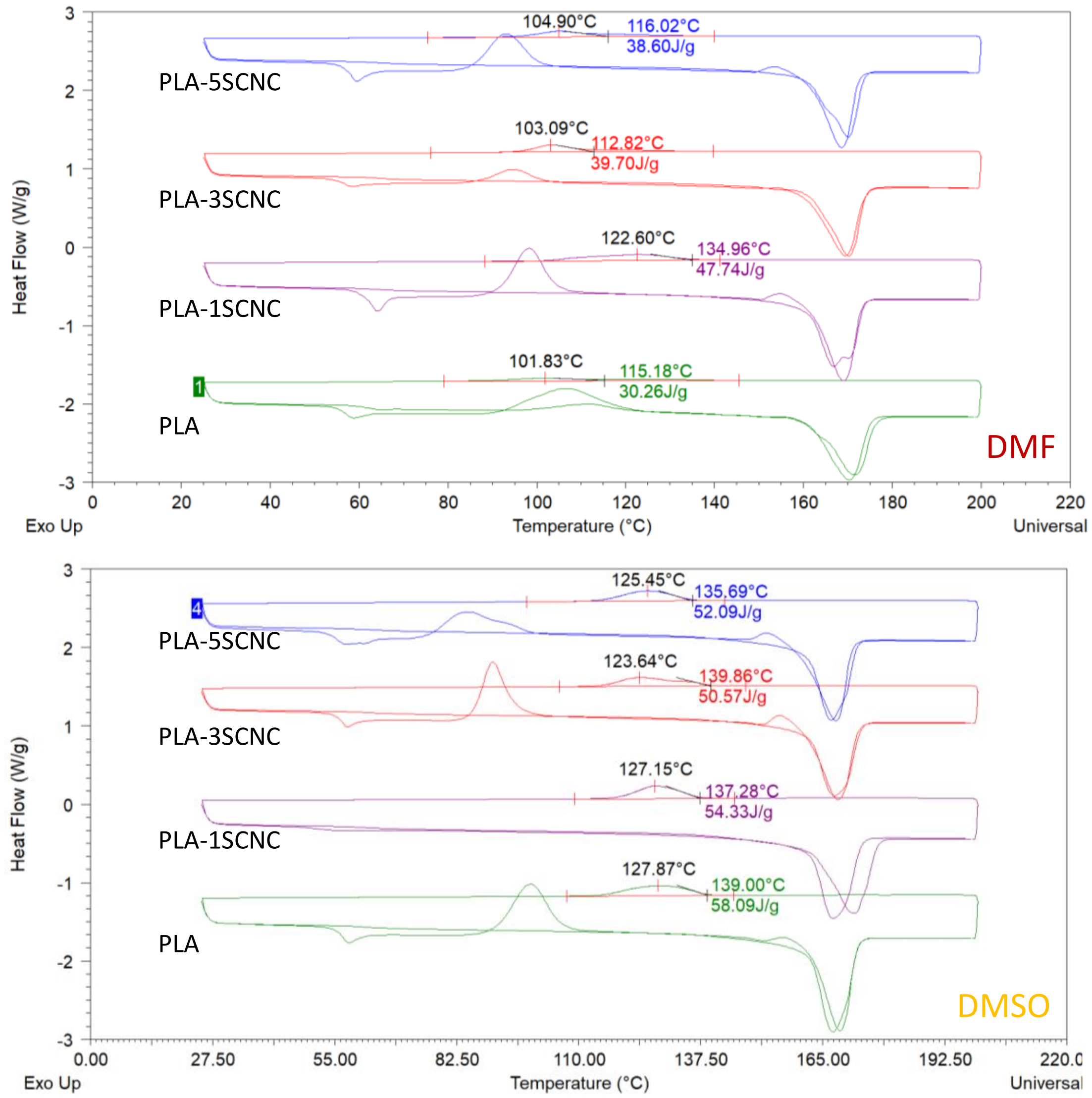

Figure 7.18: DSC heating-cooling-heating thermograms of PLA-SCNC NCs prepared with DMF and DMSO (heating: 10^{o}C/min, cooling: 2^{o}C/min).

8. CONCLUSIONS

The present work aimed to investigate the effects of solution casting method on PLA/CNC nanocomposites rheological and thermal properties. Effect of solvent type, duration and sequence of preparation was comprehensively investigated through rheological analysis. Meanwhile, effect of SCNC and FCNC on dispersion of CNC prepared with solution casted NCs was also investigated. Rheological analysis revealed that DMSO due to its high polarity, high dielectric constant, and solubility parameter was most effective to disperse CNC particles whose surface is negatively charged. SCNC was found to be more effectively and consistently dispersed in PLA matrix due to its powder form. The preparation methods were also compared by preparing PLA/SCNC and PLA/FCNC nanocomposites with DMSO. The highest improvement in viscoelastic properties was found in PLA/SCNC. The increased bath sonication time increased the dispersion of SCNC while bath sonication was not much effective for FCNC. Since the bath sonication is conducted at room temperature it didn’t successful to disperse flake-like FCNC. However, vigorous stirring at elevated temperature resulted in increased viscoelastic properties.

PLA/SCNC nanocomposites prepared with both DMF and DMSO. In nanocomposites prepared with DMF, except PLA/SCNC1, nanocomposites revealed increased rheological properties. For the NCs prepared with DMSO, this increase was more pronpunced. The rheological percolation threshold of NCs prepared with DMF and DMSO was calculated by employing the empirical power-law equation and found to be 1.59 and 0.44 wt.% respectively. The percolation concentration again revealed that DMSO is much more effective to obtain high quality dispersion of CNC.

The apparent yield stress of NCs were calculated by employing Modified Herschel-Bulkley equation. NCs prepared with DMSO revealed much higher apparent yield stress values compared to ones prepared with DMF. Both the modified cole-cole plot analysis and Herschel-Bulkley plots of NCs revealed solid like behaviour started at percolation concentration.

The nonisothermal DSC analysis of NCs revealed that due to better dispersion of CNC with DMSO, the NCs prepared with DMSO exhibit faster crystallisation kinetics. However, no significant change was observed between FCNC and SCNC. The neat PLA processes with DMSO revealed faster crystallisation compared to one with DMF. This could be due to higher plasticizing effect of DMSO since it is expected that higher amount of DMSO is remained in samples. Similarly, NCs prepared with different CNC content revealed that crystallisation time is close to that of neat PLAs. Those, results shows the effect of remaining solvent on NCs crystallisation.

REFERENCES

[1] **Hatti-Kaul R., Nilsson L.J., Zhang B., Rehnberg N., Lundmark S.** "Designing Biobased Recyclable Polymers for Plastics".(2019) *Trends Biotechnol*,

[2] **Url-1** <https://bioplasticsnews.com/wp-content/uploads/2019/04/EuBP-Fact-Sheet-automotive.pdf>, date retrieved 20.06.2020.

[3] **Pan Y., Farmahini-Farahani M., O'Hearn P., Xiao H., Ocampo H.J.J.o.B., Bioproducts.** "An overview of bio-based polymers for packaging materials".(2016) **1**,106-113.

[4] **Castro-Aguirre E., Iniguez-Franco F., Samsudin H., Fang X., Auras R.** "Poly(lactic acid)-Mass production, processing, industrial applications, and end of life".(2016) *Adv Drug Deliv Rev*,**107**,333-366.

[5] **Farah S., Anderson D.G., Langer R.** "Physical and mechanical properties of PLA, and their functions in widespread applications - A comprehensive review".(2016) *Adv Drug Deliv Rev*,**107**,367-392.

[6] **Nofar M., Park C.B.** Polylactide Foams: Fundamentals, Manufacturing, and Applications: William Andrew; 2017.

[7] **Jiménez A., Peltzer M., Ruseckaite R.** Poly (lactic acid) science and technology: processing, properties, additives and applications: Royal Society of Chemistry; 2014.

[8] **Url-2** <https://eur-lex.europa.eu/resource.html?uri=cellar:2df5d1d2-fac7-11e7-b8f5-01aa75ed71a1.0001.02/DOC_1&format=PDF>, date retrieved 20.06.2020.

[9] **Garlotta D.J.J.o.P., Environment t.** "A literature review of poly (lactic acid)".(2001) **9**,63-84.

[10] **Yasuniwa M., Tsubakihara S., Iura K., Ono Y., Dan Y., Takahashi K.** "Crystallization behavior of poly(l-lactic acid)".(2006) *Polymer*,**47**,7554-7563.

[11] **Gupta B., Revagade N., Hilborn J.** "Poly(lactic acid) fiber: An overview".(2007) *Progress in Polymer Science*,**32**,455-482.

[12] **Saeidlou S., Huneault M.A., Li H., Park C.B.** "Poly(lactic acid) crystallization".(2012) *Progress in Polymer Science*,**37**,1657-1677.

[13] **Nofar M.** "Rheological, thermal, and foaming behaviors of different polylactide grades".(2018) *Int J Mater Sci Res*,**1**,16-22.

[14] **Nofar M., Salehiyan R., Sinha Ray S.** "Rheology of poly (lactic acid)-based systems".(2019) *Polymer Reviews*,**59**,465-509.

[15] **Murariu M., Dubois P.** "PLA composites: From production to properties".(2016) *Adv Drug Deliv Rev*,**107**,17-46.

[16] **Vatansever E., Arslan D., Nofar M.** "Polylactide cellulose-based nanocomposites".(2019) *Int J Biol Macromol*,**137**,912-938.

[17] **Vatansever E., Arslan D., Sarul S.D., Durmuş A., Nofar, M.** "Effect of the molecular weight and crystallization of polymer matrix on the CNC percolation network formation".(2019) *Carbohydrate Polymers*

[18] **Ray S.S., Yamada K., Okamoto M., Ogami A., Ueda K.** "New polylactide/layered silicate nanocomposites, 4. Structure, properties and biodegradability".(2003) *Composite Interfaces*,**10**,435-450.

[19] **Chen G.-X., Kim H.-S., Shim J.-H., Yoon J.-S.** "Role of Epoxy Groups on Clay Surface in the Improvement of Morphology of Poly(l-lactide)/Clay Composites".(2005) *Macromolecules*,**38**,3738-3744.

[20] **Spitalsky Z., Tasis D., Papagelis K., Galiotis C.** "Carbon nanotube–polymer composites: chemistry, processing, mechanical and electrical properties".(2010) *Progress in Polymer Science*,**35**,357-401.

[21] **Wu D., Wu L., Zhou W., Sun Y., Zhang M.J.J.o.P.S.P.B.P.P.** "Relations between the aspect ratio of carbon nanotubes and the formation of percolation networks in biodegradable polylactide/carbon nanotube composites".(2010) **48**,479-489.

[22] **Yan S., Yin J., Yang J., Chen X.** "Structural characteristics and thermal properties of plasticized poly (l-lactide)-silica nanocomposites synthesized by sol–gel method".(2007) *Materials Letters*,**61**,2683-2686.

[23] **Raquez J.-M., Habibi Y., Murariu M., Dubois P.** "Polylactide (PLA)-based nanocomposites".(2013) *Progress in Polymer Science*,**38**,1504-1542.

[24] **Miao C., Hamad W.Y.** "Cellulose reinforced polymer composites and nanocomposites: a critical review".(2013) *Cellulose*,**20**,2221-2262.

[25] **Zakeri B**. Tailoring the Surface Charge of Cellulose Nanocrystals (CNC) Using a Polycation: École Polytechnique de Montréal; 2017.

[26] **Khoshkava V.** Polypropylene (PP) nanocomposites incorporating nanocrystalline cellulose (NCC): McGill University Libraries; 2014.

[27] **Lagerwall J.P., Schütz C., Salajkova M., Noh J., Park J.H., Scalia G., et al.** "Cellulose nanocrystal-based materials: from liquid crystal self-assembly and glass formation to multifunctional thin films".(2014) **6**,e80.

[28] **Bagheriasl D., Carreau P.J., Riedl B., Dubois C., Hamad W.Y.** "Shear rheology of polylactide (PLA)–cellulose nanocrystal (CNC) nanocomposites".(2016) *Cellulose*,**23**,1885-1897.

[29] **Bagheriasl D., Carreau P.J., Riedl B., Dubois C.** "Enhanced properties of polylactide by incorporating cellulose nanocrystals".(2018) *Polymer Composites*,**39**,2685-2694.

[30] **Heshmati V., Kamal M.R., Favis B.D.** "Cellulose nanocrystal in poly(lactic acid)/polyamide11 blends: Preparation, morphology and co-continuity".(2018) *European Polymer Journal*,**98**,11-20.

[31] **Bagheriasl D., Safdari F., Carreau P.J., Dubois C., Riedl B.** "Development of cellulose nanocrystal-reinforced polylactide: A comparative study on different preparation methods".(2017) *Polymer Composites*,

[32] **Khoshkava V., Kamal M.R.** "Effect of drying conditions on cellulose nanocrystal (CNC) agglomerate porosity and dispersibility in polymer nanocomposites".(2014) *Powder Technology*,**261**,288-298.

[33] **Kamal M.R., Khoshkava V.** "Effect of cellulose nanocrystals (CNC) on rheological and mechanical properties and crystallization behavior of PLA/CNC nanocomposites".(2015) *Carbohydr Polym*,**123**,105-114.

[34] **Url-3** <https://www.plasticseurope.org/application/files/6315/4510/9658/Plastics_the_facts_2018_AF_web.pdf>, date retrieved 29.06.2020.

[35] **Jamshidian M., Tehrany E.A., Imran M., Jacquot M., Desobry S.** "Poly-Lactic Acid: Production, Applications, Nanocomposites, and Release Studies".(2010) *Comprehensive Reviews in Food Science and Food Safety*,**9**,552-571.

[36] **Hamad K., Kaseem M., Yang H.W., Deri F., Ko Y.G.** "Properties and medical applications of polylactic acid: A review".(2015) *Express Polymer Letters*,**9**,435-455.

[37] **Auras R., Harte B., Selke S.** "An overview of polylactides as packaging materials".(2004) *Macromol Biosci*,**4**,835-864.

[38] **Nofar M., Zhu W., Park C.B., Randall J.J.I., research e.c.** "Crystallization kinetics of linear and long-chain-branched polylactide".(2011) **50**,13789-13798.

[39] **Najafi N., Heuzey M.-C., Carreau P., Therriault D.J.R.a.** "Quiescent and shear-induced crystallization of linear and branched polylactides".(2015) **54**,831-845.

[40] **Li H., Huneault M.A.** "Effect of nucleation and plasticization on the crystallization of poly (lactic acid)".(2007) *Polymer*,**48**,6855-6866.

[41] **Sungsanit K., Kao N., Bhattacharya S.** "Properties of linear poly (lactic acid)/polyethylene glycol blends".(2012) *Polymer Engineering & Science*,**52**,108-116.

[42] **Jiang L., Wolcott M.P., Zhang J.** "Study of biodegradable polylactide/poly (butylene adipate-co-terephthalate) blends".(2006) **7**,199-207.

[43] **Najafi N., Heuzey M., Carreau P.** "Crystallization behavior and morphology of polylactide and PLA/clay nanocomposites in the presence of chain extenders".(2013) *Polymer Engineering & Science*,**53**,1053-1064.

[44] **Trifol J., Plackett D., Sillard C., Szabo P., Bras J., Daugaard A.E.** "Hybrid poly(lactic acid)/nanocellulose/nanoclay composites with synergistically enhanced barrier properties and improved thermomechanical resistance".(2016) *Polymer International*,**65**,988-995.

[45] **Kamal M.R., Khoshkava V.** "Effect of cellulose nanocrystals (CNC) on rheological and mechanical properties and crystallization behavior of PLA/CNC nanocomposites".(2015) *Carbohydrate Polymers*,**123**,105-114.

[46] **Nofar M., Park C.B.J.P.i.P.S.** "Poly (lactic acid) foaming".(2014) **39**,1721-1741.

[47] **Sin L.T.** Polylactic acid: PLA biopolymer technology and applications: William Andrew; 2012.

[48] **Sinclair R.J.J.o.M.S., Part A: Pure, Chemistry A.** "The case for polylactic acid as a commodity packaging plastic".(1996) **33**,585-597.

[49] **Lim L.-T., Auras R., Rubino M.J.P.i.p.s.** "Processing technologies for poly (lactic acid)".(2008) **33**,820-852.

[50] **Cooper-White J.J., Mackay M.E.** "Rheological properties of poly (lactides). Effect of molecular weight and temperature on the viscoelasticity of poly (l-lactic acid)".(1999) *Journal of Polymer Science Part B: Polymer Physics*,**37**,1803-1814.

[51] **Al-Itry R., Lamnawar K., Maazouz A.J.E.P.J.** "Reactive extrusion of PLA, PBAT with a multi-functional epoxide: Physico-chemical and rheological properties".(2014) **58**,90-102.

[52] **Najafi N., Heuzey M.-C., Carreau P.J., Therriault D., Park C.B.J.R.A.** "Rheological and foaming behavior of linear and branched polylactides".(2014) **53**,779-790.

[53] **Palade L.-I., Lehermeier H.J., Dorgan J.R.J.M.** "Melt rheology of high L-content poly (lactic acid)".(2001) **34**,1384-1390.

[54] **Lehermeier H.J., Dorgan J.R.J.P.E., Science.** "Melt rheology of poly (lactic acid): Consequences of blending chain architectures".(2001) **41**,2172-2184.

[55] **Mihai M., Huneault M.A., Favis B.D.J.P.E., Science.** "Rheology and extrusion foaming of chain-branched poly (lactic acid)".(2010) **50**,629-642.

[56] **Carreau P., De Kee D., Chhabra R.** "Rheology of Polymeric Systems: Principles and Applications Hanser".(1997) *American Institute of Chemical Engineers: New York, NY, USA*,

[57] **Hao X., Kaschta J., Liu X., Pan Y., Schubert D.W.** "Entanglement network formed in miscible PLA/PMMA blends and its role in rheological and thermo-mechanical properties of the blends".(2015) *Polymer*,**80**,38-45.

[58] **Gu S.-Y., Zhang K., Ren J., Zhan H.** "Melt rheology of polylactide/poly(butylene adipate-co-terephthalate) blends".(2008) *Carbohydrate Polymers*,**74**,79-85.

[59] **Gui Z.-y., Wang H.-r., Gao Y., Lu C., Cheng S.-j.** "Morphology and melt rheology of biodegradable poly(lactic acid)/poly(butylene succinate adipate) blends: effect of blend compositions".(2012) *Iranian Polymer Journal*,**21**,81-89.

[60] **Wu D., Zhang Y., Yuan L., Zhang M., Zhou W.** "Viscoelastic interfacial properties of compatibilized poly(ε-caprolactone)/polylactide

blend".(2010) *Journal of Polymer Science Part B: Polymer Physics*,**48**,756-765.

[61] **Gerard T., Budtova T.** "Morphology and molten-state rheology of polylactide and polyhydroxyalkanoate blends".(2012) *European Polymer Journal*,**48**,1110-1117.

[62] **Wu D., Wu L., Wu L., Zhang M.J.P.D., Stability.** "Rheology and thermal stability of polylactide/clay nanocomposites".(2006) **91**,3149-3155.

[63] **Basilissi L., Silvestro G.D., Farina H., Ortenzi M.A.J.J.o.a.p.s.** "Synthesis and characterization of PLA nanocomposites containing nanosilica modified with different organosilanes I. Effect of the organosilanes on the properties of nanocomposites: macromolecular, morphological, and rheologic characterization".(2013) **128**,1575-1582.

[64] **Sabzi M., Jiang L., Liu F., Ghasemi I., Atai M.J.J.o.m.c.A.** "Graphene nanoplatelets as poly (lactic acid) modifier: linear rheological behavior and electrical conductivity".(2013) **1**,8253-8261.

[65] **Ding W., Kuboki T., Wong A., Park C.B., Sain M.J.R.A.** "Rheology, thermal properties, and foaming behavior of high d-content polylactic acid/cellulose nanofiber composites".(2015) **5**,91544-91557.

[66] **Safdari F., Bagheriasl D., Carreau P.J., Heuzey M.C., Kamal M.R.** "Rheological, Mechanical, and thermal properties of polylactide/cellulose nanofiber biocomposites".(2018) *Polymer Composites*,**39**,1752-1762.

[67] **Najafi N., Heuzey M.C., Carreau P.J., Wood-Adams P.M.** "Control of thermal degradation of polylactide (PLA)-clay nanocomposites using chain extenders".(2012) *Polymer Degradation and Stability*,**97**,554-565.

[68] **Xu X., Liu F., Jiang L., Zhu J., Haagenson D., Wiesenborn D.P.** "Cellulose nanocrystals vs. cellulose nanofibrils: a comparative study on their microstructures and effects as polymer reinforcing agents".(2013) *ACS applied materials*,**5**,2999-3009.

[69] **Bondeson D., Oksman K.** "Dispersion and characteristics of surfactant modified cellulose whiskers nanocomposites".(2012) *Composite Interfaces*,**14**,617-630.

[70] **Espino-Pérez E., Bras J., Ducruet V., Guinault A., Dufresne A., Domenek S.** "Influence of chemical surface modification of cellulose nanowhiskers on thermal, mechanical, and barrier properties of poly(lactide) based bionanocomposites".(2013) *European Polymer Journal*,**49**,3144-3154.

[71] **Pei A., Zhou Q., Berglund L.A.** "Functionalized cellulose nanocrystals as biobased nucleation agents in poly(l-lactide) (PLLA) – Crystallization and mechanical property effects".(2010) *Composites Science and Technology*,**70**,815-821.

[72] **Xu C., Chen J., Wu D., Chen Y., Lv Q., Wang M.** "Polylactide/acetylated nanocrystalline cellulose composites prepared by a continuous route: A phase interface-property relation study".(2016) *Carbohydr Polym*,**146**,58-66.

[73] **Dufresne A.** "Cellulose nanomaterial reinforced polymer nanocomposites".(2017) *Current Opinion in Colloid & Interface Science*,**29**,1-8.

[74] **Url-4** <https://wiki.anton-paar.com/tr-tr/reoloji-ile-ilgili-temel-bilgiler/>, date retrieved 29.06.2020.

[75] **Murariu M., Dubois P.** "PLA composites: From production to properties".(2016) *Advanced Drug Delivery Reviews*,**107**,17-46.

[76] **Nofar M., Tabatabaei A., Park C.B.** "Effects of nano-/micro-sized additives on the crystallization behaviors of PLA and PLA/CO2 mixtures".(2013) *Polymer*,**54**,2382-2391.

[77] **Nofar M.** "Effects of nano-/micro-sized additives and the corresponding induced crystallinity on the extrusion foaming behavior of PLA using supercritical CO2".(2016) *Materials & Design*,**101**,24-34.

[78] **Herrera N., Salaberria A.M., Mathew A.P., Oksman K.** "Plasticized polylactic acid nanocomposite films with cellulose and chitin nanocrystals prepared using extrusion and compression molding with two cooling rates: Effects on mechanical, thermal and optical properties".(2016) *Composites Part a-Applied Science and Manufacturing*,**83**,89-97.

[79] **Lizundia E., Vilas J.L., Leon L.M.** "Crystallization, structural relaxation and thermal degradation in Poly(L-lactide)/cellulose nanocrystal renewable nanocomposites".(2015) *Carbohydr Polym*,**123**,256-265.

[80] **Fortunati E., Armentano I., Zhou Q., Puglia D., Terenzi A., Berglund L.A., et al.** "Microstructure and nonisothermal cold crystallization of PLA composites based on silver nanoparticles and nanocrystalline cellulose".(2012) *Polymer Degradation and Stability*,**97**,2027-2036.

[81] **Habibi Y., Aouadi S., Raquez J.M., Dubois P.** "Effects of interfacial stereocomplexation in cellulose nanocrystal-filled polylactide nanocomposites".(2013) *Cellulose*,**20**,2877-2885.

[82] **Trifol J., Plackett D., Sillard C., Hassager O., Daugaard A.E., Bras J., et al.** "A comparison of partially acetylated nanocellulose, nanocrystalline cellulose, and nanoclay as fillers for high-performance polylactide nanocomposites".(2016) *Journal of Applied Polymer Science*,**133**,n/a-n/a.

[83] **Arslan D., Vatansever, E., Sarul, D. S., Kahraman, Y., Durmuş, A., Güneş, G., Nofar, R.** "Effect of preparation method on the properties of polylactide/cellulose nanocrystal nanocomposites".(2020) *Polymer composites*,

[84] **Fortunati E., Peltzer M., Armentano I., Torre L., Jimenez A., Kenny J.M.** "Effects of modified cellulose nanocrystals on the barrier and migration properties of PLA nano-biocomposites".(2012) *Carbohydr Polym*,**90**,948-956.

[85] **Casasola R., Thomas N.L., Trybala A., Georgiadou S.** "Electrospun poly lactic acid (PLA) fibres: Effect of different solvent systems on fibre morphology and diameter".(2014) *Polymer*,**55**,4728-4737.

[86] **Reichardt C., Welton T.** Solvents and solvent effects in organic chemistry: John Wiley & Sons; 2011.

[87] **Khoo R.Z., Ismail H., Chow W.S.** "Thermal and Morphological Properties of Poly (Lactic Acid)/Nanocellulose Nanocomposites".(2016) *Procedia Chemistry*,**19**,788-794.

[88] **Url-5** <https://www.sigmaaldrich.com/chemistry/solvents/dimethyl-sulfoxide-center.html>, date retrieved 29.06.2020.

[89] **Gupta A., Simmons W., Schueneman G.T., Hylton D., Mintz E.A.** "Rheological and Thermo-Mechanical Properties of Poly(lactic acid)/Lignin-Coated Cellulose Nanocrystal Composites".(2017) *ACS Sustainable Chemistry & Engineering*,**5**,1711-1720.

[90] **Pötschke P., Fornes T., Paul D.J.P.** "Rheological behavior of multiwalled carbon nanotube/polycarbonate composites".(2002) **43**,3247-3255.

[91] **Zhou Z., Zhang Y., Zhang Y., Yin N.J.J.o.P.S.P.B.P.P.** "Rheological behavior of polypropylene/octavinyl polyhedral oligomeric silsesquioxane composites".(2008) **46**,526-533.

[92] **Barick A., Tripathy D.J.A.C.S.** "Effect of organically modified layered silicate nanoclay on the dynamic viscoelastic properties of thermoplastic polyurethane nanocomposites".(2011) **52**,312-321.

[93] **Han C.D., Jhon M.S.J.J.o.a.p.s.** "Correlations of the first normal stress difference with shear stress and of the storage modulus with loss modulus for homopolymers".(1986) **32**,3809-3840.

[94] **Abbasi S., Carreau P.J., Derdouri A., Moan M.** "Rheological properties and percolation in suspensions of multiwalled carbon nanotubes in polycarbonate".(2009) *Rheologica Acta*,**48**,943-959.

[95] **Du F., Scogna R.C., Zhou W., Brand S., Fischer J.E., Winey K.I.J.M.** "Nanotube networks in polymer nanocomposites: rheology and electrical conductivity".(2004) **37**,9048-9055.

[96] **Hu G., Zhao C., Zhang S., Yang M., Wang Z.J.P.** "Low percolation thresholds of electrical conductivity and rheology in poly (ethylene terephthalate) through the networks of multi-walled carbon nanotubes".(2006) **47**,480-488.

[97] **Bagheriasl D., Safdari F., Carreau P.J., Dubois C., Riedl B.** "Development of cellulose nanocrystal-reinforced polylactide: A comparative study on different preparation methods".(2019) *Polymer composites*,**40**,E342-E349.

CURRICULUM VITAE

Name Surname : Burcu ÖZDEMİR

Place and Date of Birth : BURSA, 12.04.1994

E-Mail : ozdemirburcu@itu.edu.tr

EDUCATION

B.Sc. : 2017, Istanbul Technical University, Chemical and Metallurgical Engineering Faculty, Metallurgical and Materials Engineering Department

PROFESSIONAL EXPERIENCE

- (2015-2017) Prof.Dr. Adnan Tekin Material Science and Production Technologies Applied Research Center (Istanbul, TURKEY), *Student Assistant*
- (2018-2019) Turkish Steel Pipe Manufacturers Association, *Specialist*
- (2019-) Istanbul Techincal University, Chemical and Metallurgical Engineering Faculty, Metallurgical and Materials Engineering Department**,** *Research Assistant*